THE EFFECTS OF USING ALKALI-SILICA REACTION AFFECTED RECYCLED CONCRETE AGGREGATE IN HOT MIX ASPHALT

A Thesis

by

BRIAN JAMES GEIGER

Submitted to the Office of Graduate Studies of
Texas A&M University
in partial fulfillment of the requirements for the degree of

MASTER OF SCIENCE

August 2010

Major Subject: Civil Engineering

THE EFFECTS OF USING ALKALI-SILICA REACTION AFFECTED RECYCLED CONCRETE AGGREGATE IN HOT MIX ASPHALT

A Thesis

by

BRIAN JAMES GEIGER

Submitted to the Office of Graduate Studies of
Texas A&M University
in partial fulfillment of the requirements for the degree of

MASTER OF SCIENCE

Approved by:

Co-Chairs of Committee,	Dan G. Zollinger
	Anal K. Mukhopadhyay
Committee Members,	Amy Epps Martin
	Mohammed Haque
Head of Department,	John Niedzwecki

August 2010

Major Subject: Civil Engineering

ABSTRACT

The Effects of Using Alkali-Silica Reaction Affected Recycled Concrete Aggregate in Hot Mix Asphalt. (August 2010)

Brian James Geiger, B.S., Michigan Technological University

Co-Chairs of Advisory Committee: Dr. Dan G. Zollinger,

Dr. Anal K. Mukhopadhyay

The effects of using alkali-silica reaction (ASR) affected recycled concrete aggregate (ASR-RCA) in hot mix asphalt (HMA) were investigated in this study. Dilatometer and modified beam tests were performed to determine the possibility of new ASR occurring in reactive aggregates within the HMA or re-expansion of existing gel. The Lottman test and micro-calorimeter were used to determine the moisture susceptibility of HMA made with ASR-RCA. A differential scanning calorimeter (DSC) with thermogravimetric analysis (TGA) was used to evaluate the drying of an artificial gel and x-ray diffraction (XRD) was used to check for the potential presence of gel in the filler fraction of the ASR-RCAs. Micro-deval and freeze-thaw tests were evaluated for their potential to indicate the presence of excess micro-cracks or ASR gel.

Expansion testing indicated that both ASR-RCAs were still reactive with 0.5 N NaOH solution saturated with calcium hydroxide (CH) at 60°C. Dilatometer testing of HMA specimens in NaOH+CH solution at 60°C indicated a reaction between the asphalt binder and the solution, but little, if any, ASR. The lack of expansion in the modified beam test supports the binder-solution interaction. However, dilatometer testing in deicer solution at the same temperature indicated that some ASR may have occurred along with the primary binder-solution interaction. The volume change characteristics associated with the binder-solution interaction with and without ASR was supported by the change in pH and alkali concentration of the test solution.

DSC/TGA testing indicated that the artificial gel dehydrated at approximately 100°C. XRD analysis of the filler indicated that some gel may have accumulated in this fraction. Moisture damage testing indicated good resistance to moisture damage by HMA mixtures made with ASR-RCA especially compared to a virgin siliceous aggregate. Micro-deval and freeze-thaw tests can detect the presence of micro-cracks due to ASR in ASR-RCAs as higher mass loss than the virgin aggregate.

The potential distress mechanisms that may occur when using ASR-RCA in an HMA pavement were identified. Results obtained using accelerated laboratory conditions were extrapolated based on anticipated field conditions. Guidelines for the mitigation of potential distresses in HMA made with ASR-RCA are presented.

DEDICATION

This thesis is dedicated to my parents for all of their love and support throughout my life.

ACKNOWLEDGEMENTS

I would like to thank my committee co-chairs, Dr. Zollinger and Dr. Mukhopadhyay, and my committee members, Dr. Epps Martin, and Dr. Haque, for their guidance and support throughout the course of this research.

Thanks also go to my friends and colleagues and the Civil Engineering faculty and staff for making my time at Texas A&M University a great experience. I would also like to thank the Air Force Base personnel who helped to provide me with material for this study and the companies who graciously provided materials. I would like to thank the Federal Aviation Administration for supporting my research through the Airfield Asphalt Pavement Technology Program.

Finally, thanks to my mother and father for their encouragement and to my fiancée for her patience and love.

NOMENCLATURE

AFB	- Air Force Base
AASHTO	- American Association of State Highway and Transportation Officials
ASR	- Alkali Silica Reaction
ASR-RCA	- RCA from PCC that has suffered ASR
ASTM	- American Society for Testing and Materials
Ca	- Calcium
$CH/Ca(OH)_2$	- Calcium Hydroxide
DSC	- Differential Scanning Calorimeter
ED RCA	- RCA from Edwards AFB
EDL	- Electrical Double Layer
EDS	- Elemental Dispersive Spectroscopy
ESEM	- Environmental Scanning Electron Microscope
HL RCA	- RCA from Holloman AFB
HMA	- Hot Mix Asphalt
K	- Potassium
KOH	- Potassium Hydroxide
Li	- Lithium
LVDT	- Linear Variable Displacement Transducer
Na	- Sodium
NaOH	- Sodium Hydroxide
OH	- Hydroxyl
PCC	- Portland Cement Concrete
ppm	- parts per million
RCA	- Recycled Concrete Aggregate
SEM	- Scanning Electron Microscope
Si	- Silicon
SMA	- Stone Matrix Asphalt

TEOS	- Tetraethoxysilane
TGA	- Thermogravimetric Analysis
WMA	- Warm Mix Asphalt
XRD	- X-Ray Diffraction
ΔG_f	- Gibbs Free Energy

TABLE OF CONTENTS

Page

LIST OF FIGURES

Page

Page

Page

Page

Page

LIST OF TABLES

1. INTRODUCTION

Alkali-Silica Reaction (ASR), a reaction between siliceous aggregates and alkali hydroxides in concrete pore solution to form an expansive gel, is one of the main chemical distress problems that may occur within concrete. If the damage caused by ASR and other problems is significant, removal or replacement of the concrete will be necessary. Disposal of this concrete can be problematic due to decreasing landfill space and increased focus on reuse of materials to promote sustainability. One way to reuse the concrete is to crush it in order to form recycled concrete aggregate (RCA). Since the expansion of ASR is a result of the gel absorbing water, it is desirable to reuse recycled concrete aggregate that has suffered from ASR (ASR-RCA) in a manner that will minimize its exposure to moisture. RCA has been used successfully as a base material, but the exposure to moisture would be undesirable for an ASR-RCA. Also, ASR-RCA used in concrete would not only expose it to moisture, but there would likely be fresh faces of the reactive aggregates created during crushing that could cause additional ASR to occur. As an alternative, the ASR-RCA could be used as an aggregate in hot mix asphalt (HMA) with the hope that the asphalt film surrounding the aggregates would protect them from moisture.

The objective of this study was to provide comprehensive technical guidance on the use of alkali silica reaction (ASR) damaged recycled Portland cement concrete (PCC) aggregate in hot mix asphalt (HMA) pavements. To achieve this objective, the following work was undertaken:

- Determination of proper techniques and classifications for condition assessment of existing PCC pavements suffering from ASR distress. ASR-RCA can be used most effectively if the distress level of the existing PCC pavement is known.

This thesis follows the style of the *Transportation Research Record.*

- Determination of the allowable severity of ASR damage in ASR-RCA. This included identifying potential tests to measure the damage present in ASR-RCA.
- Assessment of the potential for continued ASR as well as the effects of pre-existing reaction products (ASR gel) and distress features (micro-cracking) within the HMA mixture. This included identifying potential tests to determine the reactivity of ASR-RCA alone and in HMA specimens made using ASR-RCA.
- Determination of potential remedial measures to prevent any new ASR and mitigate the damage present in ASR-RCA.
- Evaluation of the effects of ASR-RCA on long-term performance of HMA pavement subject to field conditions. These conditions include climate (rainfall, temperature, etc.), traffic loading, and deicer applications.

This report is organized into six sections. The second section presents the literature review of the topics of ASR, RCA, ASR-RCA, and moisture damage in HMA pavements. The third section describes the laboratory test program including the materials used and the tests that were performed on the selected materials. Section four presents the results of the laboratory test program and a discussion of how those results apply to the use of ASR-RCA in HMA pavements. The fifth section discusses the difference between the laboratory tests and actual field conditions as well as the potential impacts of those differences. Section six presents the conclusions drawn from the study along with recommendations for using ASR-RCA in HMA pavements and additional research for better understanding of the subject.

2. LITERATURE REVIEW

In order to avoid repeating past work and to understand better the topic of using RCA suffering from ASR in HMA, a literature review and discussions with knowledgeable individuals were conducted. An extensive literature review on the physical, chemical, and mechanical properties of RCA and their effects on HMA mix were conducted. An attempt was made to identify any lab studies or field projects that used ASR-affected RCA materials in HMA pavements. Studies on related topics such as alkali-silica reactivity along with the use of RCA and ASR affected RCA in PCC, were also reviewed. The following subsections describe ASR including the necessary conditions for it to occur and theories of the mechanism by which expansion occurs, RCA and its use in PCC and HMA, ASR-RCA and its use in PCC and HMA, and finally moisture damage in HMA.

2.1 Alkali-Silica Reaction

Alkali-silica reactivity is a potential cause of chemical distress in PCC. T.E. Stanton of the California Highway Department identified ASR in 1940 and since then, it has been observed all around the world (*1*,*2*). The reaction between the alkaline pore solution of the PCC and reactive silica in the aggregates produce a reaction product called alkali-silica gel. If this gel absorbs sufficient moisture, it expands, creating internal pressures in the PCC. If these internal pressures exceed the tensile strength of the concrete, the PCC will crack.

2.1.1 Causes/Conditions

The mechanism by which ASR occurs is quite complex and has been the subject of a primary focus of ASR research. The three basic requirements for ASR to occur are:

- Reactive silica in the aggregates
- Sufficient available alkalis
- Sufficient moisture in the PCC (*1-14*)

In addition to the three requirements listed above, the presence of calcium hydroxide [$Ca(OH)_2$] in the pore water solution also appears to be an important factor (*4-6*). If any one of the three factors is not present in the concrete, then the reaction will not proceed. Several chemical reactions take place during the alkali-silica reaction, which result in the formation of gel and/or reaction rims around aggregate particles.

Since silica is one of the most abundant compounds in the earth's crust, it is found in most aggregates that are used in concrete (*1,2*). However, the reactivity of silica depends on its crystal structure. Amorphous silica and fine-grained forms of crystalline silica tend to be reactive while coarse-grained forms tend to be nonreactive. Amorphous forms of silica include opal and volcanic glasses. The cryptocrystalline and microcrystalline forms of silica are basically made of fine-grained quartz whereas macrocrystalline forms of silica contain coarse-grained quartz. The greater reactivity of amorphous and fine-grained silica when compared to coarse-grained silica is attributed to the greater surface area of the material. The increased surface area results in more surface defects where reactions can occur. A pessimum effect has been found in some of the more reactive aggregates in which maximum reactivity occurs with a certain amount of reactive aggregates in the concrete and then reactivity decreases with larger amounts of aggregates.

Alkalis, sodium (Na) and potassium (K), are naturally present as substituted cations inside silicate cement phases and alkali-sulfates (*1*). During the hydration of the cement, the alkali sulfates tend to form hydroxides (NaOH and KOH), which increase the alkalinity of the pore solution. The alkali levels in the cement are related to the alkali levels in the raw materials used in its production as well as the method used to produce the cement. Modern air regulations and increased energy costs have led to the use of methods that result in increased cement alkali contents. Other sources of alkalis in the concrete pore solution are aggregates that contain alkalis and admixtures such as fly ash. The amount of alkalis that are soluble in the concrete pore solution and hence available for the reaction is more important than the total alkali content of the concrete materials. Alkalis may also become concentrated in a portion of the concrete through

migration with moisture. One example where this could occur is in a slab in a hot, dry area where moisture in the surface evaporates and the migration of moisture from the bottom brings additional alkalis to the surface. External sources may also contribute additional alkalis to the concrete. Examples of external sources are deicing salts, seawater, and ground water.

Moisture is already present in the concrete from the excess mix water needed for workability. Additional moisture can come from the environment, although the effects of external moisture can be reduced by decreasing the permeability of the concrete. A minimum internal relative humidity of 80-85% can be sufficient to cause a deleterious reaction (*2*). The moisture plays two roles in the alkali-silica reaction. First, it provides the method of transport for alkali and hydroxyl ions to reach the reactive aggregate particles. Second, the moisture is absorbed by the gel that the reaction produces causing it to expand.

Chatterji (*4-6*) has found that calcium hydroxide is also an important factor in the alkali-silica reaction. Calcium hydroxide plays two roles in the reaction. One role is as a source of hydroxyl (OH^-) ions that break down the silica. The other role is that excess calcium ions in the pore solution surrounding the aggregate particle restrict the migration of silica out of the aggregate. The role of calcium hydroxide is discussed further in the following subsection.

2.1.2 Expansion Mechanism

There are five main theories of the mechanisms by which ASR occurs. These are:

- Hansen's Theory (*15*)
- McGowan and Vivian's Theory (*16*)
- Powers and Steinour's Theory (*17*)
- Chatterji's Theory (*5-10*)
- Electrical Double Layer Theory (*11, 18-20*)

Hansen proposed that the cracking that occurred in the concrete was due to the formation of an osmotic pressure cell surrounding the aggregate. He stated that the cement paste would act as a semi-permeable membrane toward silicate ions (i.e. water and alkali ions/molecules could diffuse through the paste but the silicate ions could not). Alkali-silicate that formed on the surface on an aggregate surface would draw solution from the cement paste to form a liquid-filled pocket. The liquid that was drawn in would then exert an osmotic pressure against the confining cement paste (*15*).

McGowan and Vivian challenged Hansen's theory of the mechanism for ASR on the basis that cracking of the concrete should relieve the osmotic pressure and prevent additional damage. They believed that the reacted aggregate particles absorb water and swell in the gel condition to cause cracks. The expansion of the concrete was then caused by widening of the cracks cause by ASR (*16*).

Powers and Steinour believed that the theories proposed by both Hansen and McGowan and Vivian were fundamentally similar. They thought that the primary damage mechanism was swelling of the solid reaction product as controlled by the amount of lime it contained, but that osmotic pressure might also develop. Their theories for both mechanisms are explained below.

The reactivity of silica is determined by the number of incomplete silicon-oxygen-silicon linkages in the particle, meaning that reactivity is a function of specific surface and holes due to atomic disorder. When a silica particle is exposed to a strong base, the hydroxyl ions attack the surface and gradually penetrate the particle. As the available water increases, the reaction product becomes softer and may eventually become a colloidal solution or sol. The hydroxyl ions break the silicon-oxygen bonds producing colloidal particles with higher hydroxyl concentrations resulting in smaller colloidal particles. If the attack occurs in the presence of excess lime, then a non-swelling lime-alkali-silica complex is formed when chemical equilibrium with the lime is reached. However, if the alkali-silica complex is not in equilibrium with the lime, then swelling will occur. When the alkali-silica complex imbibes water, they felt the swelling is due to displacement of colloidal units with respect to one another. One cause

of insufficient lime is that lime is depressed by alkalis in the solution so not enough lime may be available at the reaction site to form the non-expansive gel. Another cause is that the lime-alkali-silica complex can hinder the diffusion of the calcium ion to the reaction site while allowing the other ions to diffuse to form additional gel that can swell. This also explains the persistence of the swelling gel long after its formation even though lime is present in the concrete.

For the osmotic pressure to buildup, they explained that water within concrete would tend to move to regions where it has the lowest free energy. The water held by the alkali-silica complex has lower free energy than water external to the complex. As the strength of the solution within the alkali-silica complex increases, greater osmotic pressure is required to prevent the entry of additional water into the complex. If the alkali-silica complex is fluid and confined, then osmotic pressure may be generated. If the alkali-silica complex is solid, pressure may still be generated by the swelling of the reaction rim (*17*).

Chatterji proposed a new theory based on his belief that the previous theories did not fully explain the observed phenomena. His theory can be summarized in five steps as follows:

i. Hydroxyl ions penetrate the silica grains in the high pH environment of the concrete pore solution. An increase in pH or ionic concentration will increase the rate at which the hydroxyl ions penetrate.
ii. In a mixed electrolyte, such as $Ca(OH)_2$ and NaCl, both cations will penetrate the silica grains with the hydroxyl ions to maintain a charge balance. However, the smaller hydrated cation will penetrate in greater amounts than the larger one. The order of increasing size of cations typically found in a concrete pore solution is K^+, then Na^+, then Li^+, then Ca^{2+}.
iii. The hydroxyl ions hydrolyze the siloxane bonds according to:

$$\equiv Si\text{-}O\text{-}Si\equiv + OH^- \rightarrow \equiv Si\text{-}OH + Si\text{-}O^-$$

This reaction opens the reactive grains to further attack by hydroxyl ions and frees silica that diffuses out of the aggregate and into the solution.

iv. The diffusion of silica out of the reactive grains is controlled by the calcium concentration of the surrounding pore solution. Higher concentrations of calcium will reduce the amount of silica that can diffuse out.

v. Expansion occurs when more materials, Na^+, Ca^{2+}, OH^-, and H_2O, enter the grain than silica diffuses out.

According to this theory, the low expansion of high calcium gels and the reduction of expansion by lithium are explained by the large size of the hydrated calcium and lithium ions, which prevent them from penetrating the reactive grain. This theory also offers an explanation as to why the extent of the alkali-silica reaction is not always related to the level of distress that it causes (*5-10*). If large amounts of silica are leaving the grain then the reaction may continue without causing harmful expansion.

The electrical double layer (EDL) theory was first proposed by Chatterji (*11*) to explain the expansive nature of ASR gel as well as the errors that have been encountered when measuring the concentrations of ions in pore solutions expressed from concrete. Prezzi et. al. (*18,19*) used the EDL to estimate the expansive pressure that would be generated by an ASR gel. According to the EDL, after the silica is dissolved from the aggregate by the high pH solution, it exists as a colloidal suspension in the pore solution. The colloidal silica particles have a negative surface charge, which must be balanced by positive ions from the solution in order to maintain charge neutrality. These positive ions form a diffuse double layer around the colloidal silica particle, which consists of the Stern layer and the Gouy-Chapman layer. The Stern layer is adsorbed on the surface of the silica particle and its charge is dependent on the number of adsorption sites on the surface of the particle as well as other factors. The Gouy-Chapman layer is the diffuse outer layer and its charge is dependent on the dielectric constant of water as well as other factors. The charge in both layers is also dependent on the number of adsorption sites on the surface of the silica particles and the valency and concentrations of the positive ions

in the solution. Because it is double charged, Ca^{2+} has a greater affinity for the negatively charged silica surface than the single charged Na^{+} or K^{+} ions. Also, Rodrigues et. al. (*20*) have demonstrated that Ca^{2+} is chemically adsorbed on the surface due to a nonelectrostatic affinity.

The thickness of the EDL is a function of the concentration and type of ions in the surrounding solution. As the ionic concentration increases, the EDL thickness and repulsion forces between particles decrease. Conversely, as water is added and the solution concentration decreases, the EDL thickness increases along with the repulsion force. The expansive pressure generated by the gel can be calculated from the thickness of the EDL as well as other factors. Prezzi et. al. calculated pressure ranging from 2.2 to 10.3 MPa. This range of values is in agreement with published figures from Diamond, who found pressures of 6-7 MPa (*21*), and Figg, who found expansion pressures can exceed 10 MPa (*22*).

2.1.3 Impact/Results

The expansion caused by ASR typically results in cracking of the concrete resulting in a map-like pattern of cracks. In addition, expansion due to ASR may cause movement of the concrete structural elements relative to other elements.

2.2 Recycled Concrete Aggregate

Attempts have been made to recycle waste concrete for use as aggregate in base courses, Portland cement concrete, and hot mix asphalt.

2.2.1 Properties

Several studies of RCA have found that recycled concrete aggregates have a greater water absorption capacity than typical natural aggregates. This increased water absorption was attributed to the higher porosity of the cement mortar, compared with most natural aggregates, that remains attached to the aggregates. The aggregate particles were also found to be very angular and irregularly shaped (*23-41*). RCA has been documented to produce high pH (greater than 11) solutions when combined with water (*42*).

2.2.2 Use in Portland Cement Concrete

The increased absorption capacity and high angularity of the RCA were attributed to the increased water demand of mixes made with RCA compared to natural aggregates. Some studies have found that the use of RCA reduces the mechanical properties of the concrete while others found the RCA to have insignificant impact on the mechanical properties. There was a general agreement that the fine fraction of the RCA was more likely to have a deleterious impact than the coarse fraction (*26-36*).

2.2.3 Use in Hot Mix Asphalt

Several states allow the use of RCA in hot mix asphalt (HMA). Several studies have been performed to determine the properties and performance of HMA containing RCA. These studies have found that, in comparison to mixes made with virgin aggregates, HMA made with RCA will either have a higher air void content for the same asphalt binder content or a higher optimum binder content for the same air void content (*37-41*). This has been attributed to the increased porosity of the cement paste attached to the aggregate similar to that found in the studies of RCA in Portland cement concrete. The more absorptive RCA particles usually absorb more asphalt into the larger pores and absorb asphalt more deeply into the particle. Therefore, design asphalt contents when using RCA can be expected to be relatively high. Wong et al., (*40*) found that RCA lowers abrasion resistance and bond strength of HMA made of RCA when compared to HMA made of virgin granite aggregate. The studies have had differing results for the stripping potential of HMA made with RCA. Paranavithana and Mohajerani (*39)* found that HMA mixes made with RCA had a greater potential for stripping while Heins (*38*) found that HMA mixes made with RCA had stripping potential similar to mixes made with virgin aggregates. Paranavithana and Mohajerani (*39*) also found that HMA mixes made with RCA had significantly lower resilient modulus and indirect tensile strength than those made with virgin aggregates. However, Wong et al (*40*) found that the use of RCA fines in the mix improved the rut resistance of the HMA mixture. Some studies have found that the RCA particles have a greater tendency to break down during mixing and compacting of the HMA (*39,41*).

2.3 Alkali-Silica Reaction Affected Recycled Concrete Aggregate

Studies on the use ASR-RCA have not been as extensive as those on the use of ordinary RCA. However, some studies were found on the use of ASR-RCA in Portland Cement Concrete.

2.3.1 Use in Portland Cement Concrete

A study by Gottfredsen et. al. (*43*) found that RCA from concrete in which the aggregates had only partially reacted caused a delayed yet significant reaction. In contrast, RCA from concrete in which was severely deteriorated caused only a minor expansion. This was attributed to the reactive portion of the silica having most likely been completely reacted. In a study by Li and Gress (*44*), ASR-RCA still caused significant expansion when used to produce new concrete.

2.3.2 Use in Hot Mix Asphalt

The literature review did not find any studies of the use of recycled concrete aggregate that had suffered from alkali-silica reactivity in hot mix asphalt. Discussions with national experts also did not provide any evidence of the use of RCA suffering from ASR in HMA. While these searches cannot be considered exhaustive, it is reasonable to assume that no research on this topic has been published to date.

2.4 Moisture Damage

Moisture damage in asphalt pavements is the degradation of the mechanical properties of the asphalt composite due to the action of water. Moisture damage in HMA concrete can be defined more precisely as “the progressive functional deterioration of a pavement mixture by loss of the adhesive bond between the asphalt cement and the aggregate surface and/or loss of the cohesive resistance within the asphalt cement principally from the action of water” (*45*). Moisture damage is a complex phenomenon involving chemical, physical, and mechanical processes; therefore, characterization and modeling of moisture damage is a challenging task. Moisture transport can occur in asphalt mixtures through the following different mechanisms: (*46*)

- Infiltration through cracks [both adhesive failure (along the aggregate - paste interfaces) and cohesive-failure (within the asphalt cement)] and interconnected voids
- Vapor diffusion through small pores (smaller than air voids)
- Capillary rise, although this is not normally a prominent mechanism
- Severe environmental conditions (high ambient relative humidity, high annual rainfall, high temperature fluctuations, etc.) can enhance the intensity and/or relative importance of the above three mechanisms and increase the severity of moisture damage

These three modes of moisture transport and their relationship with moisture damage were discussed in a companion paper (*47*). ASR cannot be a cause of distress in HMA concrete provided there is insufficient moisture vapor or water inside the mixture. Moisture is essential to create a high pH situation wherever cement mortar portions are attached with the aggregates and to cause any gel that forms to swell. Therefore, the greater the moisture damage, the higher the chances of ASR, provided the other conditions for ASR are also satisfied. Any remedial measures to formulate moisture damage resistant HMA mixtures would ostensibly reduce ASR related issues, if any. However, the most common antistripping agents (i.e., hydrated lime and liquids containing amines or ammonium compounds) will increase the alkalinity of the mix and may, in fact, favor ASR.

2.4.1 Mechanism

The moisture susceptibility of an HMA is a function of the surface free energy of the asphalt binder and the aggregates. The combined effect of the surface free energy of the two materials to produce the adhesive bond energy, or Gibbs free energy, (ΔG_f) is modeled by:

$$\Delta G_f = 2 * \sqrt{\gamma_A^{LW} \gamma_S^{LW}} + 2 * \sqrt{\gamma_A^{+} \gamma_S^{-}} + 2 * \sqrt{\gamma_A^{-} \gamma_S^{+}}$$

Where the subscripts A and S refer to the asphalt binder and the aggregate respectively, γ^{LW} is the non-polar Lifshitz van der Waals component of the surface free energy, and the + and - superscripts refer to the Lewis acid and base components respectively (*48-51*). Mixes containing aggregates with a more basic nature, such as limestone, tend to have lower moisture susceptibility than those containing aggregates of a more acidic nature, such as siliceous aggregates (*49-52*).

2.4.2 Mitigation

The moisture susceptibility of an HMA can be reduced by adding lime to the mixture or through the use of liquid anti-strip agents.

3. LABORATORY TEST PROGRAM

The laboratory test program describes the materials used and the tests that were performed on those materials.

3.1 Materials

Three different aggregates were used in this study, a virgin chert aggregate and ASR-RCAs from two different United States Air Force Bases (AFB). Other materials used in this study include asphalt binder, chemical reagents, and deicer solution. These materials are described below.

3.1.1 Chert

The chert consists primarily of cryptocrystalline quartz, which is known to be reactive with alkaline solution. Chert particles were separated from a Chert-rich Texas Gravel to generate reactive virgin aggregate for use in the dilatometer testing. The Texas gravel primarily contains chert (65%) with lesser amounts of quartzite (10%), limestone (18%), and volcanics (7%). The chert was selected to provide a control against which the test results of the RCAs could be compared. In addition, chert provides alkali-silica reactivity without the increased complexity caused by the mortar fraction attached to the RCA. Therefore, it provides the basic understanding of the reaction mechanisms.

In addition to the as-received chert, special samples were fabricated using selected particles of chert for a detailed study of the microstructure of the reaction products. These particles were cast in an epoxy resin in the form of a disk. After the epoxy set, the disk was cut to a thickness slightly greater than the height of the chert particles. The disk was then sanded and polished to create an exposed surface on the chert on one face of the disk. The exposed face was polished using 0.25µm diamond powder. This high degree of polishing was selected to allow for easy observation of any reaction products that formed on the surface of the chert. An image of these special chert samples is presented in Figure 1 .

Figure 1 Special Polished Chert Specimens Used in Detailed Microstructure Study

3.1.2 Alkali-Silica Reaction Affected Recycled Concrete Aggregate from Air Force Bases

The criteria for material selection were prepared in a form of standard questionnaire, which is provided in Appendix A. The potential AFBs were contacted to provide the necessary information by filling those questions. All the available information is summarized in Appendix B. Only two AFBs were qualified as potential sources of ASR-RCA based on the criteria provided in Appendix A. However, ready to use RCA was not available from these two selected sources. In Seymour Johnson AFB, the ettringite related distress was found to be the dominant mechanism rather than ASR. The New Mexico Department of Transportation was also identified as a potential source, but the material was not received.

3.1.2.1 ED RCA

ED RCA is a recycled concrete aggregate from Edwards AFB, California. The original diagnosis of ASR was determined by the Geotechnical Branch of the Sacramento District of the Army Corp of Engineers as a result of an investigation into map-cracking of the runway and taxiway pavements in 1995. An example of this map-cracking is presented in Figure 2.

Figure 2 Map-Cracking of Pavement Surface for Edwards AFB

A total of four cores from two map-cracked areas were selected for the investigation. X-ray diffraction, stereo light, polarized light, and scanning electron microscopy were used to confirm the presence of ASR. ASR gel was found in cracks and air voids, and darkened reaction rims were observed surrounding some aggregate particles.

Twenty-two cores from Edwards AFB were sent to the Concrete and Materials Branch of the US Army Corp of Engineers for investigation of possible ASR in 2004.

Some of the cores were sawn longitudinally and all cores were fractured to expose fresh faces. The sawn cores were examined for the presence and depth of cracks. Cracks caused by ASR were coated with ASR products. Sodium cobaltinitrite and rhodamine B dye were applied to the fresh fracture faces to react with potassium and calcium to stain the ASR products yellow and pink. The siliceous coarse aggregate used in the concrete was determined to be the reactive component for the ASR. An image of the stockpile of ASR affected concrete at Edwards AFB is presented in Figure 3.

Figure 3 Stockpile of ASR Affected Concrete at Edwards AFB

Additional petrographic observation by TTI confirmed that the coarse aggregate and reactive component of the ED RCA is a granitic aggregate containing strained quartz. The concrete was received in large pieces as presented in Figure 4, which were then crushed to the proper size range using a jaw crusher, a picture of which is presented in Figure 5 .

Figure 4 As-Received Edwards RCA

Figure 5 Jaw Crusher Used to Crush RCAs

Many of the larger pieces required breaking with a sledgehammer prior to crushing in the jaw crusher. The jaw crusher reduced the pieces to the size range needed for the study without any additional crushing.

After crushing, aggregate particles from the ED RCA were selected for petrographic analysis. A stereomicroscope image of gel on a particle of ED RCA is presented in Figure 6.

Figure 6 Stereomicroscope Image of Gel on Surface of ED RCA Particle at TTI

The white material on the particle presented in Figure 6 has the appearance of a typical ASR gel. The circled area, as observed under the SEM, is presented in Figure 7 .

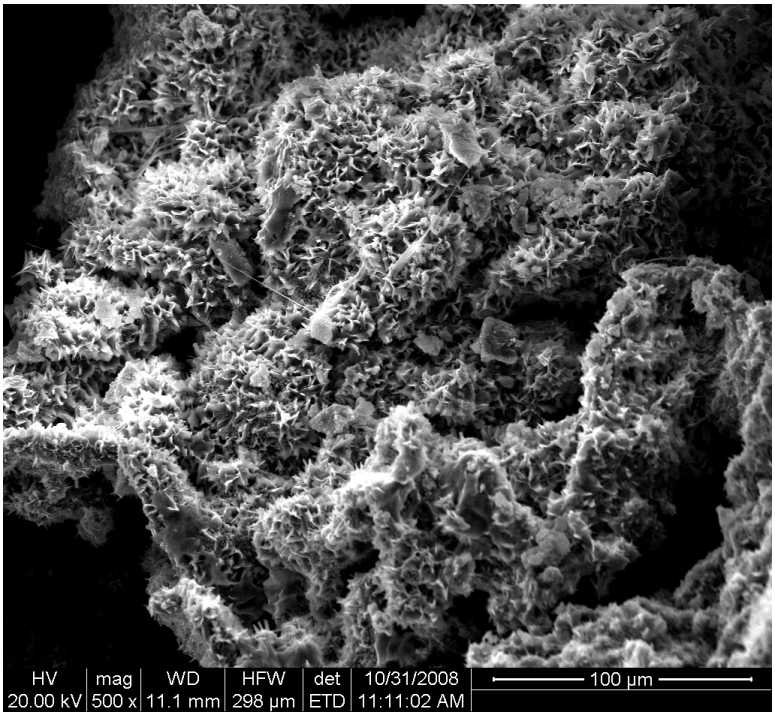

Figure 7 SEM Image of Gel from ED RCA, Magnified View of the Marked Portion in the Image of Figure 6, TTI

The Energy Dispersive Spectroscopic (EDS) analysis from this gel is presented in Figure 8.

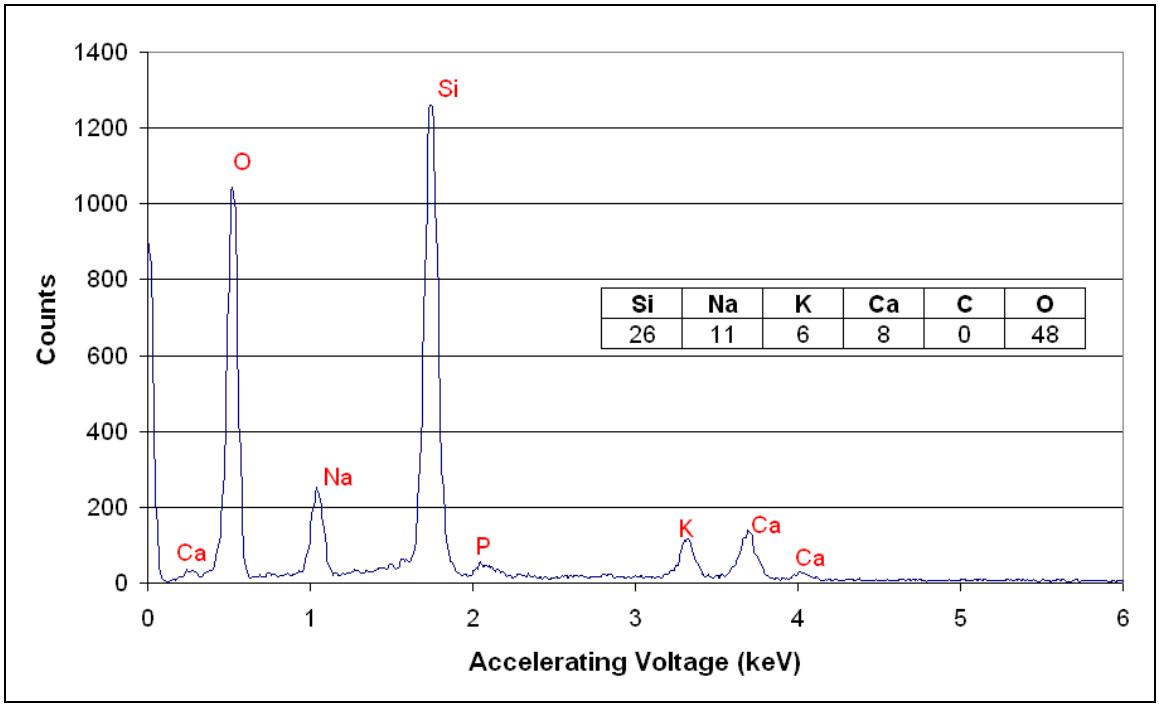

Figure 8 EDS Analysis of Gel from ED RCA

The EDS analysis confirms that the material on the surface of the ED RCA particle is ASR gel containing sodium, potassium, and calcium.

3.1.2.2 HL RCA

HL RCA is a recycled concrete aggregate from Holloman AFB, New Mexico. At Holloman AFB, the ASR was concentrated in the top 2-3 inches of the pavement. Material was collected during patch work to replace areas affected by ASR. The sand, which was the reactive component, used in the concrete was a natural sand with a high silica content from the Rio Grande River Valley. The ASR resulted in severe map cracking of the surface and misalignment of trench drains in the concrete as presented in Figure 9.

Figure 9 Map-Cracking and Misaligned Trench Drain at Holloman AFB

Holloman AFB has a mild climate regarding ASR with dry conditions and few moist freeze-thaw cycles with no use of deicers. Type V cement is used in the concrete to prevent issues with the high sulfate contents of the soils. No petrographic reports were available to confirm that the distress observed was due to ASR. Some additional details can be obtained from Appendix C.

Petrographic observation at TTI revealed that the coarse aggregate is primarily a relatively smooth limestone. Traces of rhyolitic rocks and quartzite were also observed. The primary reactive component was the fine aggregate, which was a rough sand. The mortar fraction has a relatively high air void content. The concrete was received in large pieces, which were then crushed to the proper size range using a jaw crusher. Figure 10 shows a stereomicroscope image of the white material, indicated by the arrow, on the surface of a specimen from Holloman AFB. This material appears to have an amorphous form when viewed under the stereomicroscope.

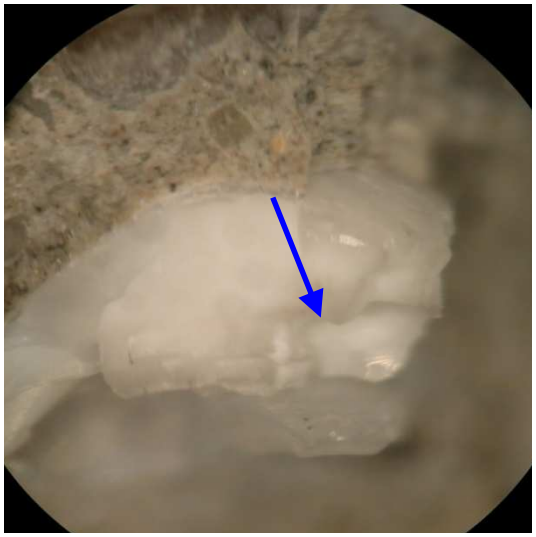

Figure 10 White Material on Holloman, Sample 5

An ESEM image of this white material is shown in Figure 11. The presence of typical massive ASR gel is evident from Figure 11.

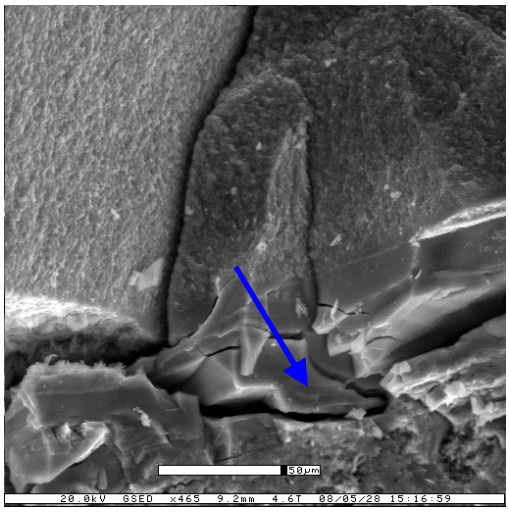

Figure 11 ESEM Image of White Material on Holloman Sample 5. Arrow Indicates Presence of Massive ASR Gel.

Figure 12 shows a reaction rim with white material, indicated by the arrow, inside of a fine aggregate particle in another sample from Holloman AFB. ESEM images of the white material are shown in Figure 13 a, b.

Figure 12 White Material and Aggregate Rim on Holloman Sample 6, Stereomicroscope

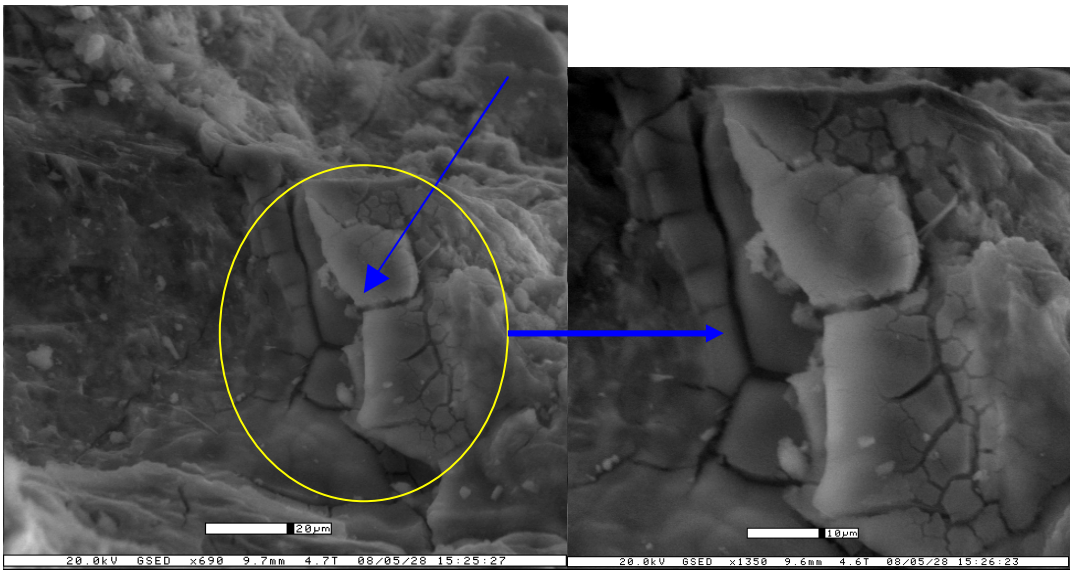

Figure 13 (a) ESEM Image from White Material on Holloman Sample 6, (b) A Magnified View of Figure 13a

The typical appearance of massive ASR gel with micro-cracks is clearly evident in Figure 13. The presence of aggregate cracking and gel (typical ASR distress features) is clearly evident from thin section petrography as presented in Figure 14.

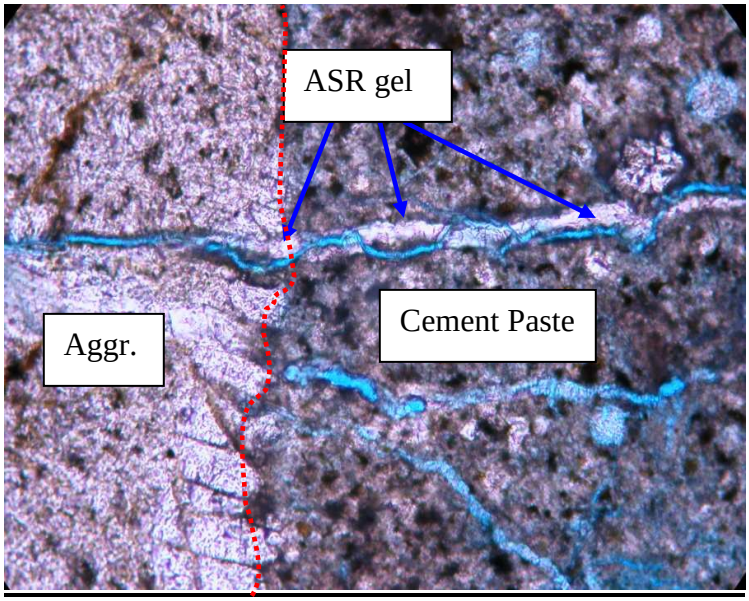

Figure 14 Presence of ASR Gel, Aggregate Cracking in RCA from Holloman AFB

An additional specimen of the HL RCA was observed using the SEM in order to confirm that the observed materials were in fact ASR gel. An image of the gel on the HL RCA is presented in Figure 15.

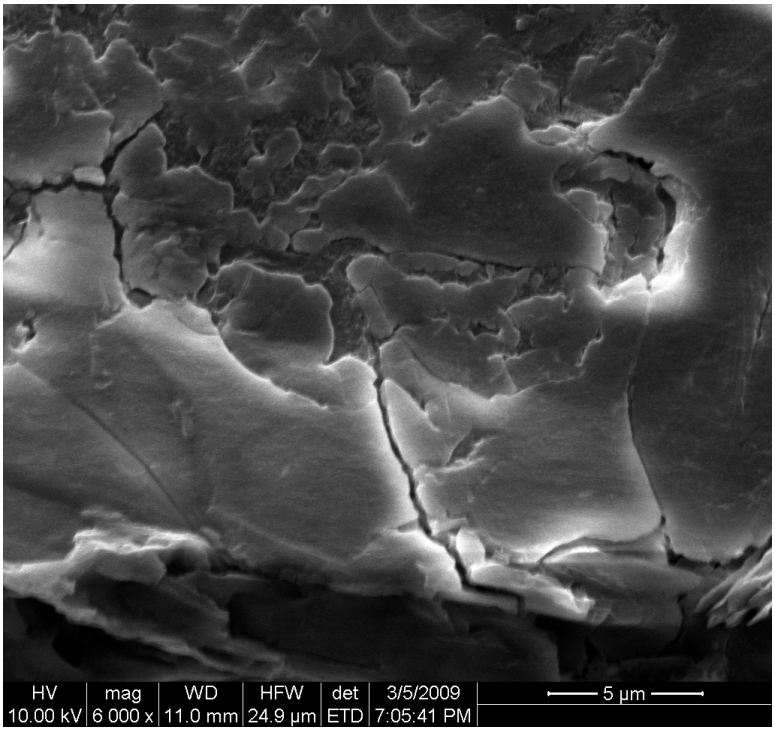

Figure 15 SEM Image of Gel from Holloman RCA

The EDS analysis of the gel is presented in Figure 16.

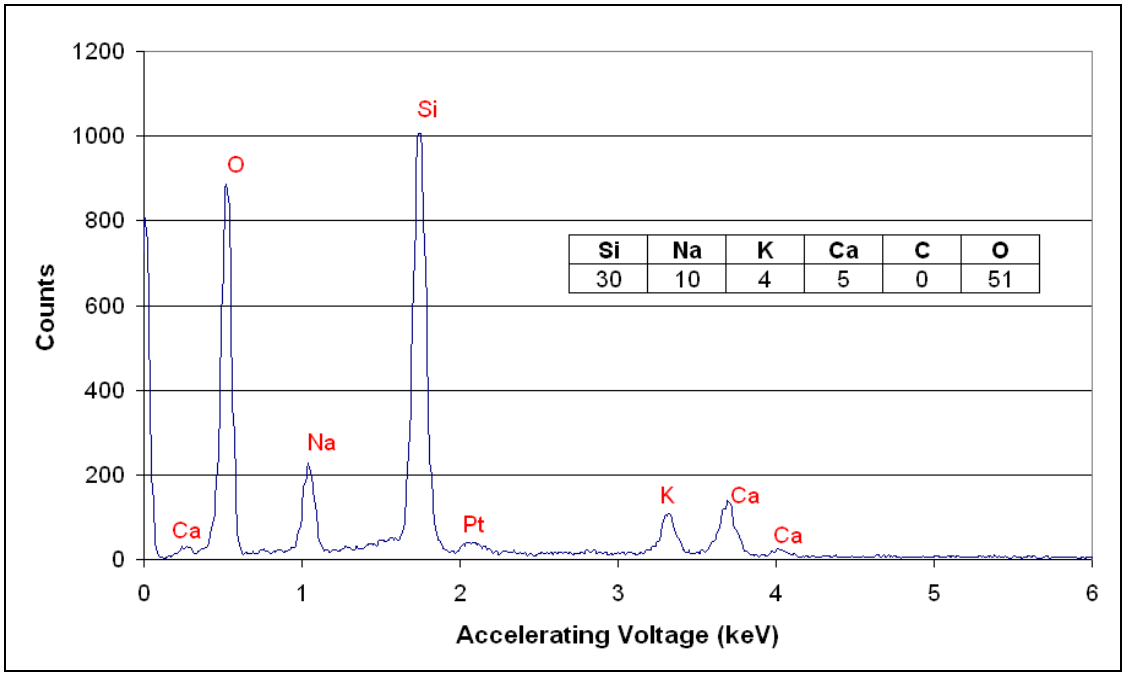

Figure 16 EDS Analysis of Gel from HL RCA

The EDS analysis confirms that the product is an ASR gel containing sodium, potassium, and calcium.

3.1.3 Asphalt Binder

The asphalt binder used in the study is a PG76-22 produced by Valero. The mixing temperature of the binder was 163°C (325°F) and the compaction temperature was 149°C (300°F).

3.1.4 Chemical Reagents

The chemical reagents used were of analytical grade. The analysis of the lot for the sodium hydroxide is presented in Table 1.

Table 1 Analysis of Lot for Sodium Hydroxide

NaOH	99%
Ca	<0.005%
Cl	<0.005%
Cu	<0.001%
Heavy Metals	<0.001%
Insoluble Matter	<0.003%
Fe	0.0001%
Mg	0.001%
Hg	<0.1ppm
Ni	0.0002%
N	<0.0003%
PO4	<0.0002%
K	0.01%
Na2CO3	0.4%
SO4	<0.0005%

The analysis of the lot for the calcium hydroxide is presented in Table 2.

Table 2 Analysis of Lot for Calcium Hydroxide

Heavy Metals (as Pb)	< 20 ppm
Magnesium and Alkali Salts	< 0.1 %

Tetraethoxysilane (TEOS) was used to create the artificial gel. The analysis of the lot for the TEOS is presented in Table 3.

Table 3 Analysis of Lot for Tetraethoxysilane

Ethanol (GC-TCD)	< 0.1 %
Purity (GC-TCD)	99.9%
Color (Pt-Co)	< 5
Chloride	< 2 ppm

3.1.5 Deicer

The deicer used was a potassium acetate solution from Cryotech, Inc. The solution is a blend of 50% potassium acetate and 50% water by weight with less than 1% proprietary corrosion inhibitors. The solution is clear and colorless with no suspended material. At 20°C, the deicer has a specific gravity of 1.28g/cm^3 and a maximum viscosity of 10cp. The deicer solution was transported and stored in five-gallon polyethylene containers.

3.2 Test Methods

A summary of the tests performed on the materials used in this study are presented in Table 4 .

Table 4 Summary of Test Methods

Material	Tests
Aggregate	Freezing and Thawing (AASHTO T 103), Gradation (AASHTO T 27/AASHTO T 11, ASTM C 136/ASTM C117), Micro Deval (AASHTO T 327, ASTM D 6928/ASTM D 7428), Petrography (ASTM C295), Dilatometer
Uncompacted HMA	Micro Calorimeter
Compacted HMA	HMA Beam Test similar to ASTM C 1293, Dilatometer, Chemistry of Soak Solution, Petrography, Lottman Test (AASHTO T 283, ASTM D 4867)

The testing for each material is applicable to both ASR-RCA and virgin aggregates. The basic concept for each test method and any differences between testing of different materials are outlined in the following sections. All equipment that was needed to perform the tests was available at TTI.

3.2.1 Gradation

The gradation of the chert samples was determined using a loss by washing (ASTM C117) and a sieve analysis (ASTM C136). These gradations were then used to create a master gradation meeting the requirements of Federal Aviation Administration

(FAA) specification P401 for use in producing asphalt specimens and for dilatometer testing. The remaining chert and the RCA samples were sieved to separate the materials into the different size fractions so that they could be recombined to meet the desired fixed gradation.

3.2.2 Dilatometer

The dilatometer is a device designed to measure the volumetric expansion of a system as a reaction occurs (*53-55*). The dilatometer consists of a stainless steel container, a brass lid, a stainless steel tower, a stainless steel float, a cap, a linear variable displacement transducer (LVDT), and a thermocouple. The set-up of the dilatometer system is presented schematically in Figure 17 .The stainless steel container has dimensions of 6 inches in both diameter and height and is used to hold the test specimen and solution. The brass lid is angled on the bottom and coated with Teflon to allow entrapped air to escape. The stainless steel tower is attached to the top of the brass lid and provides room for the float to move as the volume of the system changes. An LVDT core is attached to the top of the stainless steel float to provide measurement of volume changes. The cap is placed on top of the stainless steel tower and secures the LVDT for accurate measurement of the float's movement. The thermocouple is located inside of the dilatometer to provide accurate measurement of the system temperature.

The LVDTs and thermocouples are connected to a computer data acquisition system. Due to the low strength of the signals generated by the LVDTs and thermocouples, a signal-conditioning unit is placed between the dilatometer and the computer. The computer automatically measures the displacement and temperature at the specified time interval, which for this study was every fifteen minutes. The data are then recorded to an excel spreadsheet for data analysis.

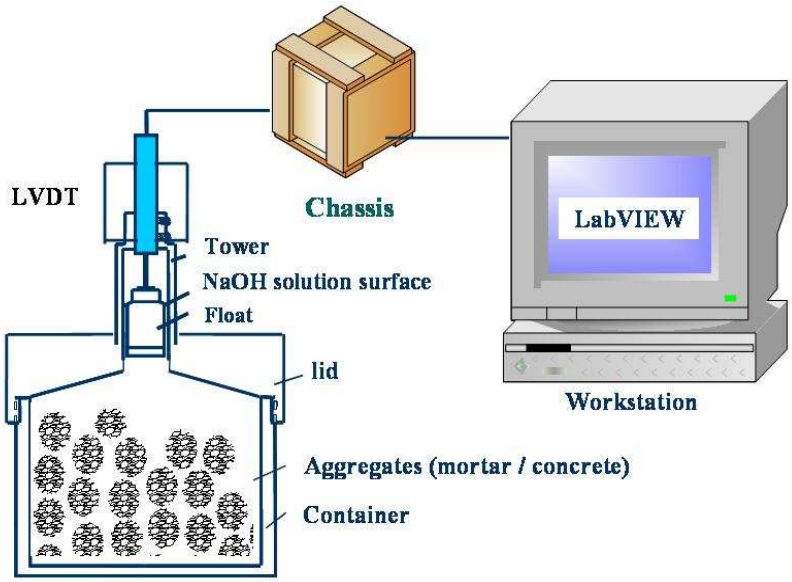

Figure 17 Schematic Representation of Dilatometer System

Except in cases where a large degree of reaction occurs, there is a downward movement of the LVDTs during the dilatometer tests, which appears to be a consequence of two phenomena. One phenomenon is a pressure build-up inside the dilatometer and the other being incomplete saturation of the sample. The pressure build-up occurs because the dilatometer is a sealed system. As the water or solution in the dilatometer vaporizes, it creates an increase in the pressure at the top of the dilatometer tower. This pressure forces some vapor to escape through the O-ring junctions. The incomplete saturation is a result of the difficulty of fully saturating a specimen, especially HMA specimens. As the specimens become more fully saturated during the dilatometer test process, the level of the solution decreases and therefore the position of the float is also decreased. To remove these effects, a test using distilled water is run in parallel with the solution tests for use as a calibration.

The dilatometer set-up process begins by soaking the test specimens in the desired test solution for approximately twelve to fifteen hours. After soaking, the dilatometers containing the specimens are placed on a vibrating table and subject to

vacuuming for approximately two hours. When this initial vacuuming is completed, the dilatometers are placed in an oven at the target test temperature to raise the specimen temperature to the target. After the specimen reaches the second temperature, the dilatometers are returned to the vibrating table and subject to vacuuming for an additional forty-five minutes at the target temperature. After the second vacuuming, the solution level is adjusted to the desired initial level and the cap and LDVT are secured in position. After all of the dilatometers are properly adjusted and placed in the oven, the data acquisition program on the computer is started. The set-up process for the dilatometer and the time required for each step are presented in Table 5 .

Table 5 Dilatometer Set-Up Process

Task	Time Required
Acquire Samples	0.5-2 hrs
Soak Samples*	~12-15 hrs
Initial Vacuum	2 hrs
Heat to Target Temperature	2-4 hrs
Second Vacuum	45 min
Adjust Solution Level	~30 min
Record Displacement	7 days

*HMA samples were not soaked

Data monitoring is conducted periodically to ensure that the data was recorded properly and that no sticking of the LVDT occurred. The data analysis begins by plotting the measured displacement for each dilatometer over time. This initial plot also helps to determine the point at which the temperature in the dilatometer stabilized. The displacement curves are then adjusted so that this initial point reads zero displacement. In order to remove the effects of incomplete saturation of the specimens and pressure build-up within the dilatometer as discussed above, the adjusted curve from a water test is subtracted from the adjusted curve of a solution test. This calibrated curve is then multiplied by the cross-sectional area of the tower and divided by the specimen volume

to calculate the percent volume change that occurred with time. A detailed dilatometer test protocol is provided in Appendix C.

Samples of loose aggregate were prepared by weighing out the desired amount of aggregate according to the HMA gradation without any mineral filler. The aggregate samples were placed in the dilatometer along with the test solution to be used. The samples were allowed to soak overnight prior to the start of the dilatometer set-up.

Samples of compacted HMA were produced using the Superpave gyratory compactor, which produces cylindrical specimens. The cylindrical specimens can be compacted to the exact height needed to produce a single specimen for each test without any cut faces with either 4-inch (10cm) or 6-inch (15cm) diameters. Since the internal diameter of the dilatometer container is approximately 6 inches, 4-inch diameter specimens were used to allow room for the solution and expansion of the samples within the dilatometer. The following describes the procedure used to fabricate HMA specimens. Sufficient aggregate to produce the desired number of samples was weighed out according to the design gradation. Crushed limestone filler was used in place of the filler from the aggregates used in the study. The aggregates were then heated overnight at 163°C (325°F) to dry them thoroughly and to ensure that they were at the proper temperature for mixing with the asphalt binder. The asphalt binder was heated at 163°C (325°F) for two hours prior to mixing with the aggregates. The aggregate was placed in a heated bucket and the asphalt binder was added in the amount necessary for the desired binder content. The aggregate and asphalt binder were thoroughly mixed and then cured at 149°C (300°F) for two hours. After curing, uncompacted samples were spread thin on a table for cooling. For compacted specimens, the proper amount of material was weighed to produce one specimen. The material was placed in the gyratory mold and then compacted to the desired density. After compaction, the specimen was removed from the mold and allowed to cool. An example of two 4-inch diameter specimens made using ED RCA with 6.0% binder content is shown in Figure 18 .

Figure 18 Superpave Gyratory 4 Inch Diameter Specimens

Some of the RCA at the top of the specimens was observed to have severely fractured during compaction. This may be partially attributed to the greater compactive effort needed for the low binder content (more than 100 gyrations) of this mixture and the high angularity and texture along with the relatively low fracture strength of the RCA. An image of one of these specimens in the dilatometer is shown in Figure 19 .

Figure 19 Superpave Gyratory Specimen in Dilatometer

The white areas visible on top of the specimen are the broken aggregates as mentioned above. The significant amount of space surrounding the specimen can also be seen in this image. The HMA specimens were not soaked overnight in order to avoid causing moisture damage prior to the start of testing.

3.2.3 Solution Analysis

The solutions from the dilatometer tests were analyzed for pH as well as sodium, calcium, and potassium concentrations. At the completion of testing, the solution from each dilatometer was poured into a large plastic beaker and thoroughly mixed to ensure homogeneity. Samples of the solution were then removed for pH and ion analysis. The pH analysis was conducted using an Accumet Excel XL-25 pH meter. The XL-25 provides pH measurements to the nearest 0.001 that are corrected for temperature. The XL-25 was calibrated using 1N sodium hydroxide solution and 0.01N sodium hydroxide solution to allow for measurement in the pH range of 12-14. Sodium hydroxide solution was used for the calibration to maintain a similar ionic environment between the calibration and the measurements to ensure accurate readings. The hydroxyl ion

concentrations were calculated from the pH of the solution using the equation presented below.

$$OH = \frac{K_W}{10^{-pH}}$$

Where OH is the concentration of hydroxyl ions in parts per million (ppm), K_w is the dissociation constant of water, and pH is the negative log of the concentration of hydrogen ions. The sodium, calcium, and potassium concentrations were measured using a Cole-Palmer flame photometer. The solution samples were filtered using Whatman filter paper to remove any particulate matter that could clog the uptake of the flame photometer. In order to measure the concentration, the solutions were diluted to have concentrations between 0.0 and 10.0 ppm. The diluted solutions were then filtered again to ensure that there were no particulates in the solution. The flame photometer was calibrated using solutions having a known concentration. The percent change in concentration for each ion type between the start of testing and the completion of testing was calculated using the equation presented below.

$$\%ION = \frac{ION_f - ION_i}{ION_i} * 100$$

Where %ION is the percentage change in concentration in the test solution of a particular ion, ION_f is the concentration in ppm of the ion in solution at the completion of testing, and ION_i is the concentration in ppm of the ion in the solution before testing was started.

3.2.4 ESEM/SEM-EDS

Microstructural evaluation of the materials and the reaction products that occurred was performed using an Electroscan Environmental Scanning Electron Microscope (ESEM) and an FEI Quanta 600 Field Emission Scanning Electron Microscope with Elemental Dispersive Spectroscopy (SEM-EDS). The ESEM offers the advantage that samples may be viewed in a more natural state as it does not require as

high of a vacuum or coating of the specimens with a conductive material. However, for materials with low conductivity, such as those used in this study, the resolution of the images is not as good as it is for the SEM. In addition, the ESEM in the Texas A&M EM Center does not have EDS capabilities and therefore cannot provide the elemental composition of the specimen. The SEM requires that non-conductive specimens be coated with a conductive material, which for this study was a platinum-palladium alloy. In addition, because of the high vacuum requirements of the SEM, the samples must be thoroughly dried to prevent moisture from the specimen from reducing the vacuum. The EDS capabilities of the SEM allow for analysis of elemental composition of points on the surface of the specimen. This is particularly useful for determining if deposits on the surface of a specimen have the composition of an ASR gel.

3.2.5 Modified Beam

A beam test based on ASTM C 1293 was performed for this study. An asphalt beam was fabricated using the linear kneading slab compactor. The finished dimensions of this beam were eighteen inches by six inches by three inches. The beam was cut to a length of 11 ¼ inches and then in half lengthwise to create two beams with cross-sections of approximately three inches by three inches. Holes were then drilled in the ends of these beams for mounting of the measurement studs. The measurement studs were mounted using a marine grade epoxy to resist the effects of the alkaline solution. An example of the measuring stud mounted in the trial beam is presented in Figure 20.

Figure 20 Measuring Stud Mounted in the End of Sample Beam

The beams were placed in a water bath at 60°C for approximately twenty-four hours to saturate them and reach the target temperature. After an initial measurement was made, the beams were placed in a 0.5N NaOH solution saturated with $Ca(OH)_2$ and periodic length change measurements were made.

3.2.6 Lottman

The Lottman test (AASHTO T 283) is intended to indicate the moisture sensitivity of an asphalt mixture. It consists of comparing the indirect tensile strength of specimens conditioned in water at 60°C for 24 hours to the strength of dry specimens. For this study, additional testing was performed on specimens conditioned in 0.5N NaOH solution at 60°C for 24 hours and 6.5 days and in water at 60°C for 6.5 days. Higher ratios of indirect tensile strength indicate a lower susceptibility to moisture damage with most agencies requiring a minimum ratio of 70%.

3.2.7 Micro Calorimeter

The micro calorimeter measures the total energy of adhesion between an aggregate and asphalt binder. The test is performed on a sample of aggregate between 150µm and 75µm (No. 100 to No. 200) which has been washed and dried. The asphalt

binder is dissolved in toluene to allow for testing at ambient temperatures. It has been shown that a solution of asphalt binder in toluene does not compromise the physio-chemical properties of the asphalt binder (*56-57*). The solution was prepared by dissolving 1.5g of asphalt binder in 11mL of toluene and allowing the solution to sit for 12-24 hours. The reaction cells used for the micro calorimeter tests were glass vials having open top plastic lids with a PTFE-silicon septa to maintain an airtight seal. Approximately eight grams of material was placed in each vial for testing. These vials, along with an equal number of empty vials used for reference cells, were subject to vacuum at 150°C for three hours. After vacuuming, the vials were allowed to return to room temperature. A vial containing a sample and an empty reference cell were then placed in the micro calorimeter along with two syringes per vial containing 2mL of asphalt-toluene solution each. The heat flow between the two vials was allowed to reach equilibrium and then the solution was injected into the vials. The computer system records the heat flow between the two vials. After the heat flow returns to equilibrium, the software calculates the area under the time-heat flow curve to determine the total energy of adhesion between the asphalt binder and the aggregate.

3.2.8 Differential Scanning Calorimeter / Thermogravimetric Analysis

The Differential Scanning Calorimeter (DSC) was used to characterize the changes that occur in ASR gel upon heating. The DSC measures the heat flow into or out of the specimen as the temperature is changed. The DSC was equipped with a Thermogravimetric Analyzer (TGA) that measured the mass change of the specimen as the temperature changed. Samples of approximately 100mg were heated from 30°C (86°F) to 1000°C (1832°F) at a rate of 5°C (9°F) per minute.

3.2.9 X-Ray Diffraction

X-ray diffraction (XRD) was used to aid in determining if ASR gel preferentially concentrates to the finer fractions of the ASR-RCA. Samples of the filler fraction (minus 75µm/No. 200) from each RCA were ground to a powder smaller than 45µm (No. 325 sieve) using a mortar and pestle. These samples were then tested in the XRD

to determine the mineral components and the presence of any amorphous materials (especially ASR gel).

3.2.10 Micro-Deval

The Micro-Deval test measures the mass loss of an aggregate sample abraded by steel balls in the presence of water inside a steel drum. The test was performed on samples of both coarse (ASTM D6928) and fine aggregate (ASTM D7428). It is anticipated that ASR-RCA will show greater Micro Deval mass loss than the virgin unreacted aggregate. The higher loss can be correlated with poor mechanical performance (*58-60*).

3.2.11 Freeze-Thaw

The freeze-thaw test (AASHTO T 103) measures the mass loss of aggregate specimens subjected to a specified number of freezing and thawing cycles. The freeze-thaw test was selected instead of the sulfate soundness test (ASTM C88) to avoid issues with sulfate attack on the mortar fractions of the RCA. The ASR-RCAs were tested using this method, with results from virgin aggregates serving as controls. It is expected that ASR-RCA's will have greater mass loss due to higher porosity and lower strength of these RCA.

4. RESULTS AND DISCUSSION

The results of the tests performed on aggregate and HMA specimens and the implications of those results on the use of ASR-RCA in HMA are discussed in the following section.

4.1 Asphalt Mixture Designs

Two different gradations were used in this project. One is a dense-graded HMA meeting the gradation requirements of Federal Aviation Administration specification P401. This gradation is intended to be typical of those used to construct the majority of asphalt pavements. The percentages passing the standard sieve sizes of the P401 gradation are presented in Table 6.

Table 6 Gradation for P401 Specification

Sieve (mm)	Sieve	% Passing	Specification
25	1	100.0	100 Max
19	3/4	95.7	76 - 98
12.5	1/2	75.5	66 - 86
9.5	3/8	59.4	57 - 77
4.75	4	43.5	40 - 60
2.36	8	31.6	26 - 46
1.18	16	20.7	17 - 37
0.600	30	11.8	11 - 27
0.300	50	7.5	7 - 19
0.150	100	6.5	6 - 16
0.075	200	3.2	3 - 6

The P401 gradation and the specifications are graphically presented on a 0.45 power chart in Figure 21.

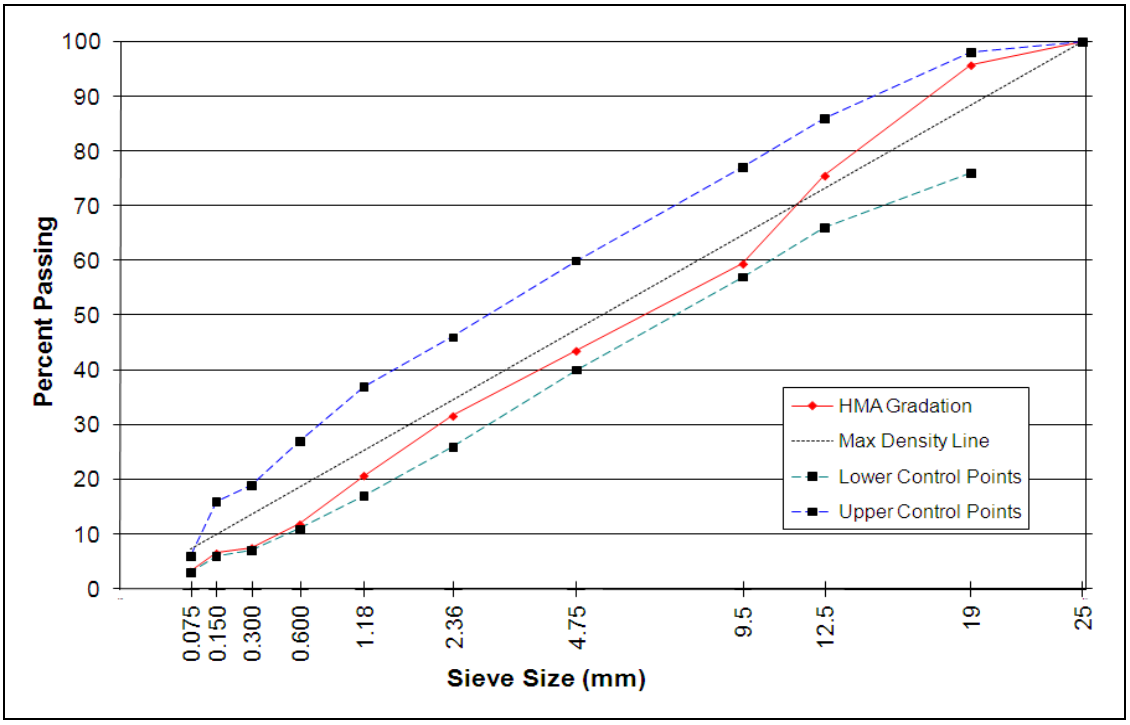

Figure 21 P401 Gradation Plotted on a 0.45 Power Chart

This was the primary gradation used for the dilatometer testing and Lottman testing. Two different binder contents representing thick and thin films of asphalt binder were selected for each material. For the virgin chert aggregate, the two binder contents were 4.0% and 6.5% by weight of the mix. For the RCAs, the higher absorption required higher binder contents so 6.0% and 8.0% by weight of the mix were selected.

The second is an SMA gradation meeting the requirements of the Unified Facilities Guide Specifications (UFGS) 32.13.17. This mix was selected primarily for use in the beam test to provide greater stone to stone contact so that expansion of the aggregates (if any) would be more likely to be transmitted to the ends of the beam rather than absorbed by the asphalt mastics. The percentages passing the standard sieve sizes of the SMA gradation are presented in Table 7.

Table 7 Gradation for UFGS 32.13.17 Specification

Sieve (mm)	Sieve	% Passing	Specification
19	3/4	100.0	100 Max
12.5	1/2	95.0	90 - 100
9.5	3/8	68.0	50 - 85
4.75	4	30.0	20 - 40
2.36	8	22.0	16 - 28
1.18	16	18.0	-
0.600	30	16.0	-
0.300	50	14.0	-
0.150	100	12.0	-
0.075	200	10.0	8 - 11

The SMA gradation and the specifications are graphically presented on a 0.45 power chart in Figure 22.

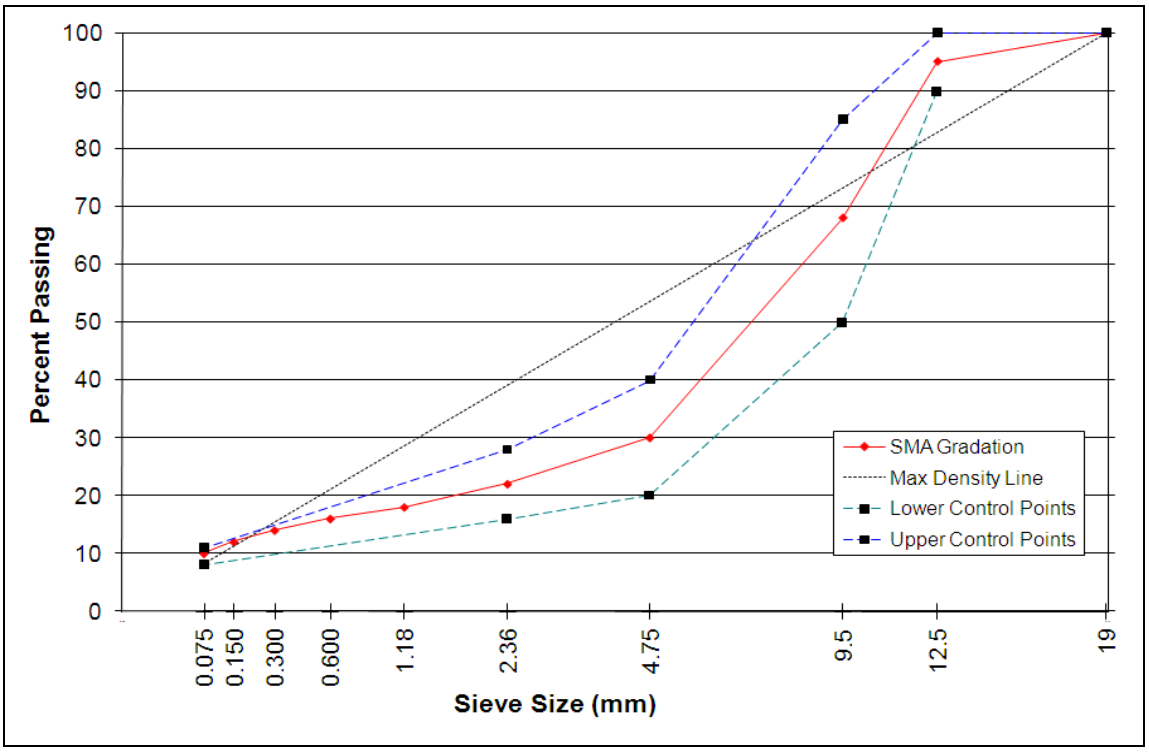

Figure 22 SMA Gradation Plotted on a 0.45 Power Chart

The SMA gradation was used to construct the beams. A binder content of 6.5% was used for the SMA gradation.

4.2 Dilatometer Test Results

Dilatometer testing was performed on the virgin chert aggregate and HMA specimens made using chert as controls to understand better the reaction mechanisms that occur during the test. These tests were performed using NaOH solution of different concentrations, 1N as well as 0.5N, saturated with $Ca(OH)_2$ [CH]. Similarly, the ASR-RCAs alone and HMA specimens made with the ASR-RCAs were also tested in the dilatometer using NaOH solution saturated with CH. Additional testing of the ED RCA was performed using potassium acetate deicer solution. The dilatometer test results are presented and discussed below.

4.2.1 Virgin Aggregate Tests

Preliminary dilatometer tests were performed at 70°C and (1N NaOH + CH) solution using virgin chert specimens as well as uncompacted HMA made using chert. Due to severe asphalt stripping of the uncompacted HMA specimens under these conditions (discussed later), the majority of the subsequent dilatometer tests were performed at 60°C and 0.5N NaOH + CH solution in order to reduce the amount of stripping that occurred. Additional testing of chert specimens was performed at 60°C and 1N NaOH + CH solution to understand the role of alkalinity at constant temperature. The expansion results of the dilatometer tests of the virgin chert specimens at these different temperatures and solution alkalinities are presented in Figure 23.

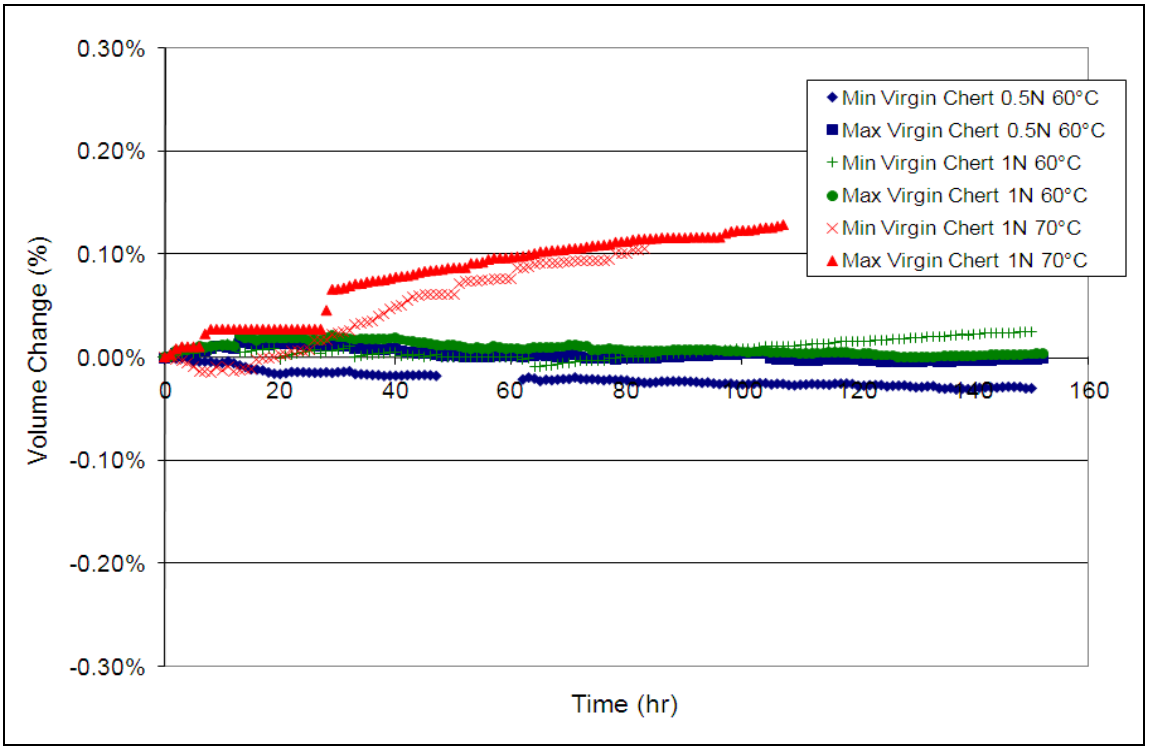

Figure 23 Percentage Volume Change of Virgin Chert Specimens Tested in 1N NaOH+CH and 0.5N NaOH+CH at 60°C and 70°C

The bands shown in Figure 23 represent the range of percentage volume-change results that were obtained for each of the three test conditions described earlier. The results show that the reactivity of chert increases with increasing solution normality and test temperature, as expected. At 60°C and 0.5N NaOH + CH, the primary test condition, a slight decrease in volume to a very small increase was measured during the testing period, approximately 6 days. Only small amounts of product (ASR gel) were observed during this time period on the surface of chert specimens (discussed later under detailed microstructure study). This indicates a very slow reactive nature of the chert specimens at the primary test conditions, i.e., 0.5 NaOH +CH and 60°C. At 1N NaOH + CH and 60°C, the chert demonstrates a small increase in volume during the test period. It seems that the increase in alkalinity, from 0.5N to 1N NaOH, has little effect on the degree of expansion at 60°C. However, when the temperature is increased to 70°C, the volumetric expansion increases substantially at 1N NaOH + CH. Therefore, thermal

activation dominates the alkaline activation for ASR in the particular chert studied. The solution analysis for these tests is presented in Figure 24 and Figure 25.

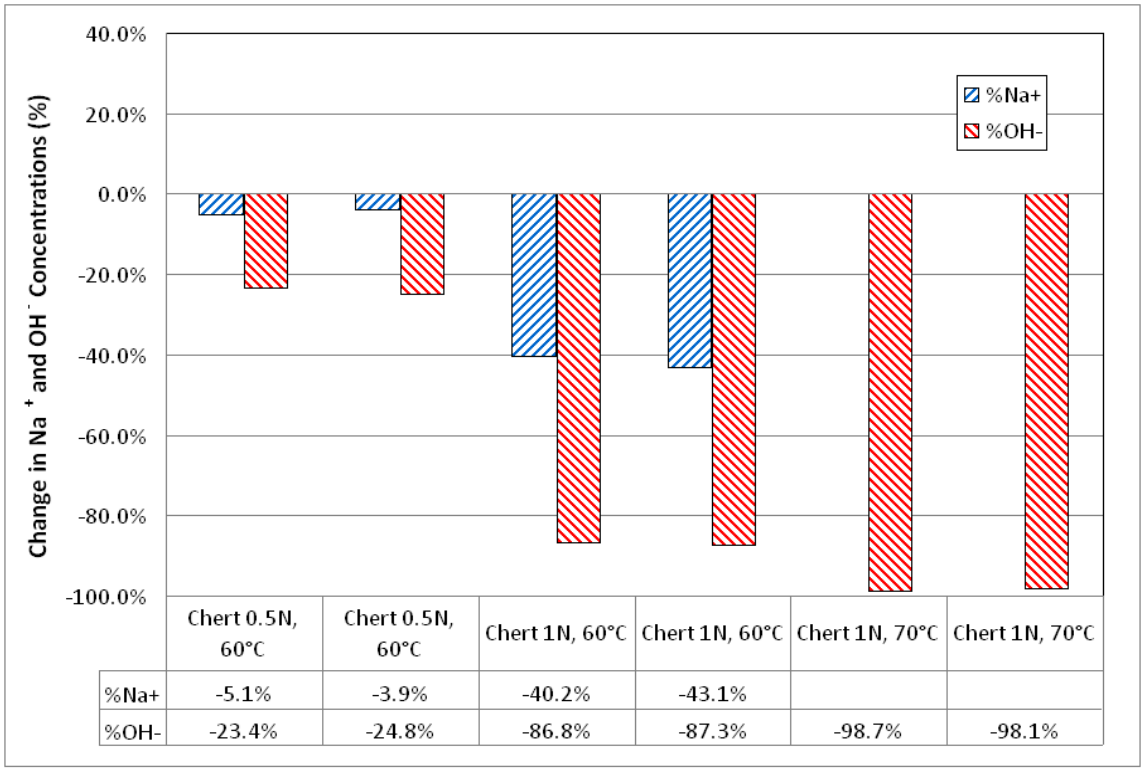

Figure 24 Percentage Change in Na^+ and OH^- Concentrations for Virgin Chert Specimens Tested in 1N NaOH+CH and 0.5N NaOH+CH at 60°C and 70°C

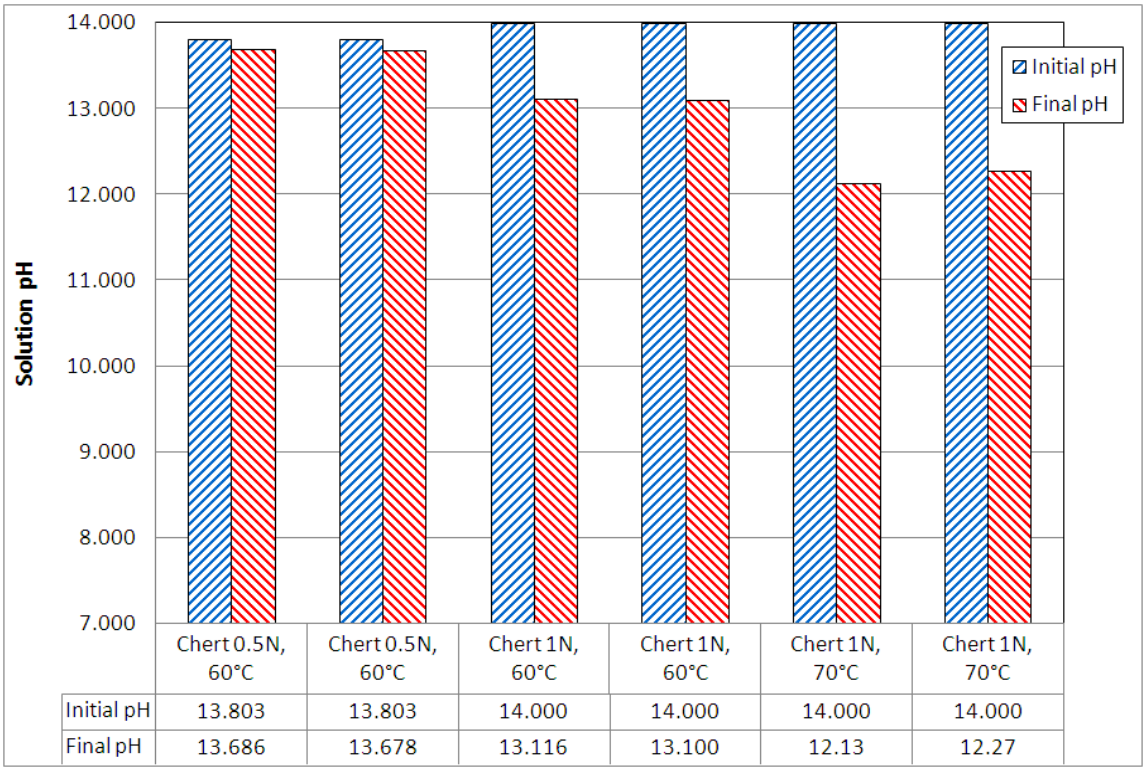

	Chert 0.5N, 60°C	Chert 0.5N, 60°C	Chert 1N, 60°C	Chert 1N, 60°C	Chert 1N, 70°C	Chert 1N, 70°C
Initial pH	13.803	13.803	14.000	14.000	14.000	14.000
Final pH	13.686	13.678	13.116	13.100	12.13	12.27

Figure 25 Comparison of Solution pH for Virgin Chert Specimens Tested in 1N NaOH+CH and 0.5N NaOH+CH at 60°C and 70°C

The very little percent reduction of both Na^+ and OH^- / pH at 60°C and 0.5N NaOH + CH presented in Figure 24 Figure 25 indicate that very little reaction occurred in the primary test conditions. On the other hand, significant reduction of both Na^+ and OH^- / pH was noticed at 1N NaOH + CH and 70°C, which supports the high expansion measured at these test conditions as presented in Figure 23. Therefore, the degree of reaction predicted from test solution chemistry and volume-change results support each other. Based on the observations of the volume expansion, solution analysis, and microstructural study as discussed later, it can be concluded that the studied chert is very slowly reactive at 0.5N NaOH + CH and 60°C.

4.2.2 Compacted HMA Made with Virgin Aggregate Tests

The expansion over time for the compacted HMA specimens made using chert (P 401 gradation, Figure 21) was measured at the primary test conditions and was compared with the results of the virgin chert tests in Figure 26.

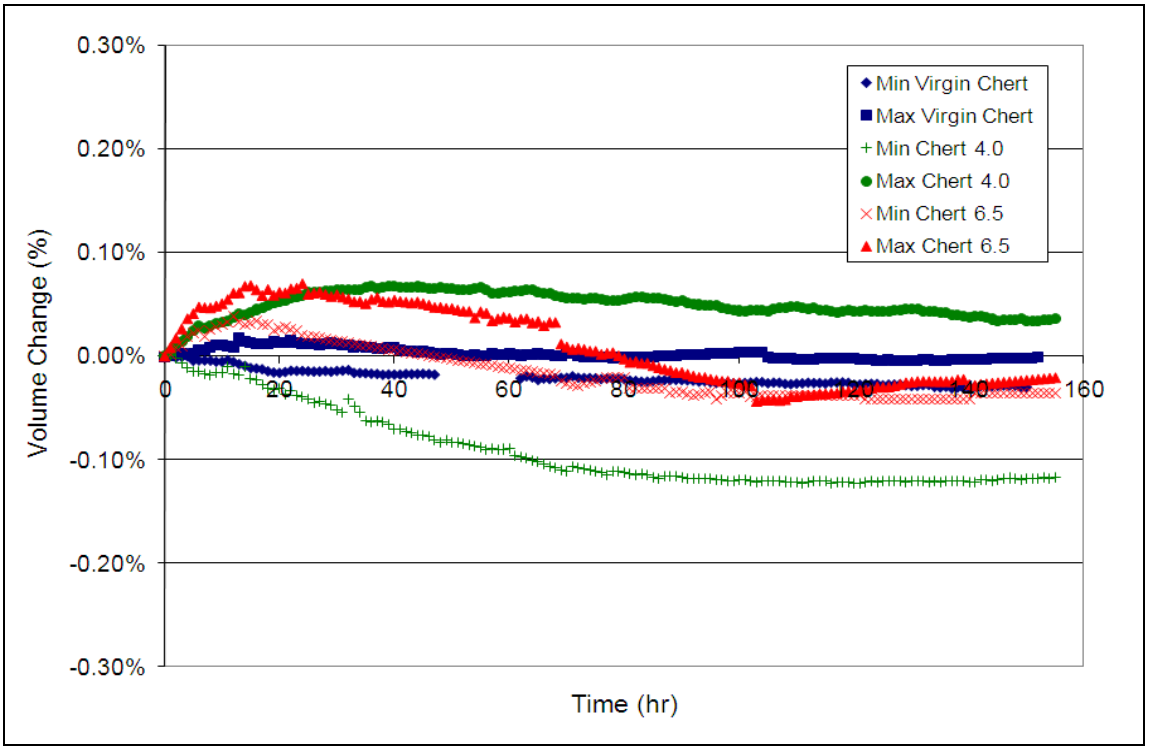

Figure 26 Percentage Volume Change of Virgin Chert and Compacted HMA Chert Specimens Tested in 0.5N NaOH+CH at 60°C

The results of the compacted HMA specimens form bands around the band of the virgin chert specimens. Since the test conditions were determined to be mild, as far as ASR is concerned (discussed earlier), the greater volume changes must be due to an interaction between the NaOH solution and the asphalt binder. In support of the observation that an interaction is occurring between the asphalt binder and the solution, the compacted HMA specimens were observed to feel significantly softer after testing and had a tendency to crack during handling. In general, a slight swelling is observed

until 60 hours, if the downward movement is assumed to be due to “error of inequality” during calibration (described below). This swelling of the HMA is believed to be due to the chemical interaction between the asphalt binder and the alkaline solution.

The use of the displacement curve of water-aggregate/HMA test to calibrate the displacement of solution-aggregate/HMA test (described earlier) was based on the assumption that the processes of vapor-solution equilibrium within the dilatometer tower and incomplete saturation of the samples were occurring in a similar way for both the water and solution tests. However, if these processes were not equivalent in both cases, or if other processes were occurring in one of the tests, errors would have been introduced in the calibration process. These errors could account for the decrease in volume measured for some of the HMA tests. The results of the Lottman test, as presented later, clearly indicate that the NaOH solution caused more damage to the specimens than the water alone. This increased damage could have been caused by two different processes that occurred at higher rates within the NaOH solution tests than in the water tests.

The first process is the absorption of moisture by the aggregates within the HMA. A diagram of this phenomenon is presented in Figure 27 .

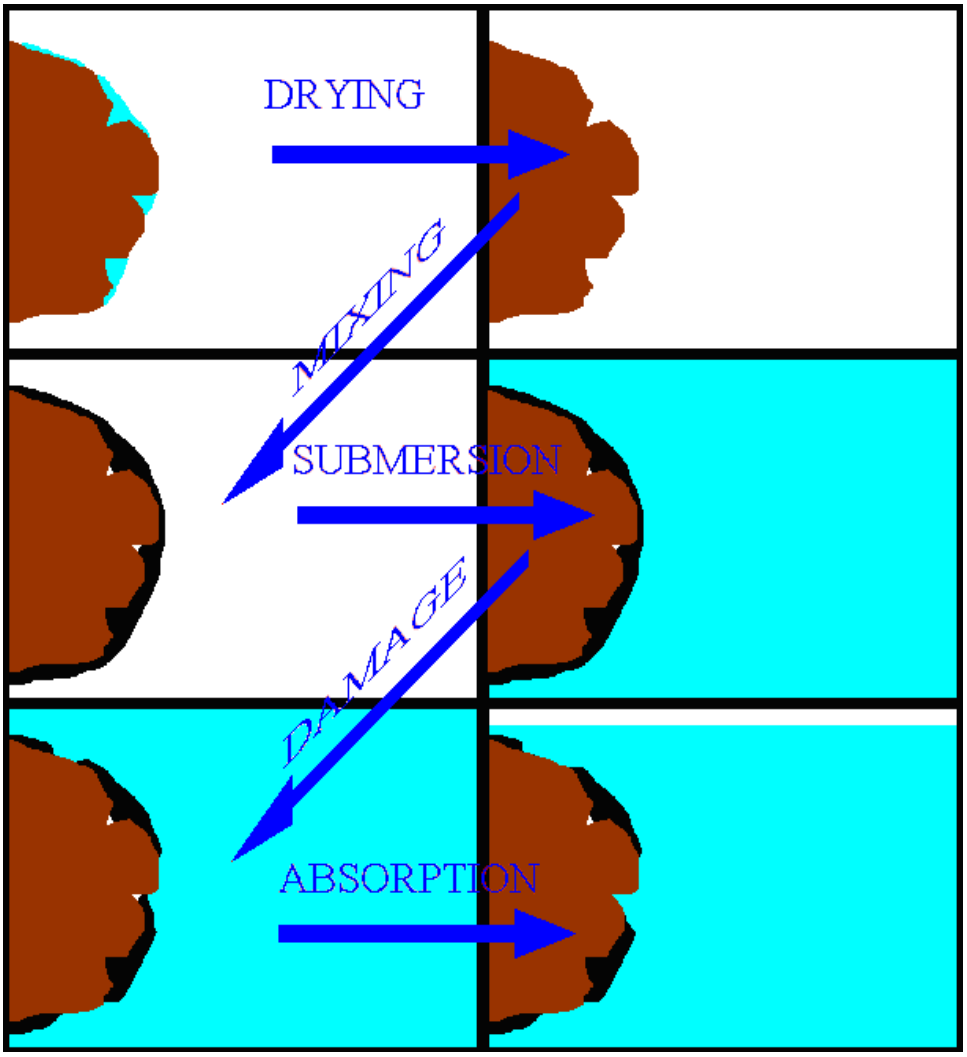

Figure 27 Diagram of Asphalt Binder Stripping and Moisture Absorption by Aggregate

The aggregates were dried overnight in an oven at 163°C (325°F) prior to mixing with the asphalt binder, which provides a protective coating against moisture. If the water or NaOH solution strips the binder from the aggregate, the dry aggregates will be able to absorb moisture from the water or solution causing an apparent drop in the measured solution volume. This would be especially true for the highly absorptive RCAs. Since the NaOH solution causes more damage than the water, more aggregate would be exposed to the solution resulting in a greater apparent decrease in the NaOH solution level than the water level.

The second process is the opening of previously inaccessible voids. A diagram of this phenomenon is presented in Figure 28.

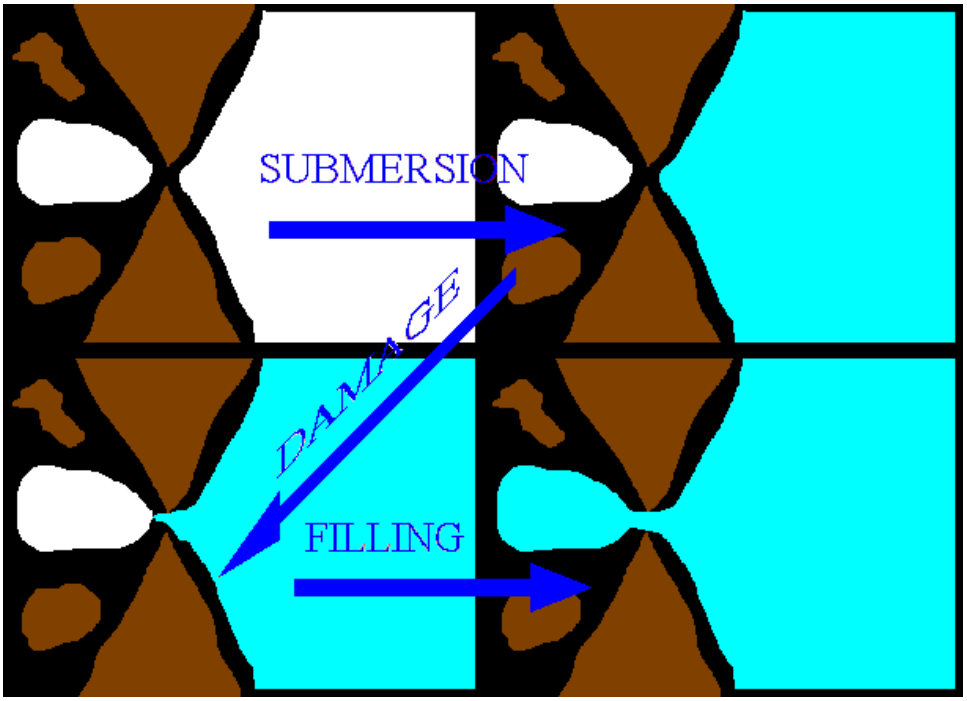

Figure 28 Diagram of Filling of Inaccessible Void

The process of compacting the HMA specimens, using dry aggregate and asphalt binder, sealed off some voids from the exterior of the specimen. When the specimens were immersed in water or the NaOH solution, these voids would have been inaccessible to the water/solution. Only a thin film of asphalt binder may have separated some of these voids from the water/solution. As the water or solution damaged the specimen, the thin film would be removed and create an opening into the previously inaccessible void. Water/solution would then enter the void resulting in an apparent drop in solution level. Since the NaOH solution caused more damage than water, more voids would have been opened by this phenomenon resulting in a greater decrease in the NaOH solution level than the water level.

If the downward movement (Figure 26) is believed to be due to error of inequality during calibration (discussed above), then the upward movement (majority) is swelling from binder-solution interaction (i.e., saponification, described later). The solution chemistry change should support this chemical reaction.

Examples of the appearance of the test solutions from low and high binder content compacted HMA specimens made with chert tested in 0.5N NaOH+CH and water are presented in Figure 29.

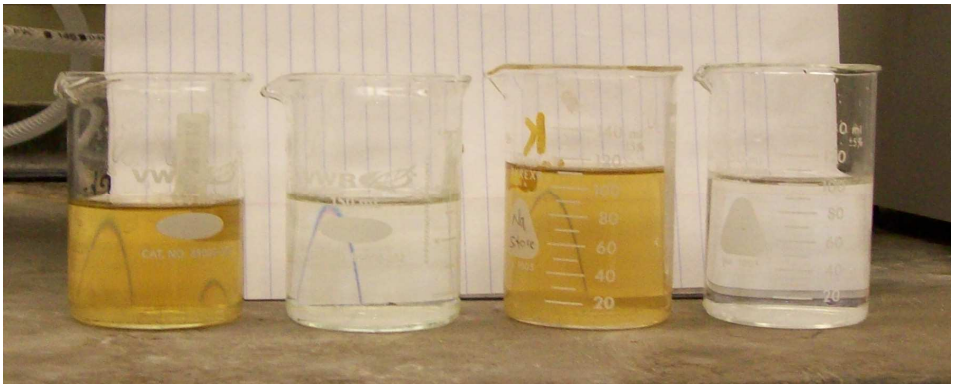

Figure 29 Water and Solution Samples from Compacted HMA Made with Chert Tested in 0.5N NaOH+CH (L to R: 4.0% Binder in NaOH, 4.0% Binder in Water, 6.5% Binder in NaOH, 6.5% Binder in Water)

The NaOH+CH solution was originally a clear solution but after testing, turned a yellowish-brown color. This color is likely due to the presence of some fraction of the asphalt binder in the solution. Color changes of this nature were not observed when testing aggregate specimens alone. The solution analysis for these tests is presented in Figure 30 and Figure 31.

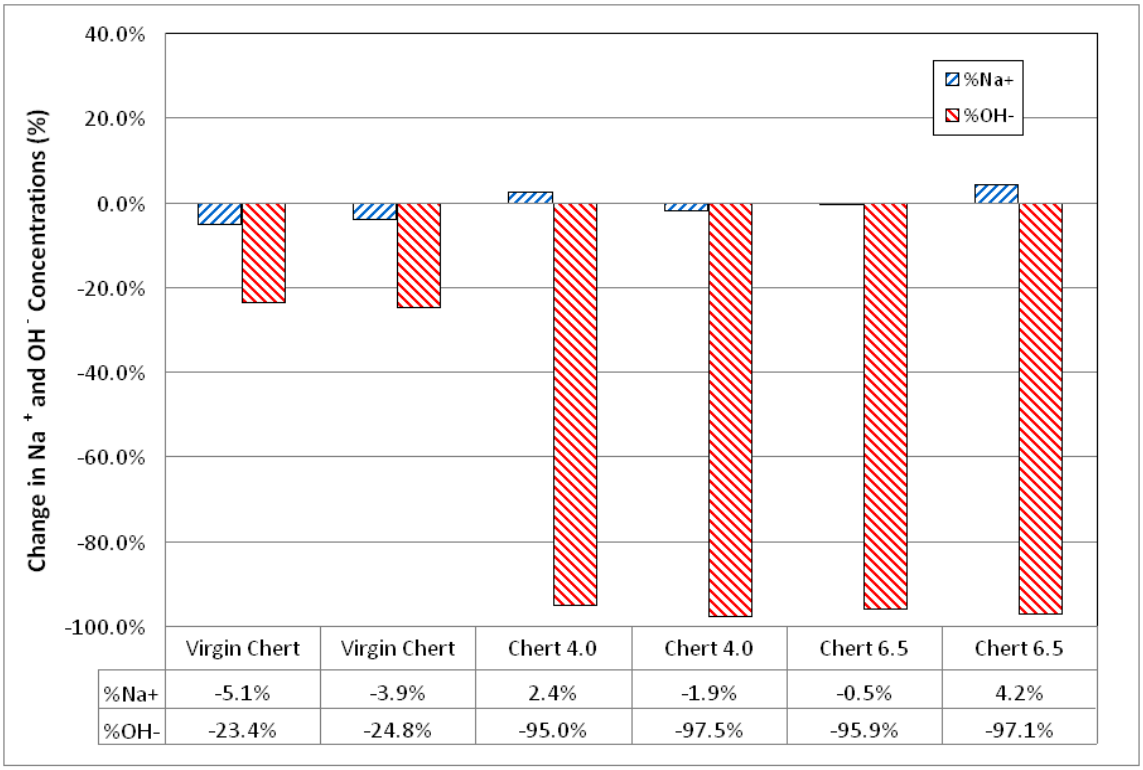

Figure 30 Percentage Change in Na^+ and OH^- Concentrations for Virgin Chert and Compacted HMA Chert Specimens Tested in 0.5N NaOH+CH at 60°C

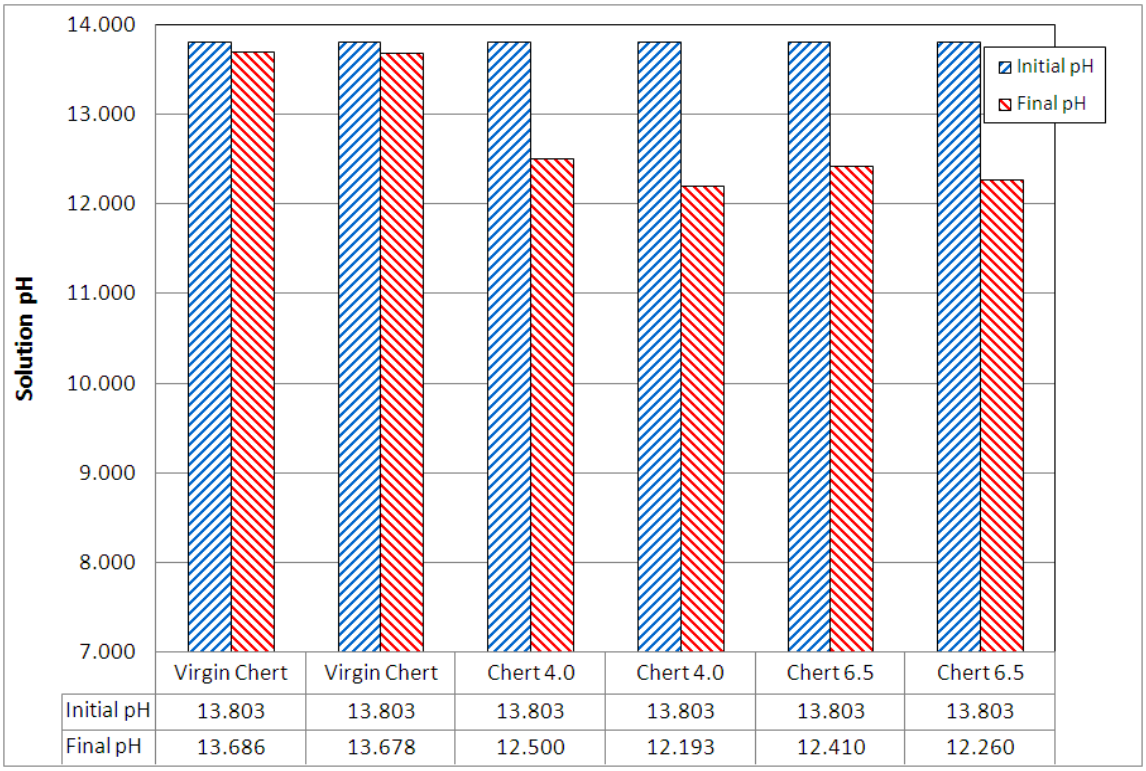

	Virgin Chert	Virgin Chert	Chert 4.0	Chert 4.0	Chert 6.5	Chert 6.5
Initial pH	13.803	13.803	13.803	13.803	13.803	13.803
Final pH	13.686	13.678	12.500	12.193	12.410	12.260

Figure 31 Comparison of Solution pH for Virgin Chert and Compacted HMA Chert Specimens Tested in 0.5N NaOH+CH at 60°C

The solution from the compacted HMA specimens exhibited relatively large decreases in pH / hydroxyl ions but very little decrease in sodium. For ASR to have occurred, decreases of both Na and OH ions with similar magnitudes would be expected. This indicates that the reaction that occurred was primarily between the asphalt binder and the test solution. The swelling observed was likely due to a saponification reaction between the asphalt binder and the solution (described later in detail). Similar expansion results were observed for the chert specimens tested in 1N NaOH+CH at 60°C, as presented in Figure 32.

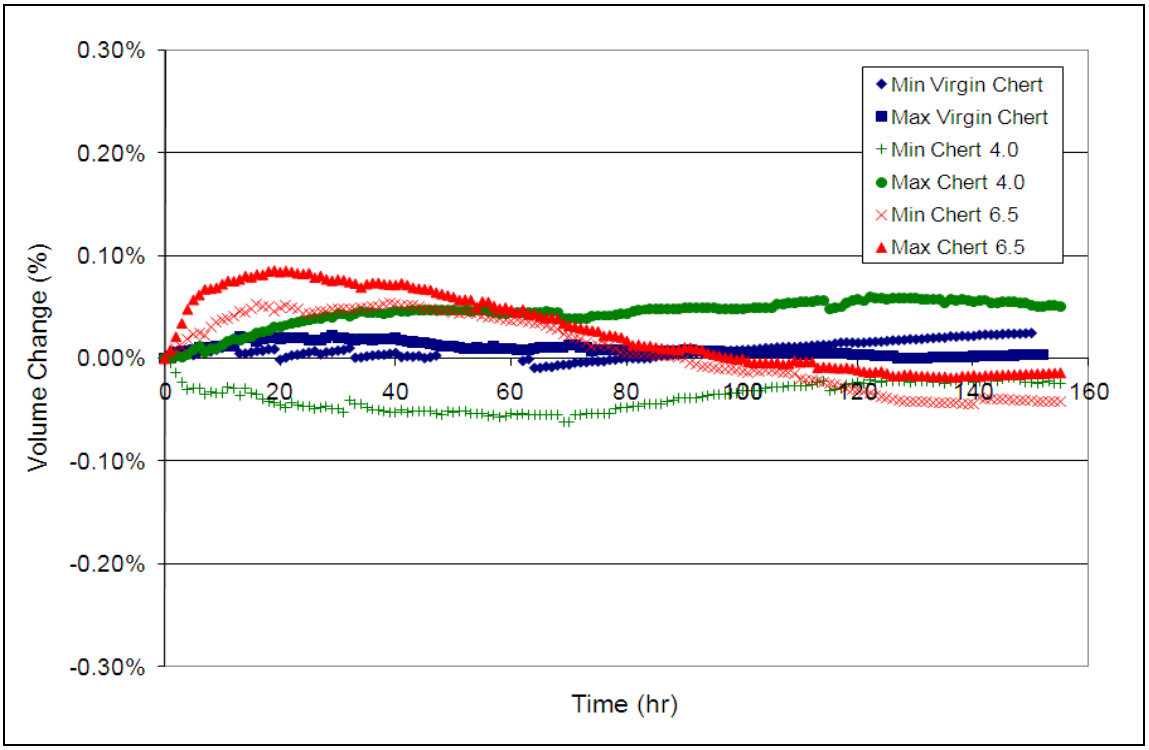

Figure 32 Percentage Volume Change of Virgin Chert and Compacted HMA Chert Specimens Tested in 1N NaOH+CH at 60°C

The results for compacted HMA tested in 1N NaOH+CH have similar trends and magnitudes of volume change to those of the 0.5N NaOH+CH results. If the volume change was due to ASR, the compacted HMA results would have greater expansion with 1N NaOH+CH than with 0.5N NaOH+CH as observed for the virgin aggregate alone. Since the trends and magnitudes of volume change for both solutions are similar, the swelling is likely due to the solution-binder interaction. The softening observed in these compacted HMA specimens was much greater than that for the 0.5N NaOH+CH tests, as the specimens tested in 1N NaOH+CH solution were partially collapsed at the completion of testing. An example of this along with examples of specimens tested in 0.5N NaOH+CH solution and water are presented in Figure 33.

a **b** **c**

Figure 33 (a) Collapsed Chert HMA Specimen at Completion of Testing at 60°C Using 1N NaOH+CH (b) Chert HMA Specimen Tested in Water at 60°C (c) Chert HMA Specimen Tested in 0.5N NaOH+CH at 60°C

The solution analysis for these tests is presented in Figure 34 and Figure 35.

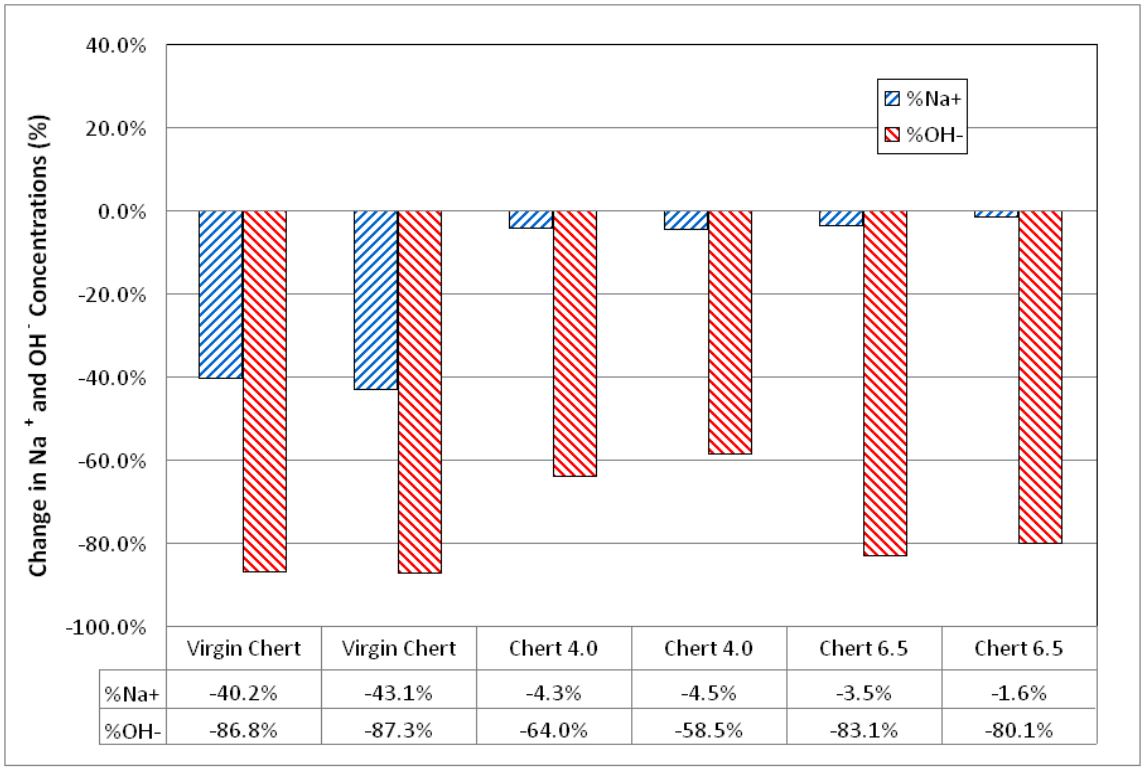

	Virgin Chert	Virgin Chert	Chert 4.0	Chert 4.0	Chert 6.5	Chert 6.5
%Na+	-40.2%	-43.1%	-4.3%	-4.5%	-3.5%	-1.6%
%OH-	-86.8%	-87.3%	-64.0%	-58.5%	-83.1%	-80.1%

Figure 34 Percentage Change in Na^+ and OH^- Concentrations for Virgin Chert and Compacted HMA Chert Specimens Tested in 1N NaOH+CH at 60°C

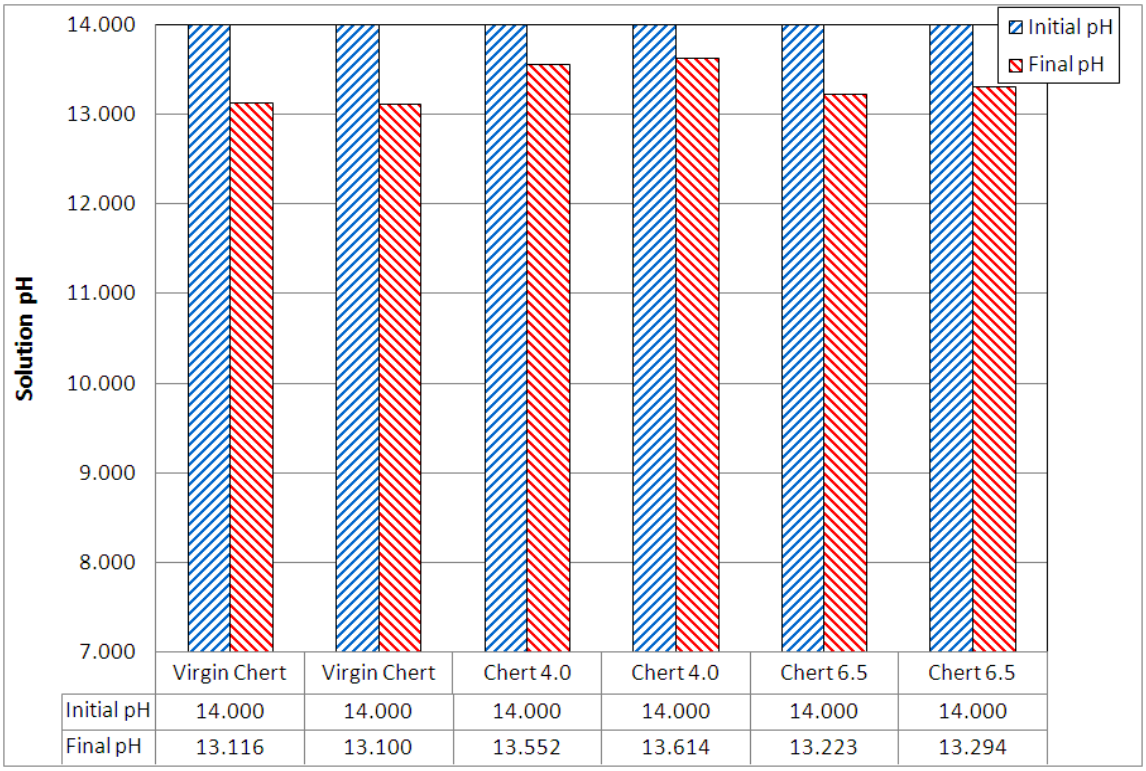

Figure 35 Comparison of Solution pH for Virgin Chert and Compacted HMA Chert Specimens Tested in 1N NaOH+CH at 60°C

Again, the solution for the compacted HMA specimens shows large decreases in hydroxyl ions but very little change in sodium ions. Combined with the observed softening of the binder, the decrease in hydroxyl, and very little change in sodium, appears to confirm that the reaction is primarily occurring between the asphalt binder and the solution. This is helpful for interpreting the volume change results of the tests of chert specimens tested at 70°C and 1N NaOH+CH, as presented in Figure 36.

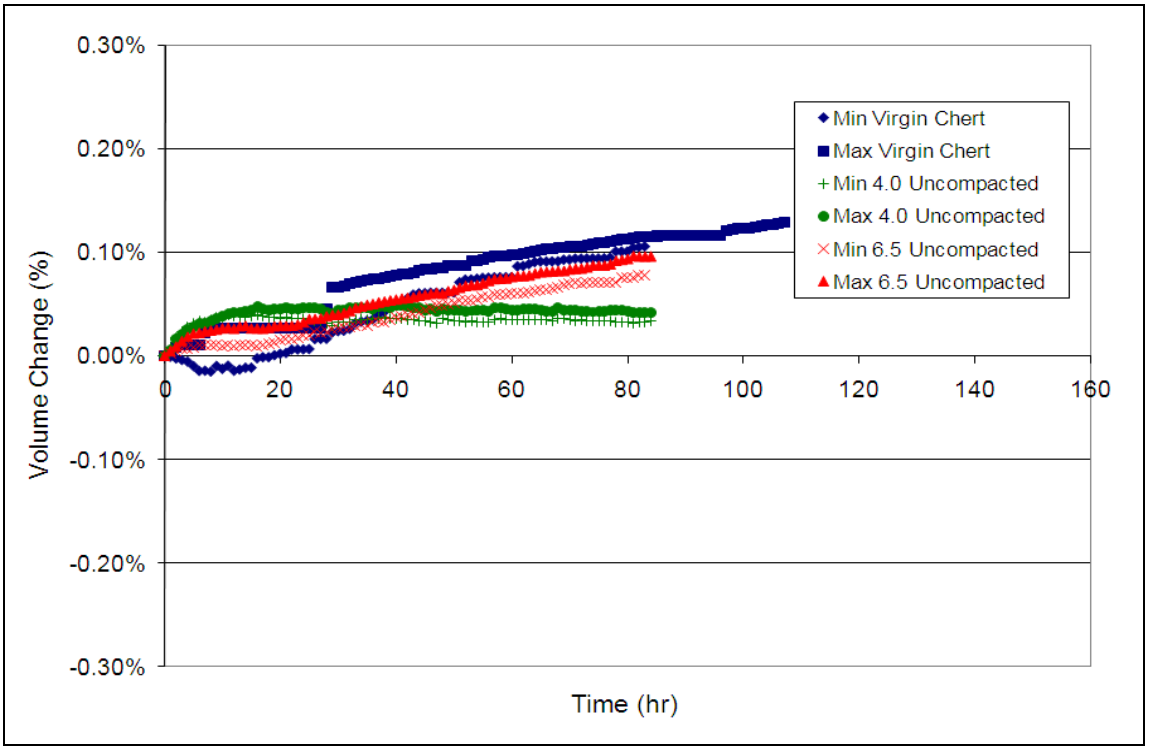

Figure 36 Percentage Volume Change of Virgin Chert and Uncompacted HMA Made with Chert Tested in 1N NaOH+CH at 70°C

These tests were the preliminary tests used to determine the desired test conditions for the dilatometer test program (mentioned earlier). The initial tests of HMA were performed on uncompacted specimens, so the degree of stripping is greater than if compacted specimens had been used. The asphalt binder appears to provide some protection against ASR during the test period as the bands for both the high and low binder contents lie below that of the virgin chert specimens (without binder). A large degree of stripping of the asphalt binder was observed in both sets of HMA specimens at the end of the test period. An example of this is presented in Figure 37.

Figure 37 Severe Stripping of Uncompacted HMA at Conclusion of Dilatometer Test

The aggregate shown in Figure 37 is typical of the aggregates observed at the completion of dilatometer testing of uncompacted HMA in 1N NaOH+CH at 70°C. This severe stripping made the majority of the aggregate surfaces available for ASR. Since it is a closed system, it is not known if the majority of the stripping occurred during the set-up of the dilatometers or after data collection began. As such, some of the observed volume change for the HMA specimens may be due to the binder-solution interaction, as discussed earlier, and therefore the protective nature of the binder may be greater than is apparent from the volume change results. The volume change results of the low binder content compacted HMA made using chert are presented in Figure 38.

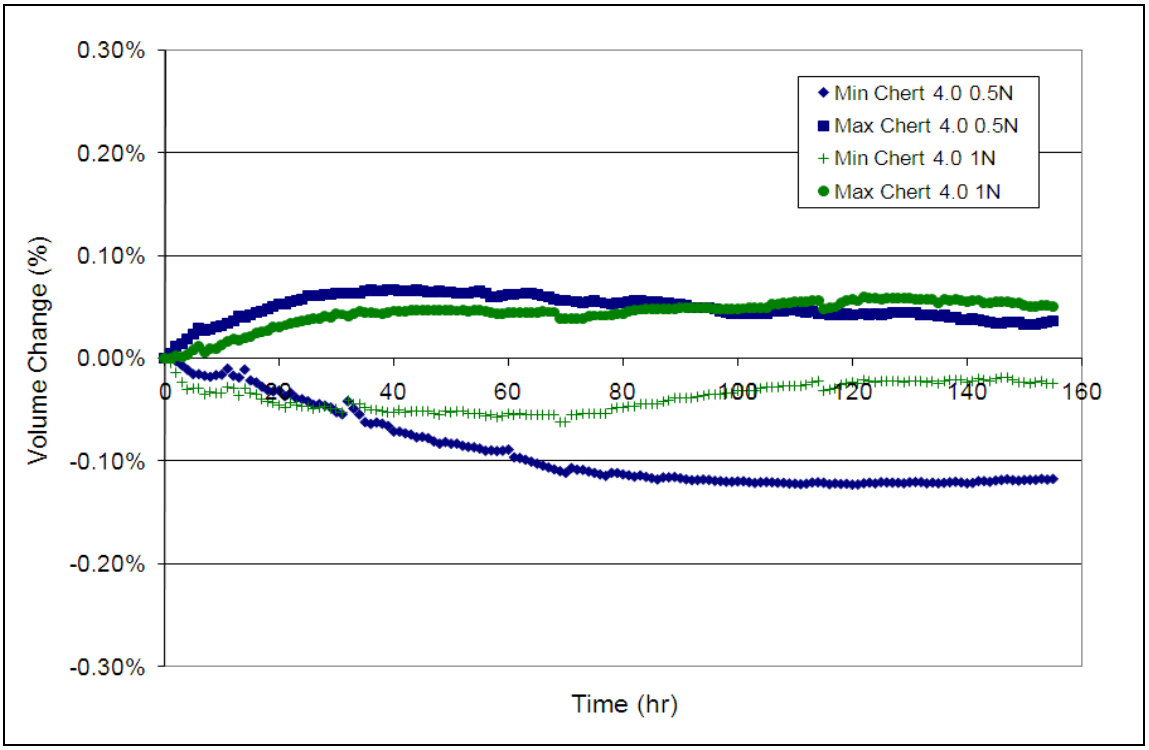

Figure 38 Percentage Volume Change of Low Binder Content HMA Specimens Made with Chert Tested in 0.5N NaOH+CH and 1N NaOH+CH at 60°C

The results for both 0.5N and 1N test solutions yielded similar trends and magnitudes of volume change. Since 1N solution produced greater expansion due to ASR than 0.5N solution (from aggregate alone tests presented earlier), if ASR was occurring in the compacted HMA specimens, then the 1N results should be slightly higher than the 0.5N results. Since the results for both are similar, the reaction that is occurring to produce a volume change is likely due to an interaction between the solution and the binder. The solution analysis from these tests is presented in Figure 39 and Figure 40.

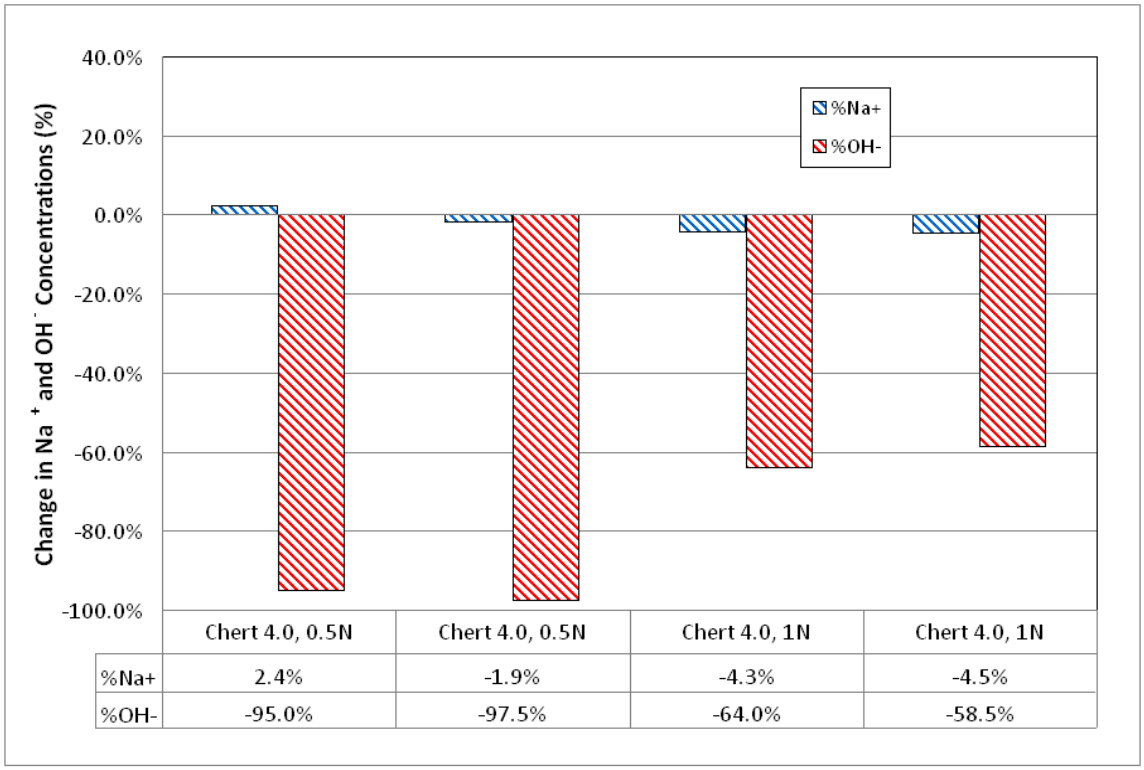

Figure 39 Percentage Change in Na^+ and OH^- Concentrations for Low Binder Content HMA Specimens Made with Chert Tested in 0.5N NaOH+CH and 1N NaOH+CH at 60°C

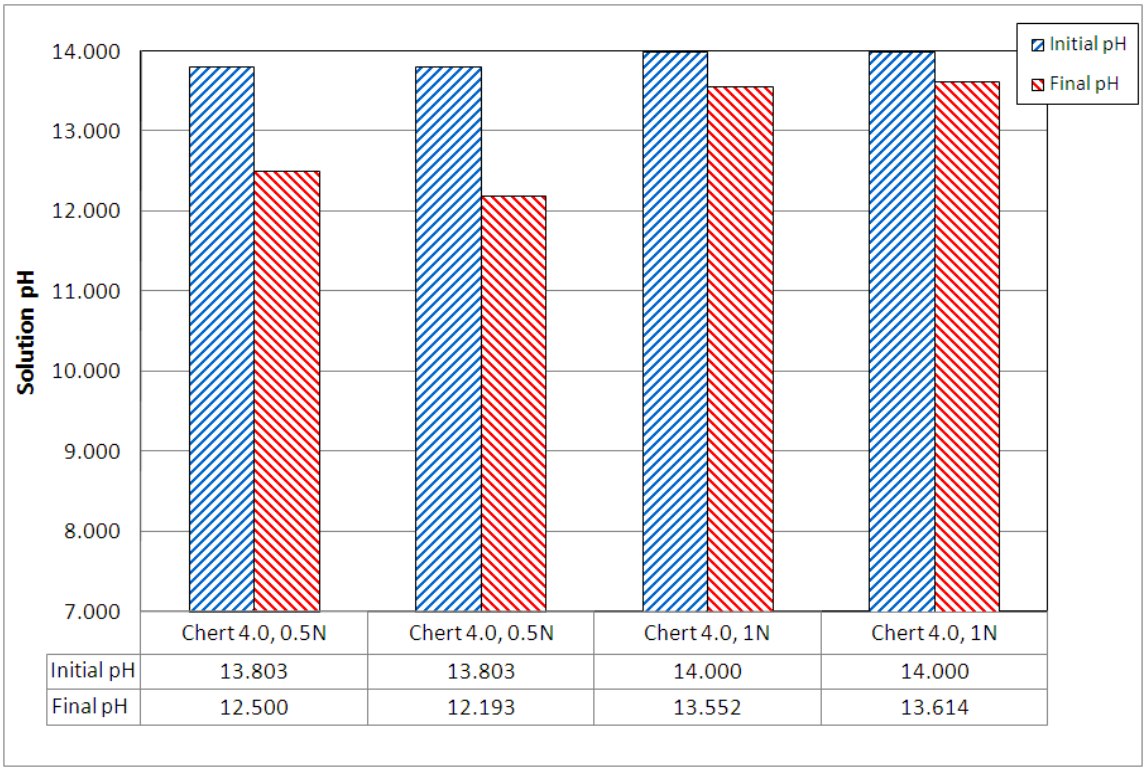

Figure 40 Comparison of Solution pH for Low Binder Content HMA Specimens Made with Chert Tested in 0.5N NaOH+CH and 1N NaOH+CH at 60°C

The changes in sodium concentrations are very small, indicating that little, if any, ASR has occurred. However, a decrease in pH is apparent for both solutions with the 0.5N solution having the greater percent decrease. Although the results of the hydroxyl concentration appear to contradict the expected trends, these graphs were included to disprove the occurrence of ASR and to maintain consistency throughout the report. This apparent contradiction of the expected result of greater decrease for greater alkalinity can be explained by examining the absolute decreases in hydroxyl concentrations, as presented in Table 8. The average pH at the beginning and ending of the tests were used to calculate the average hydroxyl concentration in the solution at the respective times, as described earlier. These average hydroxyl concentrations were then used to calculate the average absolute change in hydroxyl concentration during testing for a particular alkalinity.

Table 8 Absolute Change in Hydroxyl Concentration for Low Binder Content HMA Specimens Made with Chert Tested in 0.5N NaOH+CH and 1N NaOH+CH at 60°C

	Average Initial pH	Average Initial OH^- (ppm)	Average Final pH	Average Final OH^- (ppm)	Average Change in OH^- (ppm)
Chert 0.5N	13.803	0.642	12.347	0.024	-0.618
Chert 1N	14.000	1.01	13.583	0.388	-0.622
Percent Difference between 0.5N & 1N					0.7%

Results from both 0.5N and 1N solution tests indicate that approximately the same amount of hydroxyl ion is consumed in each reaction. This would be consistent with the neutralization of the naphthenic acids contained within the asphalt binder. Naphthenic acids are a family of complex organic acids found in most petroleum sources. There is a large variation in the chemical composition of these acids, although they are given the general formula RCOOH, where the R consists of various combinations of carbon rings. In a single California crude oil, researchers identified 1500 individual acids with boiling points ranging from 250-350°C (°F). The standard test for determining the amount of acid within a crude petroleum or a petroleum product consists of measuring the amount of KOH needed to neutralize the acids in the petroleum. These acids are typically active at the oil/water interface in systems containing both petroleum products and water (*61-69*). Since the HMA specimens from both solutions contain the same amount of asphalt binder, the amount of NaOH necessary to neutralize the acids within the binder should be the same for each. In addition, since the film of binder coating the aggregates is relatively thin for the low binder content specimens, essentially all of the acids should be able to diffuse to the binder/water interface to react. If complete neutralization of available acids occurs during the test period, the net effect of the neutralization reaction on the consumption of hydroxyl ions, at normal pavement service temperatures, will be independent of the

temperature or solution normality for specimens with relatively low binder contents. The volume change results of the high binder content compacted HMA made using chert are presented in Figure 41.

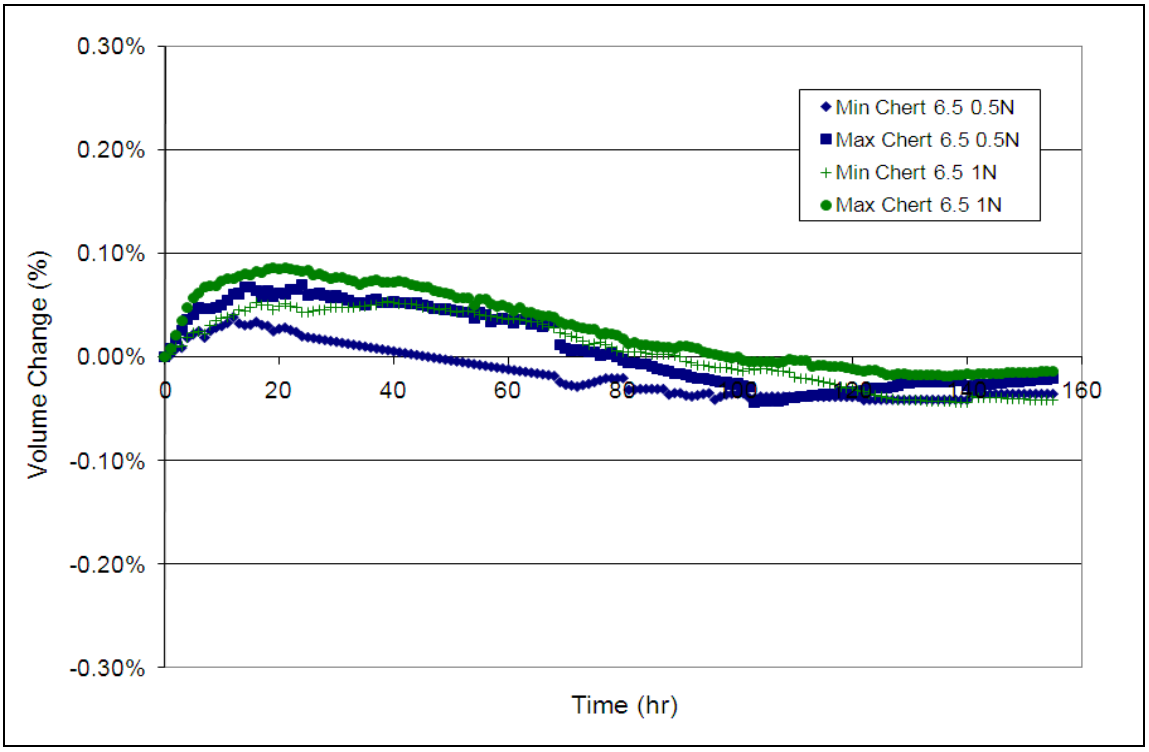

Figure 41 Percentage Volume Change of High Binder Content HMA Specimens Made with Chert Tested in 0.5N NaOH+CH and 1N NaOH+CH at 60°C

As with the low binder content specimens, the results for 0.5N and 1N tests show similar trends and magnitude of volume change. While the 1N tests initially have a slightly greater expansion, the results at the end of the testing period are very similar. This would indicate that the initial peak is due to the binder-solution interaction, and that eventually very little reaction is occurring. The solution analysis for these tests is presented in Figure 42 and Figure 43.

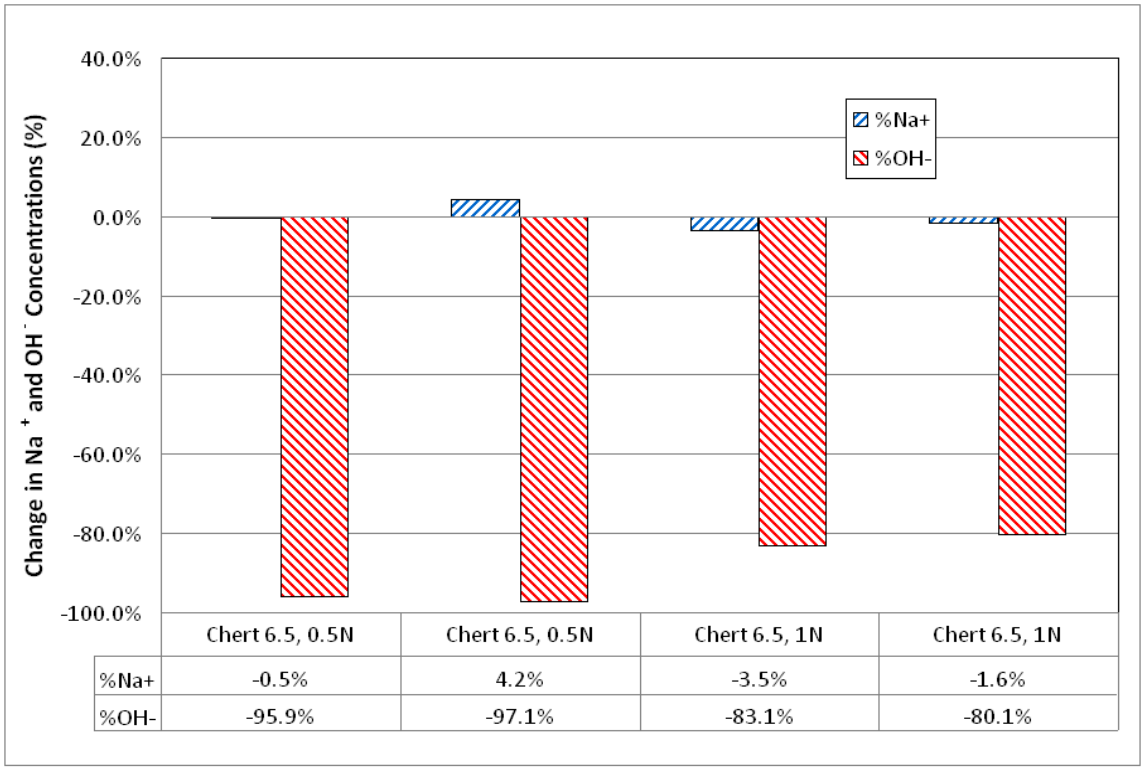

Figure 42 Percentage Change in Na^+ and OH^- Concentrations for High Binder Content HMA Specimens Made with Chert Tested in 0.5N NaOH+CH and 1N NaOH+CH at 60°C

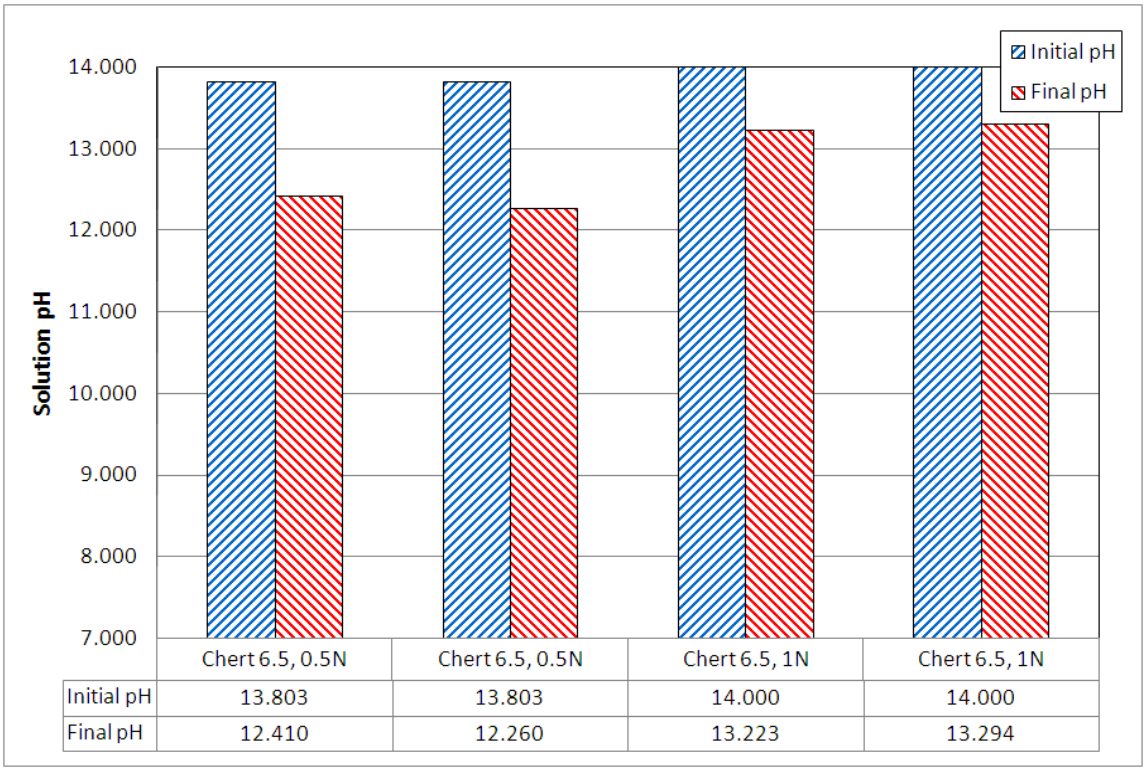

Figure 43 Comparison of Solution pH for High Binder Content HMA Specimens Made with Chert Tested in 0.5N NaOH+CH and 1N NaOH+CH at 60°C

As with the low binder content specimens, there is very little change in sodium concentrations but large decreases in hydroxyl concentrations with the 0.5N solution having the greater percent decrease. As with the low binder content results, the hydroxyl and pH results were included to disprove the occurrence of ASR and maintain consistency throughout the report. The greater percent decrease can again be explained by examining the absolute decreases in hydroxyl concentrations, as presented in Table 9.

Table 9 Absolute Change in Hydroxyl Concentration for High Binder Content HMA Specimens Made with Chert Tested in 0.5N NaOH+CH and 1N NaOH+CH at 60°C

	Average Initial pH	Average Initial OH^- (ppm)	Average Final pH	Average Final OH^- (ppm)	Average Change in OH^- (ppm)
Chert 0.5N	13.803	0.642	12.335	0.022	-0.620
Chert 1N	14.000	1.01	13.259	0.184	-0.826
Percent Difference between 0.5N & 1N					24.3%

The 0.5N solution exhibited a decrease similar to that observed for the low binder content specimens, but the 1N solution showed a larger decrease. The similar decrease for the 0.5N to the low binder content specimens indicates that, although there may be increased naphthenic acid due to the higher binder content, not all of the acid was able to diffuse to the binder/solution interface to participate in the neutralization reaction during the testing period. Therefore, in the absence of severe moisture damage, the thicker film of the high binder content reduces the effect of acid neutralization. The larger decrease for the 1N solution is likely due to the increase in total naphthenic acid due to the increased binder content and the increased ability of the 1N solution to penetrate the samples as a result of the greater damage done by the 1N solution, as demonstrated in Figure 33.

4.2.3 ASR-RCA Tests

Both ASR-RCAs were tested at 60°C using 0.5N NaOH + CH as the primary test condition for this study. HMA specimens fabricated with both high and low binder contents were tested under these conditions. In addition, ED RCA and HMA specimens made using it were tested at 60°C using a potassium acetate deicer solution. The results of the ASR-RCA tests are presented in the following subsections.

4.2.3.1 ASR-RCA NaOH Solution Tests

The volume change results of the ASR-RCAs tested at 60°C and 0.5N NaOH + CH are presented in Figure 44 and compared to the results of the virgin chert under the same conditions.

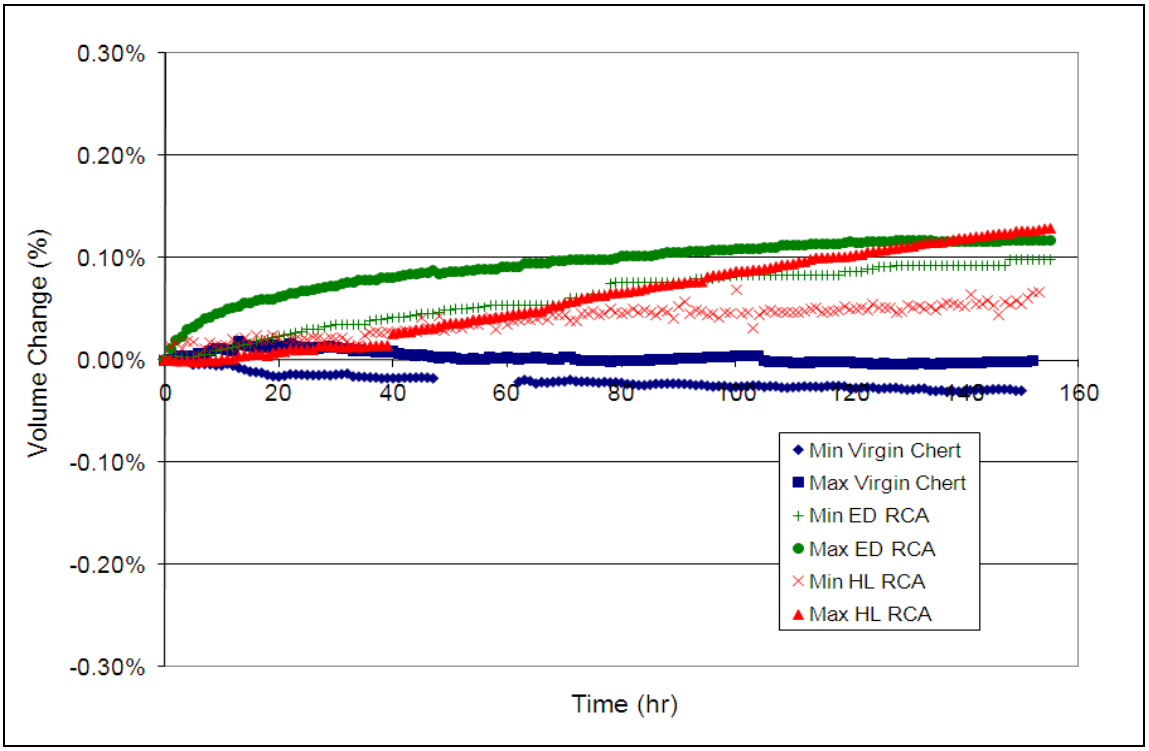

Figure 44 Percentage Volume Change of ASR-RCA and Virgin Chert Aggregate Tested in 0.5N NaOH+CH at 60°C

Although the test conditions are very mild for chert, some ASR appears to be occurring in the two RCAs. The initial expansion for the ED RCA is greater than for the HL RCA, but by the end of the test period, the two have similar expansion levels. The rate of expansion of ED RCA was initially higher than that at HL RCA, but later on (65-70 hours), the rate of expansion of HL RCA exceeded that of ED RCA. The solution analysis for these tests is presented in Figure 45 and Figure 46.

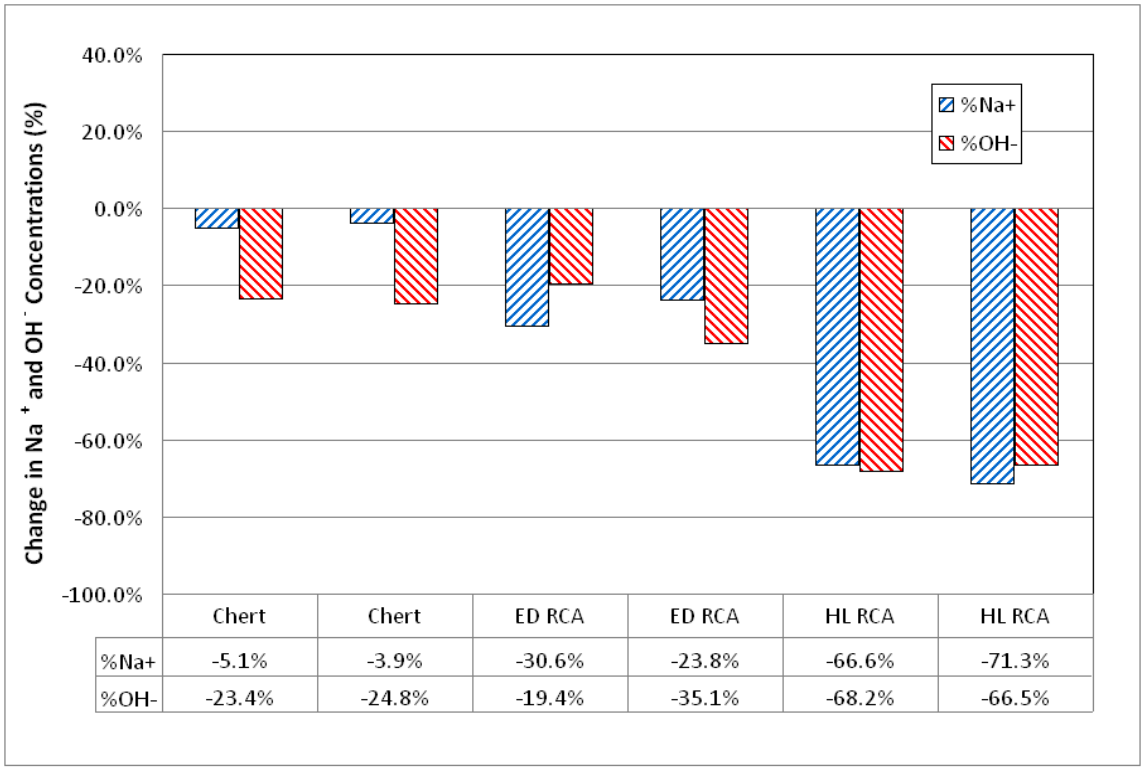

Figure 45 Percentage Change in Na^+ and OH^- Concentrations for ASR-RCA and Virgin Chert Aggregate Tested in 0.5N NaOH+CH at 60°C

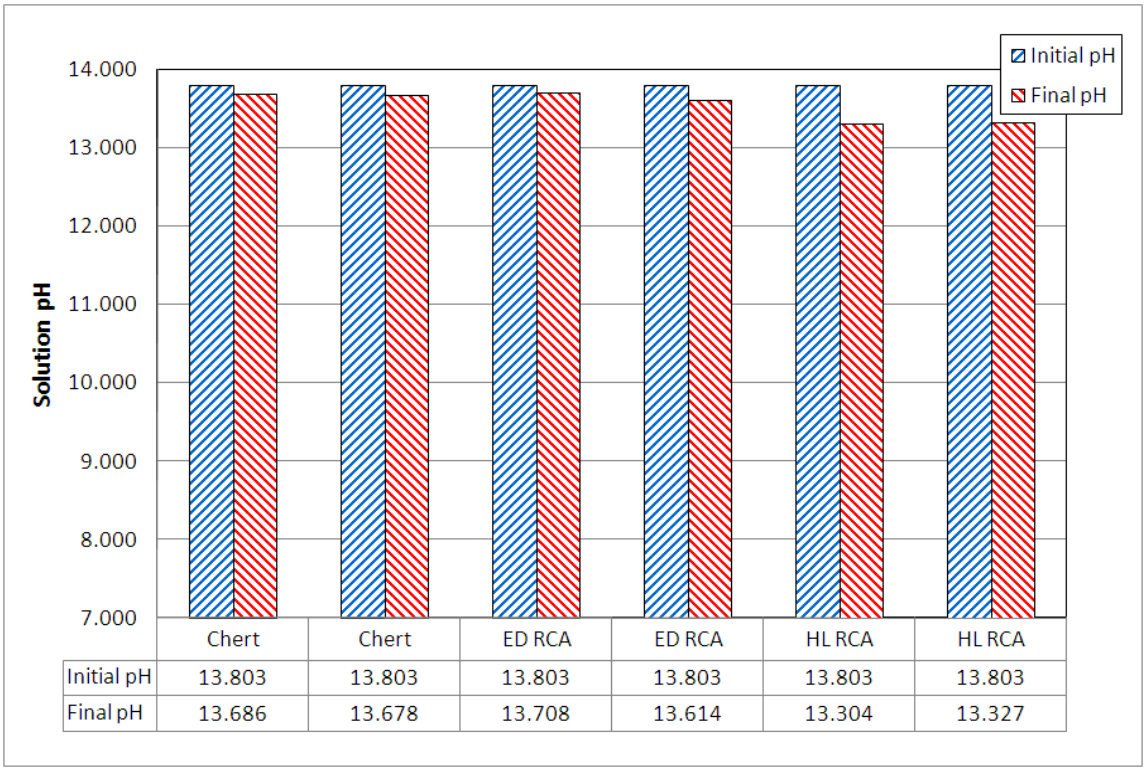

	Chert	Chert	ED RCA	ED RCA	HL RCA	HL RCA
Initial pH	13.803	13.803	13.803	13.803	13.803	13.803
Final pH	13.686	13.678	13.708	13.614	13.304	13.327

Figure 46 Comparison of Solution pH for ASR-RCA and Virgin Chert Aggregate Tested in 0.5N NaOH+CH at 60°C

The ED RCA test solutions have larger decreases in sodium than the chert specimens, despite having similar magnitudes for the decrease in hydroxyl ions. The percent reduction of both Na^+ and OH^- of HL RCA is higher than that at ED RCA and significantly higher than that of chert. The complementary decrease of both Na^+ and OH^- with similar magnitudes for all three aggregates, support the postulation that the observed expansion is due to ASR. The higher percent decrease of both Na^+ and OH^- correlated well with higher rate of overall expansion for HL RCA.

4.2.3.2 ASR-RCA Compacted HMA Tests

One of the primary concerns of this study was the re-expansion of existing gel in the ASR-RCA and the occurrence of new ASR in HMA made using ASR-RCA. The dilatometer and solution analysis results pertaining to these concerns are presented in the following subsection. The volume change results of the HL RCA alone, at these test

conditions, are compared to the results for compacted HMA made with HL RCA in Figure 47.

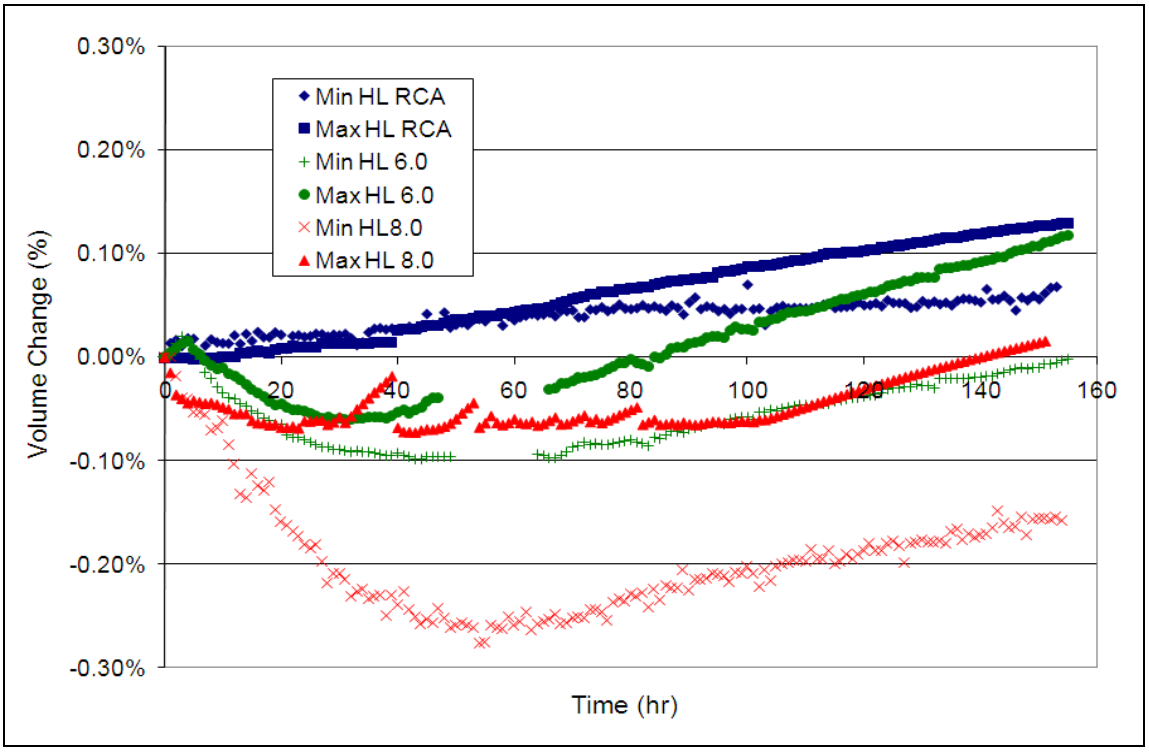

Figure 47 Percentage Volume Change of HL RCA and Compacted HMA Made with HL RCA Tested in 0.5N NaOH+CH at 60°C

The results indicate that the bands for both low and high binder contents are below that of the HL RCA. An initial downward movement (40-55 hours) followed by upward movement were the characteristics for the HMA specimens of both low and high binder contents. The initial downward movement is likely due to the error of inequality discussed earlier, while the upward movement is likely due to swelling from the binder-solution interaction. The solution analysis from these tests is presented in Figure 48 and Figure 49.

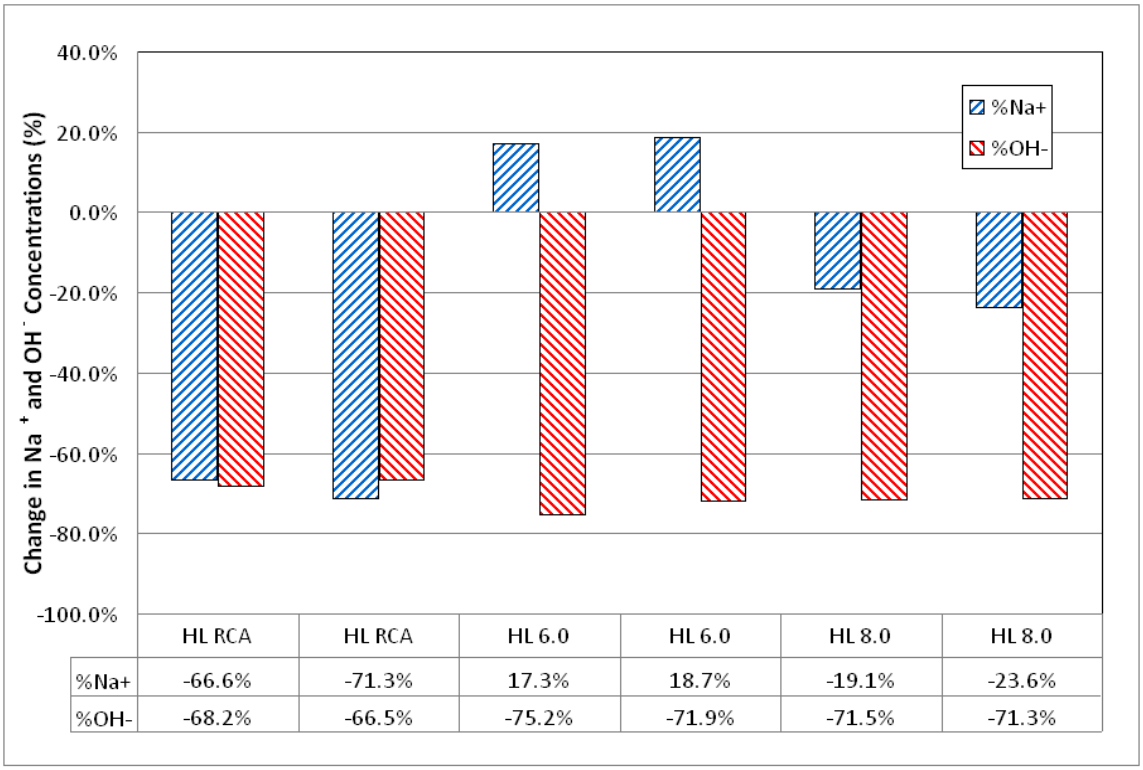

Figure 48 Percentage Change in Na^+ and OH^- Concentrations for HL RCA and Compacted HMA Made with HL RCA Tested in 0.5N NaOH+CH at 60°C

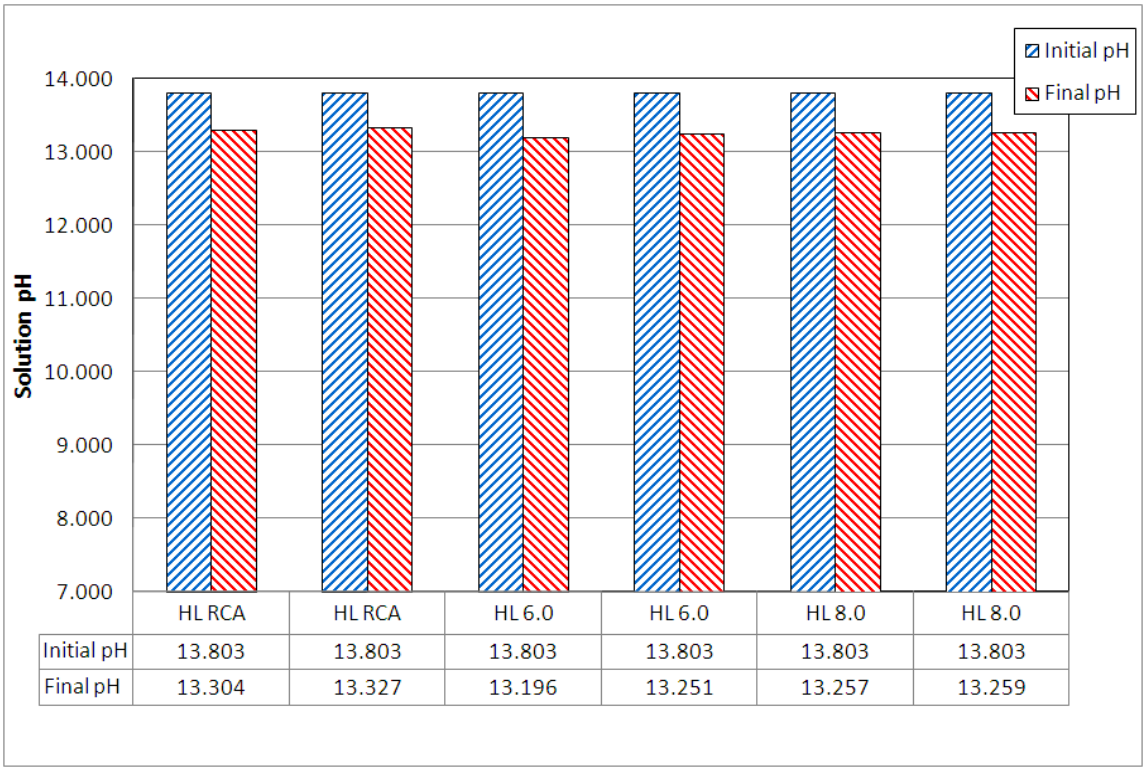

	HL RCA	HL RCA	HL 6.0	HL 6.0	HL 8.0	HL 8.0
Initial pH	13.803	13.803	13.803	13.803	13.803	13.803
Final pH	13.304	13.327	13.196	13.251	13.257	13.259

Figure 49 Comparison of Solution pH for HL RCA and Compacted HMA Made with HL RCA Tested in 0.5N NaOH+CH at 60°C

The solutions from the HMA tests have large decreases in hydroxyl ions without large decreases in sodium ions, similar to that which was observed in HMA specimens made with chert. This would indicate that the main reaction that is occurring in the HMA tests is the binder-solution interaction rather than ASR. Apparent increases in sodium with low binder content specimens are due to inherent inaccuracies in the measurement process and not as a result of additional sodium entering the system. The volume change results for the ED RCA specimens, tested under the same conditions, show similar trends as presented in Figure 50.

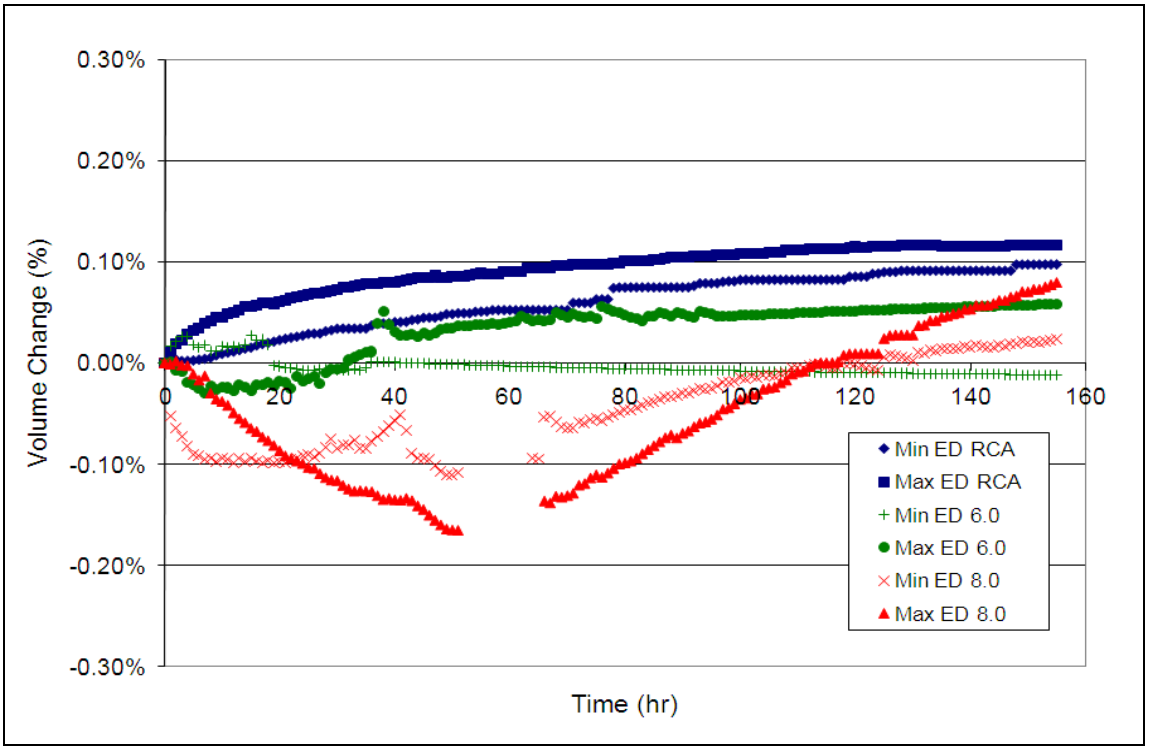

Figure 50 Percentage Volume Change of ED RCA and Compacted HMA Made with ED RCA Tested in 0.5N NaOH+CH at 60°C

As with the HL RCA specimens, both the low and high binder content bands are below those of the ED RCA. In addition, an initial downward movement until 25-55 hours, followed by upward movement, occurs. It appears that the error of inequality is occurring also, followed by swelling due to the binder-solution interaction. The solution analysis for these tests is presented in Figure 51 and Figure 52.

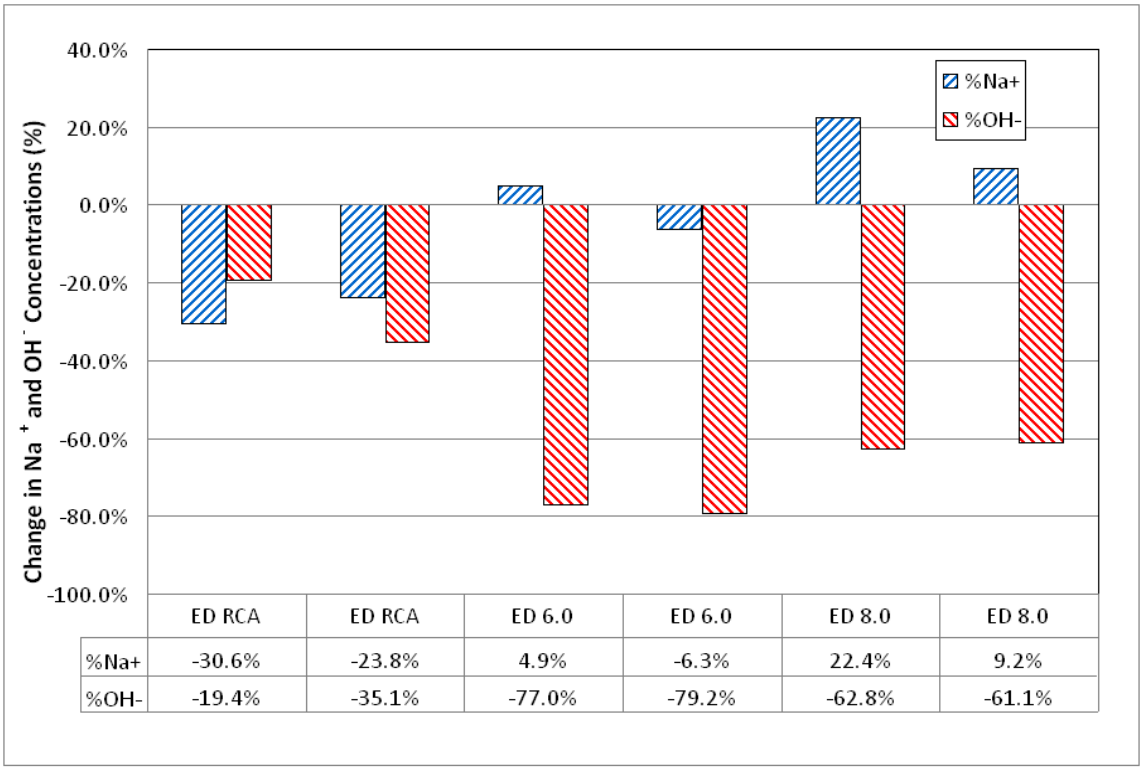

	ED RCA	ED RCA	ED 6.0	ED 6.0	ED 8.0	ED 8.0
%Na+	-30.6%	-23.8%	4.9%	-6.3%	22.4%	9.2%
%OH-	-19.4%	-35.1%	-77.0%	-79.2%	-62.8%	-61.1%

Figure 51 Percentage Change in Na^+ and OH^- Concentrations for ED RCA and Compacted HMA Made with ED RCA Tested in 0.5N NaOH+CH at 60°C

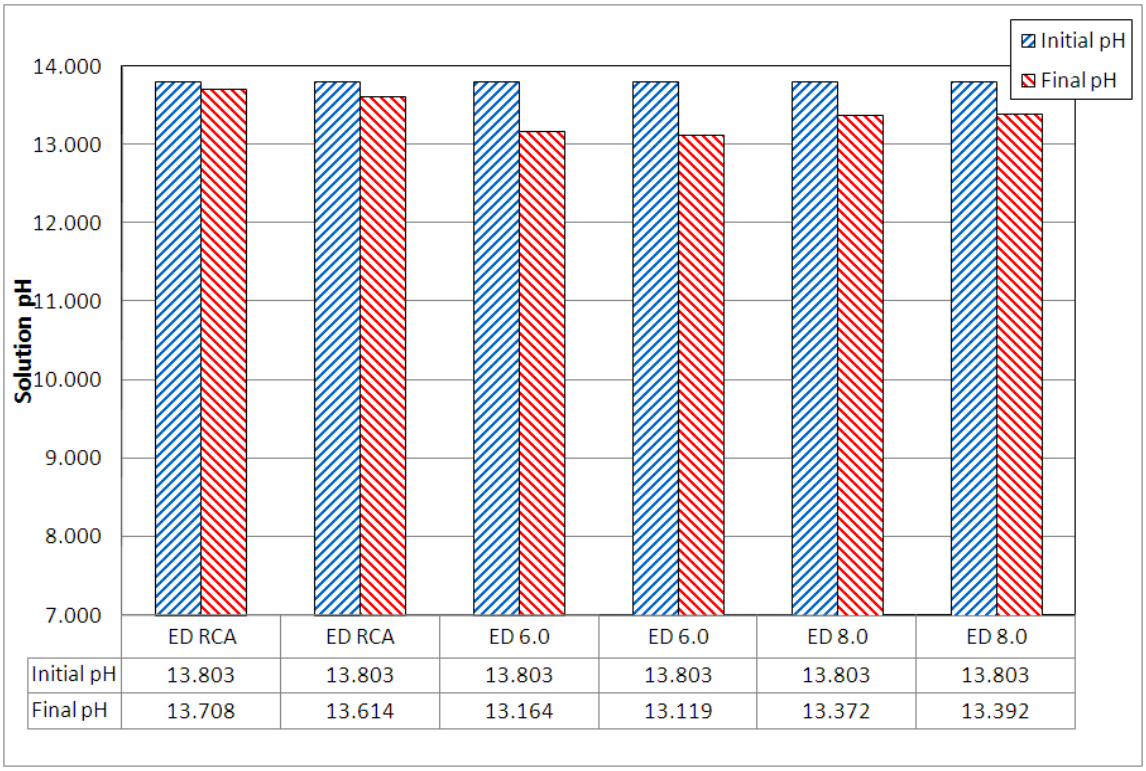

	ED RCA	ED RCA	ED 6.0	ED 6.0	ED 8.0	ED 8.0
Initial pH	13.803	13.803	13.803	13.803	13.803	13.803
Final pH	13.708	13.614	13.164	13.119	13.372	13.392

Figure 52 Comparison of Solution pH for ED RCA and Compacted HMA Made with ED RCA Tested in 0.5N NaOH+CH at 60°C

As with the solutions from the chert and HL RCA HMA specimens, the test solutions from HMA specimens made using ED RCA have large decreases in hydroxyl ions without the corresponding decrease in sodium ions. A slight increase or decrease of Na^+ is within the error limits. This would indicate that the same binder-solution interaction is occurring.

4.2.3.3 ASR-RCA Deicer Solution Tests

Specimens containing ED RCA were also tested at 60°C using a potassium acetate deicer solution. The volume change results of the ED RCA tests using deicer are compared to those from the testing using 0.5N NaOH with CH in Figure 53.

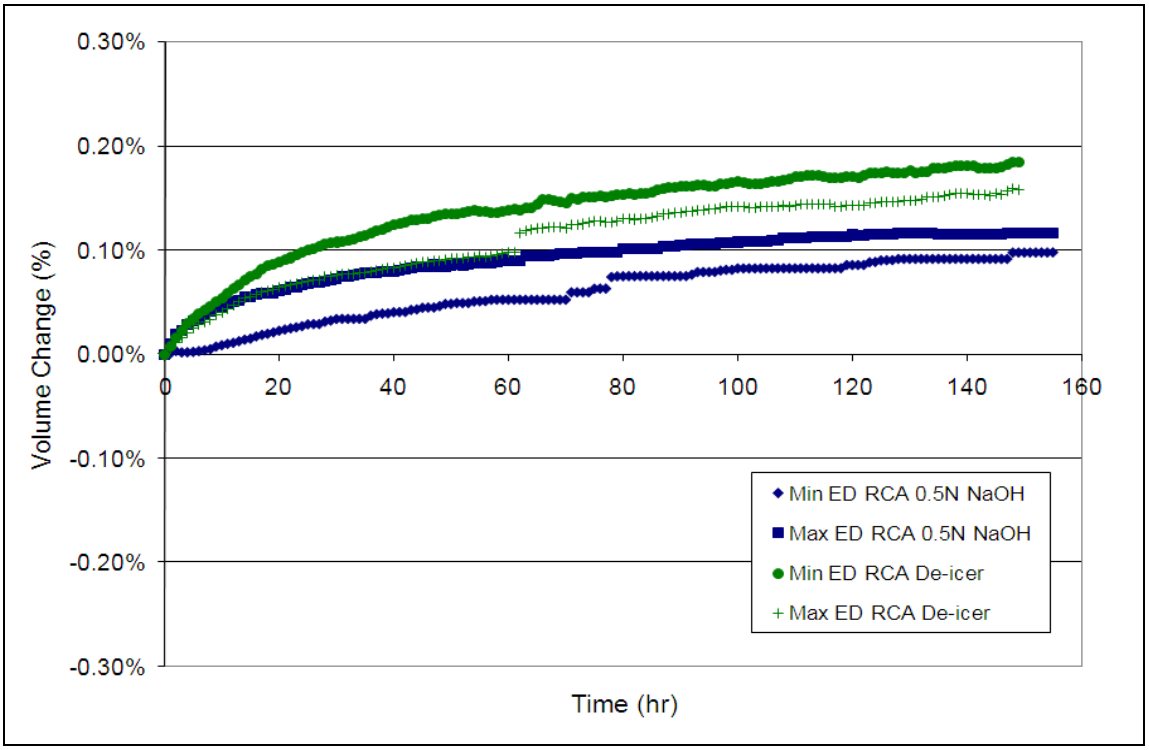

Figure 53 Percentage Volume Change of ED RCA Specimens Tested in Deicer Solution and 0.5N NaOH+CH at 60°C

The specimens tested in deicer solution demonstrate greater expansion than those tested in 0.5N NaOH with CH. This is probably due to the greater concentration of potassium in the deicer, about 6.5N, as compared to the sodium in the 0.5N NaOH. The solution analysis from these tests is presented in Figure 54 and Figure 55.

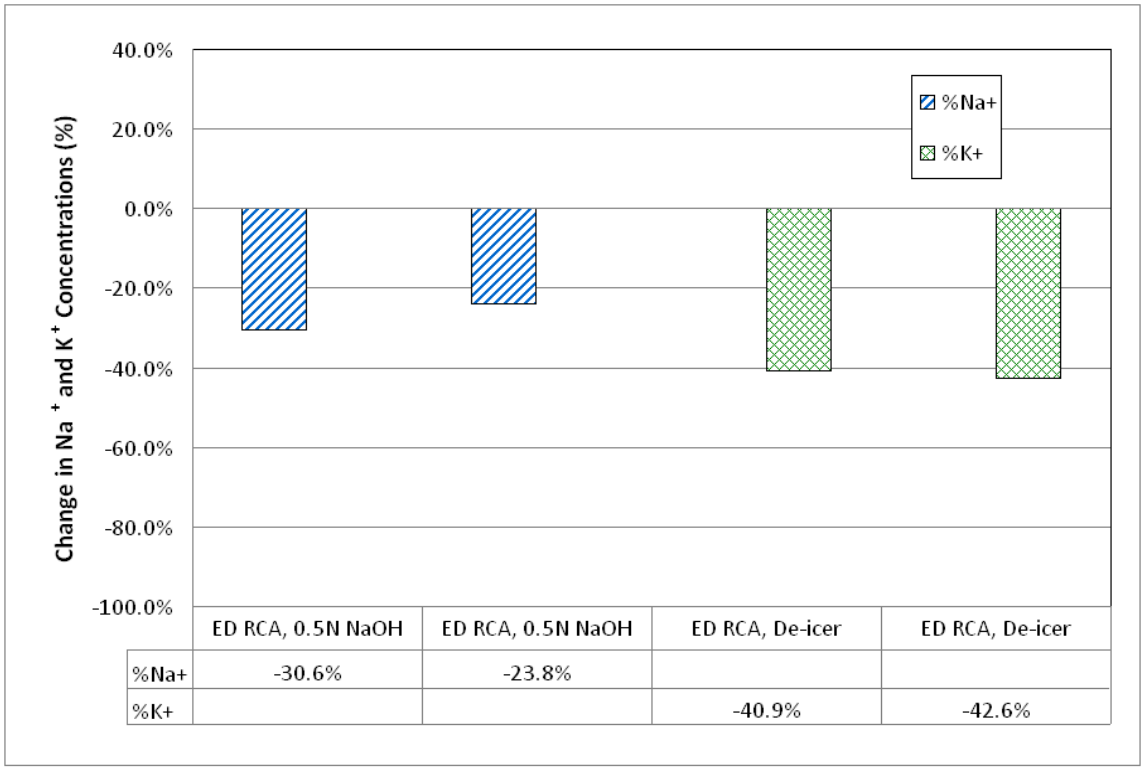

Figure 54 Percentage Change in Na^+ and K^+ Concentrations for ED RCA Specimens Tested in Deicer Solution and 0.5N NaOH+CH at 60°C

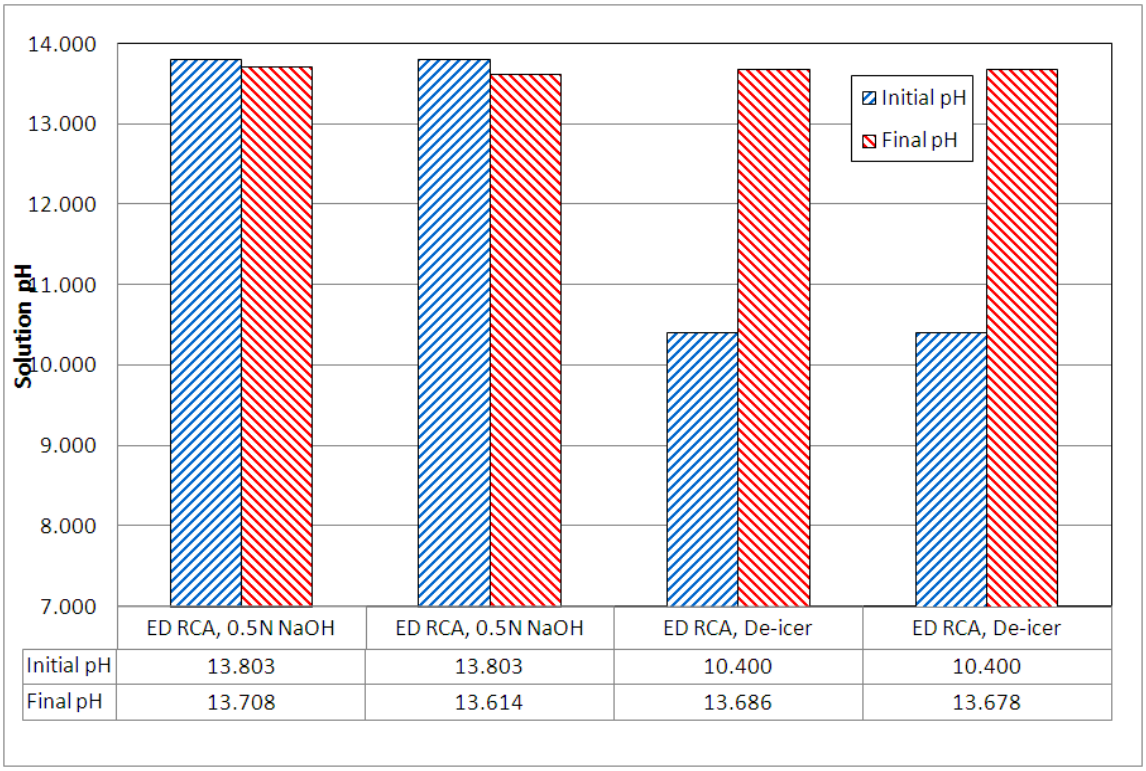

	ED RCA, 0.5N NaOH	ED RCA, 0.5N NaOH	ED RCA, De-icer	ED RCA, De-icer
Initial pH	13.803	13.803	10.400	10.400
Final pH	13.708	13.614	13.686	13.678

Figure 55 Comparison of Solution pH for ED RCA Specimens Tested in Deicer Solution and 0.5N NaOH+CH at 60°C

The solutions from both sets of tests exhibited decreases in either sodium or potassium concentrations of a similar relative magnitude. The increase in pH for the deicer solution is likely caused by hydroxyl ions from the mortar fraction of the RCA entering the solution to form KOH. Due to the high concentration of potassium in the solution, large numbers of hydroxyl ions may enter the solution. The volume change results for the low and high binder content compacted HMA specimens tested in deicer solution are compared to those from ED RCA in Figure 56.

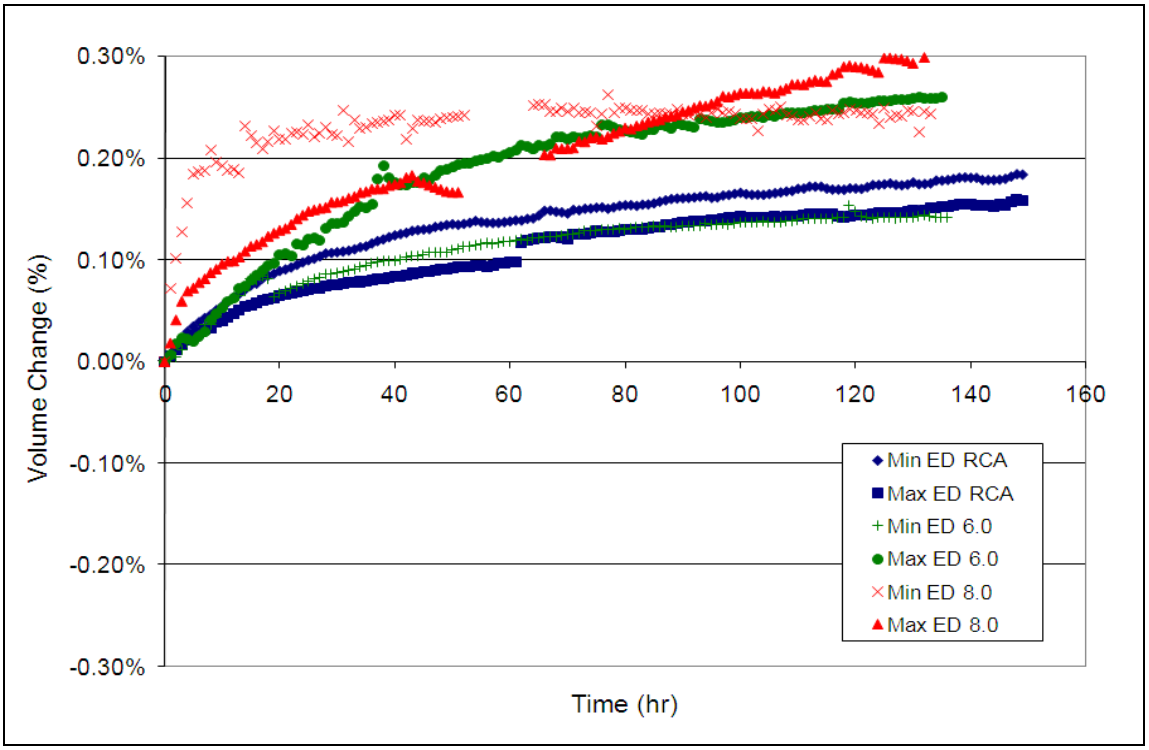

Figure 56 Percentage Volume Change of ED RCA and Compacted HMA Made with ED RCA Tested in Deicer Solution at 60°C

Results from the low binder content specimens form a band that overlaps the band from ED RCA alone. The results from the high binder content specimens fall slightly above those of the low binder content specimens. The majority of the greater increase for both sets of HMA specimens appears to occur during the first 30-40 hours of testing. This would likely indicate that, initially, the primary reaction for the HMA is the saponification reaction resulting in swelling. The similar rates for all three sets of material combinations, after the first 30-40 hours, would then indicate that ASR may be occurring at this time. Solution analysis for these tests is presented in Figure 57 and Figure 58.

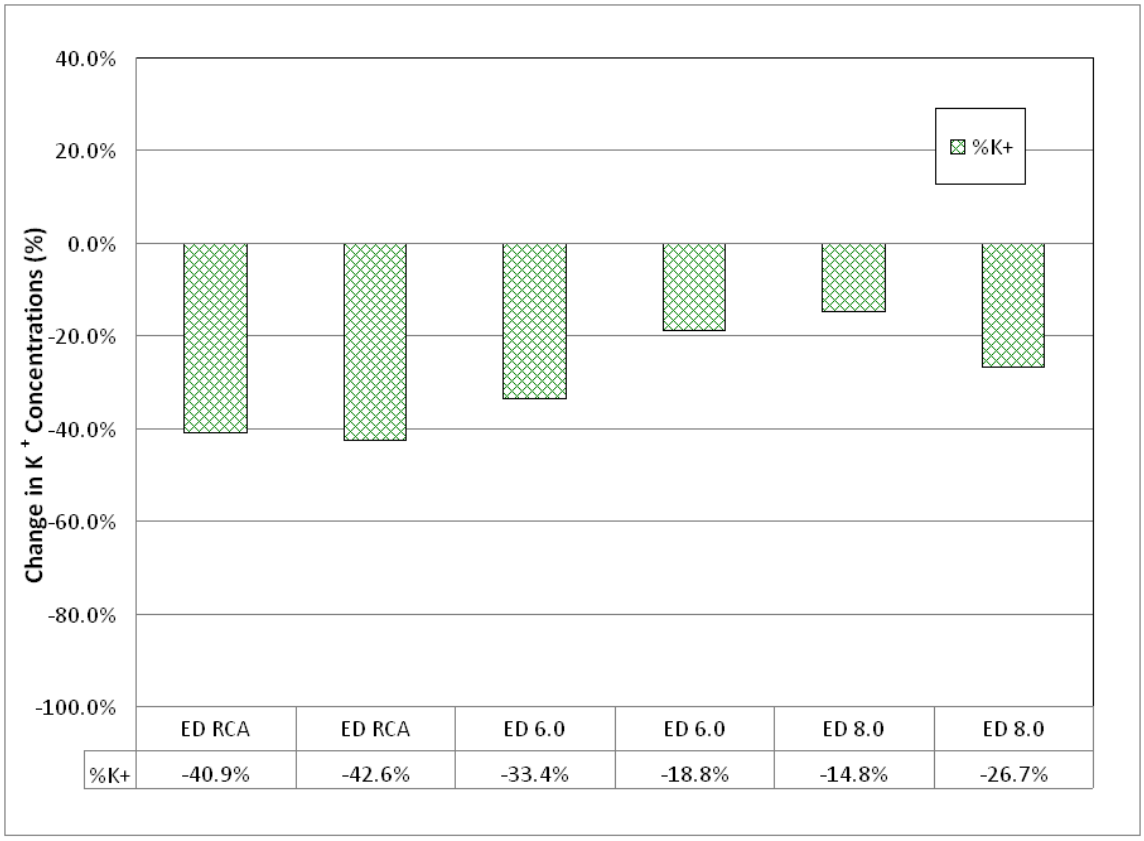

Figure 57 Percentage Change in K^+ Concentrations for ED RCA and Compacted HMA Made with ED RCA Tested in Deicer Solution at 60°C

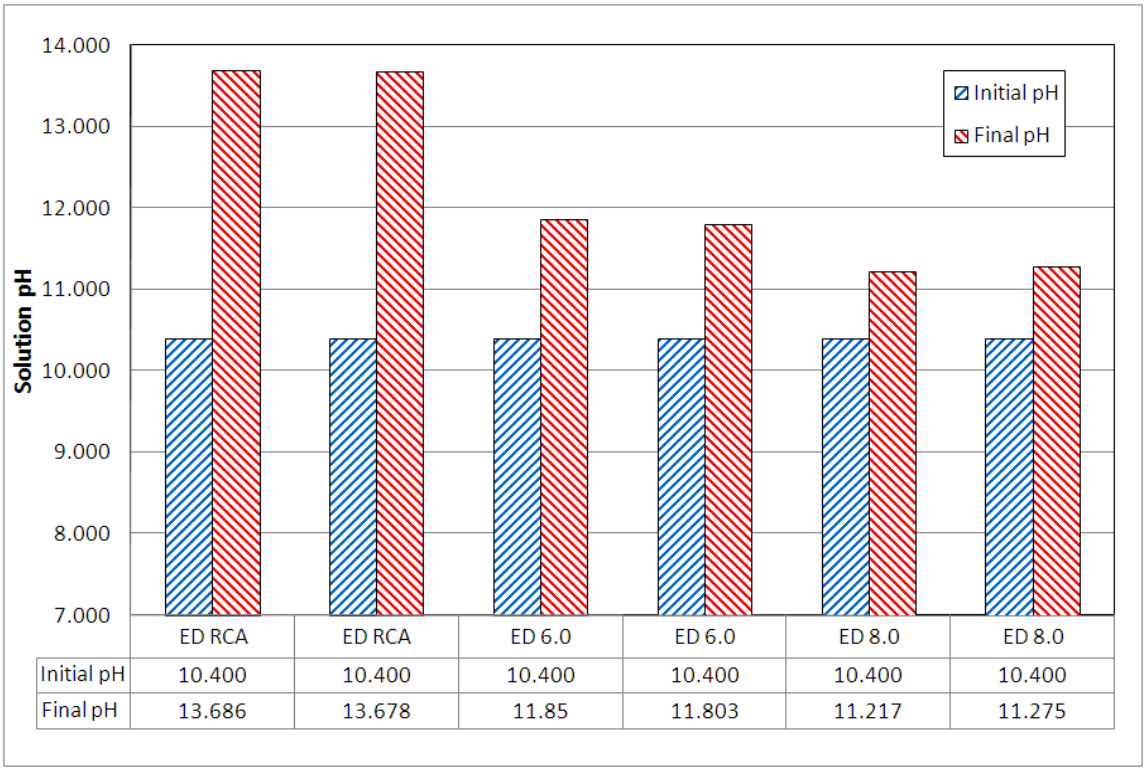

	ED RCA	ED RCA	ED 6.0	ED 6.0	ED 8.0	ED 8.0
Initial pH	10.400	10.400	10.400	10.400	10.400	10.400
Final pH	13.686	13.678	11.85	11.803	11.217	11.275

Figure 58 Comparison of Solution pH for ED RCA and Compacted HMA Made with ED RCA Tested in Deicer Solution at 60°C

The solutions from the HMA tests also have large increases in pH, as was observed for the ED RCA (Figure 55). However, the solution from the ED RCA alone shows greater increase of pH than that from the HMA specimens with both low and high binder contents. The possible explanations are the binder around RCA reducing direct contact between mortar fractions in RCA and K-acetate solution and reduction of OH^- by the binder solution interaction. The three steps involved are (I) initially, OH^- ions diffuse through the binder to the test solution, increasing the pH of the solution. This is a slow process and likely only causes a slight increase in pH over the test period. (II) The binder-solution interaction starts due to the presence of OH^- ions in the solution, which softens the binder causing some stripping and micro-cracking. (III) The stripping and micro-cracks allow direct penetration of the solution to the mortar and reactive aggregate. Direct contact between the mortar and solution allows for higher rate of

release of OH^- ions which cause more significant increases in pH. It appears that the rate of release of OH^- ions is greater than the consumption of OH^- by the binder-solution interaction and any ASR that may occur, ultimately resulting in an increase of the solution pH. A diagram of this interaction is presented in Figure 59.

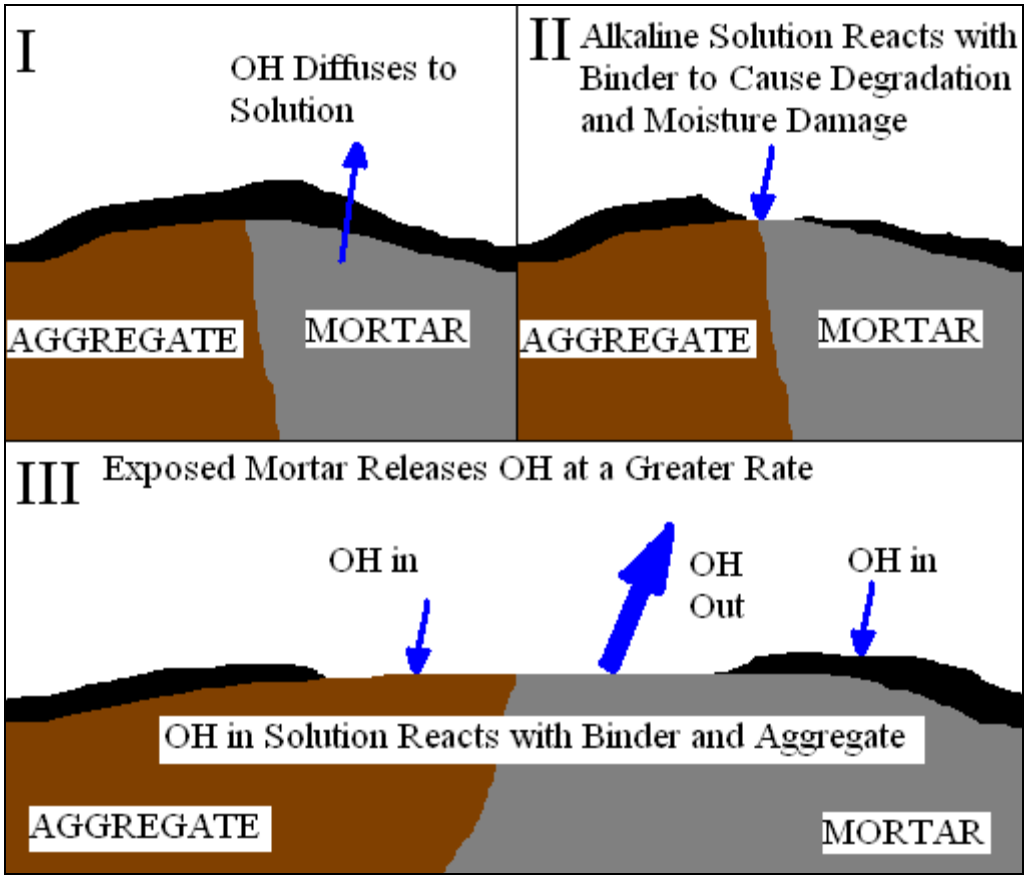

Figure 59 Diagram of Interaction Between Deicer Solution and Compacted HMA Made from ASR-RCA

The solutions from the HMA tests also show a decrease of K^+ of similar but slightly lesser magnitude than those of the ED RCA alone as presented in Figure 57. This confirms that ASR may be occurring in HMA made using ED RCA along with primary binder-solution interaction. However, if any ASR is occurring, it is of lesser intensity than ED RCA alone under the same test conditions.

The HMA specimens were still intact after testing, as presented in Figure 60. This indicates that the degradation of the binder is lower than that with NaOH + CH solution, which possibly suggests that deicer-binder interaction is different and less harmful than NaOH + CH solution-binder interaction.

Figure 60 Compacted HMA Made with ED RCA after Testing in Deicer Solution at 60°C

With deicer, binder-solution interaction may create the path for solution ingress, which creates a favorable situation for ASR. It seems that ASR contributes more in expansion measurements with deicers than those with the NaOH + CH solutions. The volume change results from the low binder content compacted HMA made using ED RCA and tested in deicer solution are compared to those from the 0.5N NaOH + CH in Figure 61.

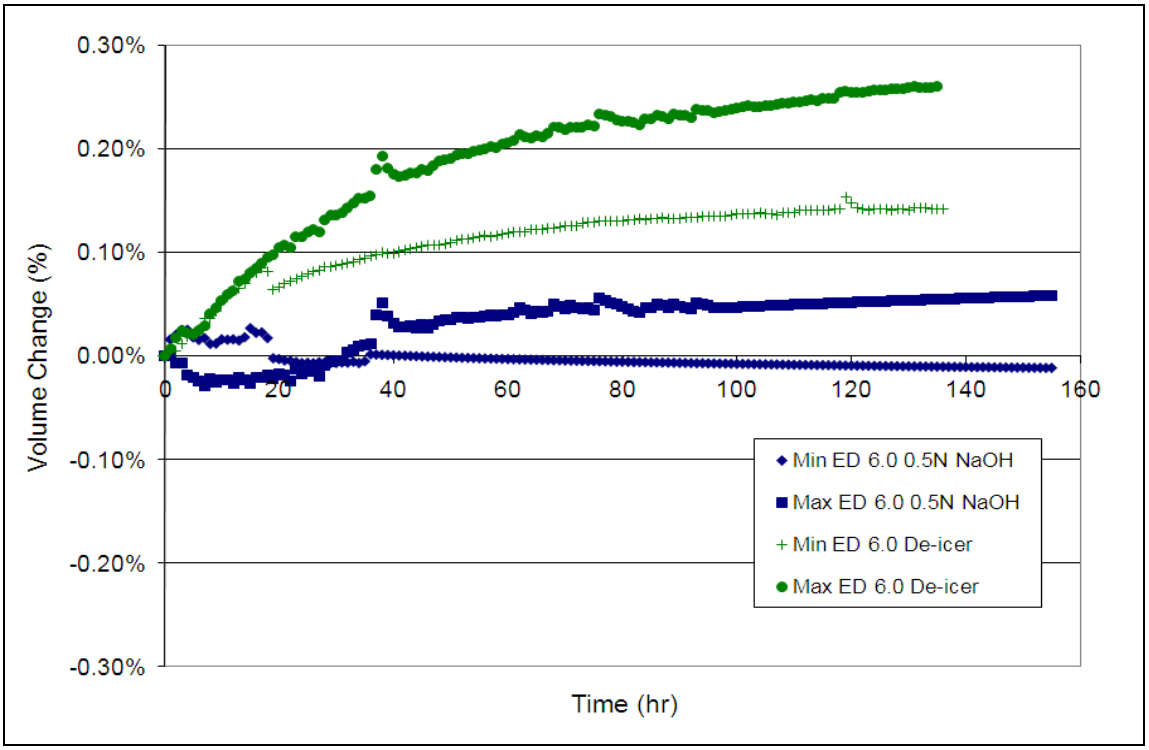

Figure 61 Percentage Volume Change of Low Binder Content Compacted HMA Made with ED RCA Tested in Deicer Solution and 0.5N NaOH+CH at 60°C

The band from the deicer tests is much higher than the band from the 0.5N NaOH with CH tests. The evidence presented above indicates that ASR may be occurring in the specimens tested in deicer solution. Interestingly, white deposits (possibly ASR gel) were observed on the surface of the HMA specimens, as presented in Figure 62, which was not observed in any of the NaOH + CH reacted HMA specimens.

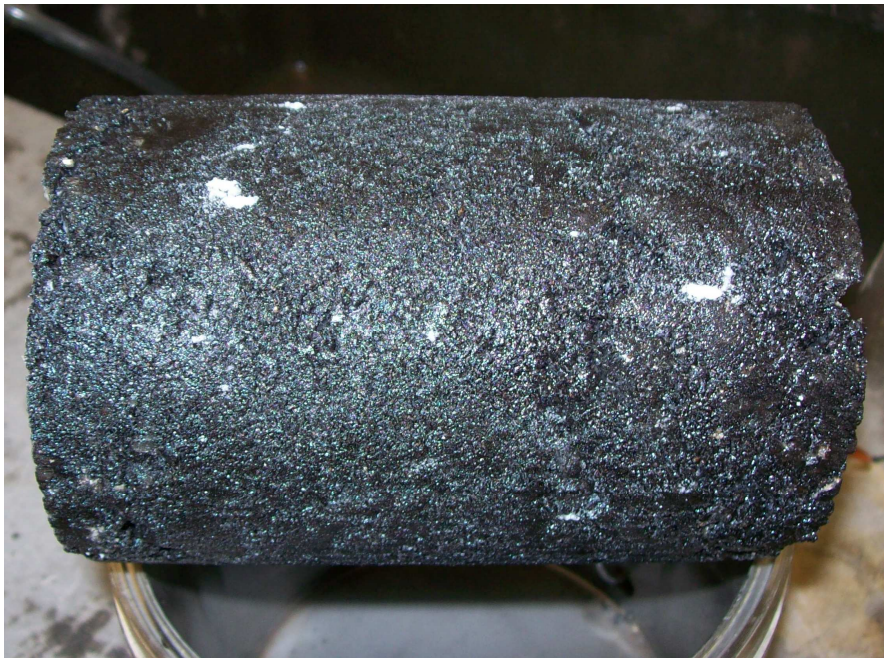

Figure 62 White Deposit on Exterior of Compacted HMA Made with ED RCA Tested in Deicer Solution at 60°C

An attempt was made to verify that the white products observed on the surface of the specimens were in fact ASR products using SEM-EDS. Oil phases present in the asphalt binder boiled off in the high vacuum of the SEM (*70*). This prevented the SEM system from achieving sufficient vacuum to view the samples. The increased volume change is likely due to a combination of asphalt binder-solution interaction and possibly some ASR. The solution analysis for these tests is presented in Figure 63 and Figure 64.

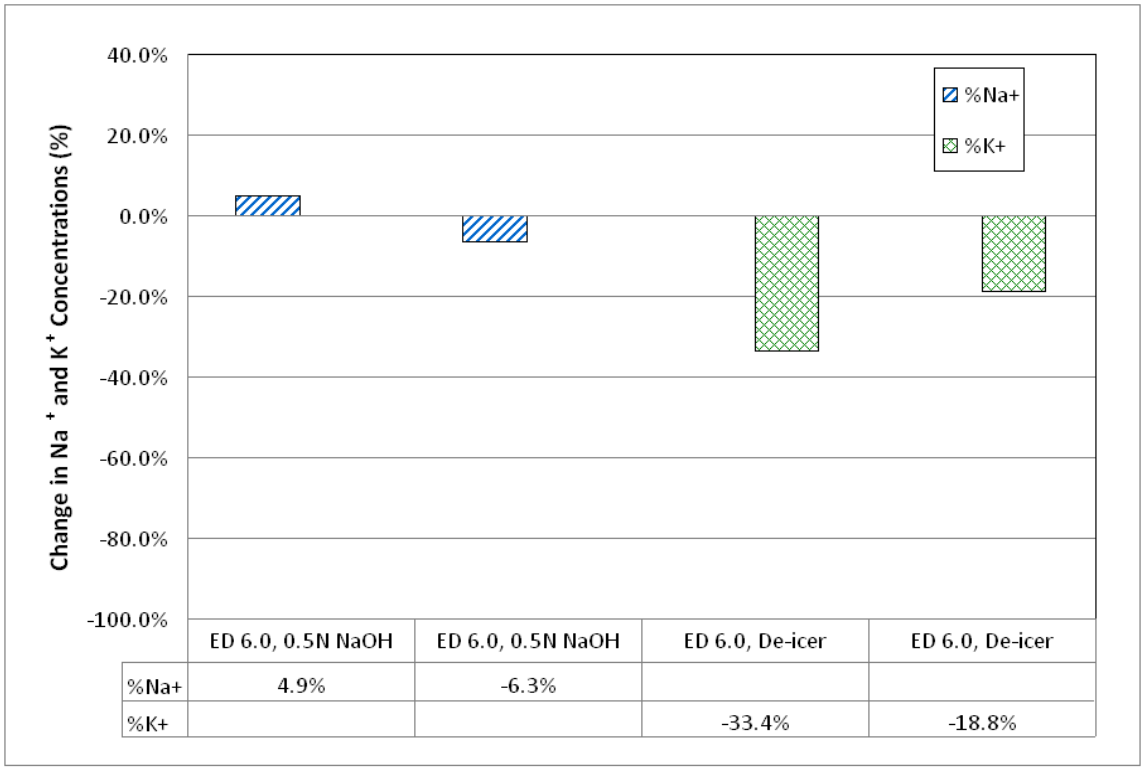

Figure 63 Percentage Change in Na^+ and K^+ Concentrations for Low Binder Content Compacted HMA Made with ED RCA Tested in Deicer Solution and 0.5N NaOH+CH at 60°C

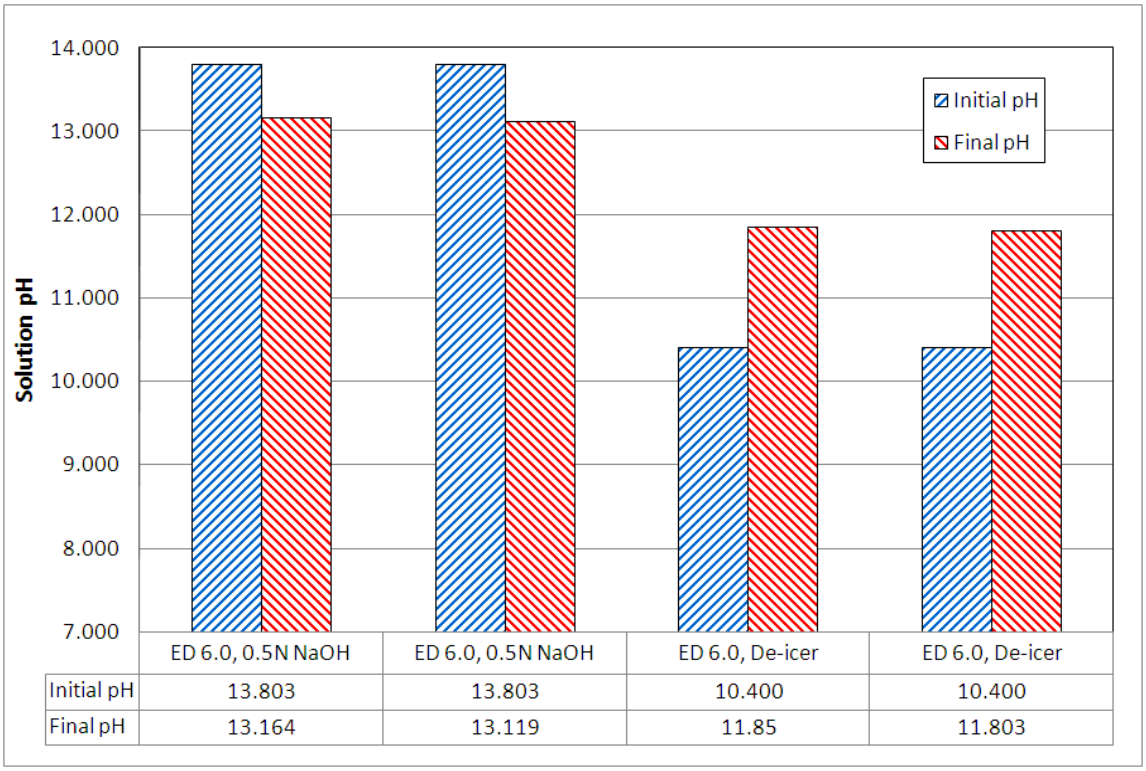

Figure 64 Comparison of Solution pH for Low Binder Content Compacted HMA Made with ED RCA Tested in Deicer Solution and 0.5N NaOH+CH at 60°C

While the volume change observed in the specimens tested in 0.5N NaOH with CH appears to be primarily due to the binder-solution interaction, based on the small decreases in sodium ions, the volume change observed in the specimens tested in deicer solution appears to be partially due to ASR. The volume change results from the high binder content compacted HMA made with ED RCA tested in deicer solution are compared to those from the 0.5N NaOH with CH in Figure 65.

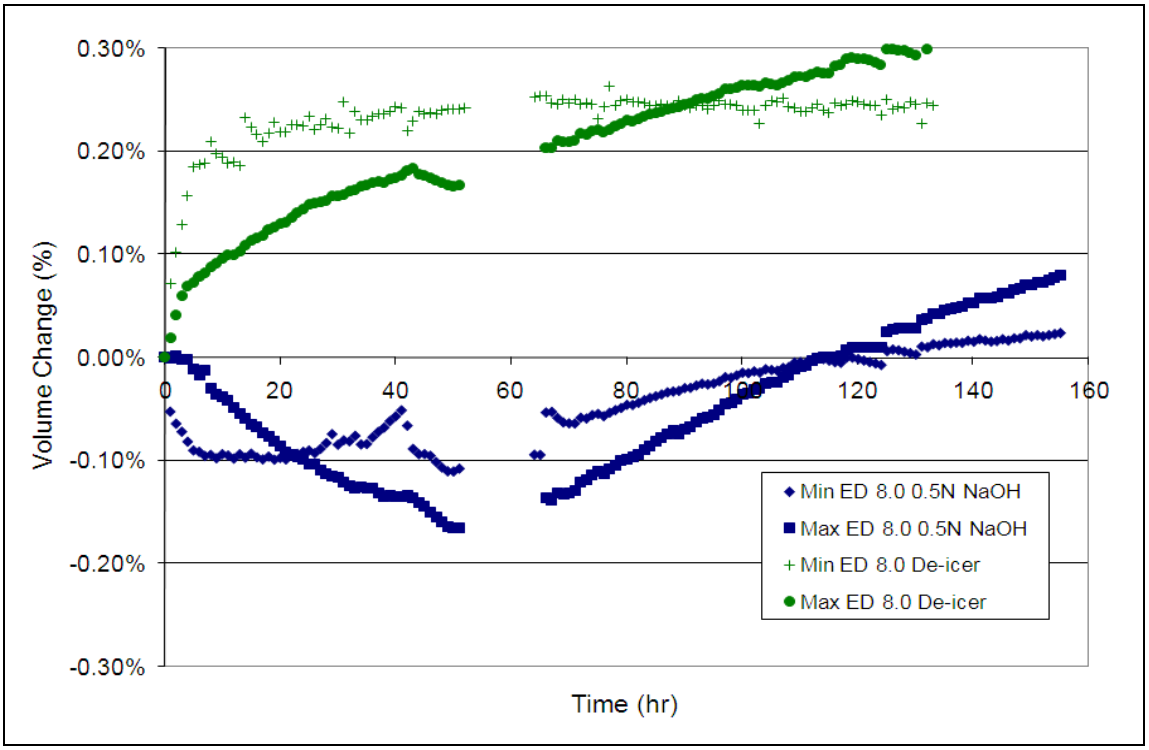

Figure 65 Percentage Volume Change of High Binder Content Compacted HMA Made with ED RCA Tested in Deicer Solution and 0.5N NaOH+CH at 60°C

There does not appear to be any strong similarities between the two bands for the high binder content compacted HMA specimens. The lack of similarity is possibly due to (i) the nature of binder-deicer interaction is different, and (ii) some ASR is possibly occurring in the specimens tested in deicer solution but not in specimens tested in 0.5N NaOH + CH. The reasons for initial downward movement of the 0.5N NaOH + CH curves are provided earlier in the discussion corresponding to Figure 47 and Figure 50. It was mentioned earlier that the binder-deicer interaction is less harmful than binder-(NaOH+CH) interaction, which is probably the reason for not getting any initial downward movement (less or no "error of inequality" during calibration) with deicer tests. The solution analysis from these tests is presented in Figure 66 and Figure 67.

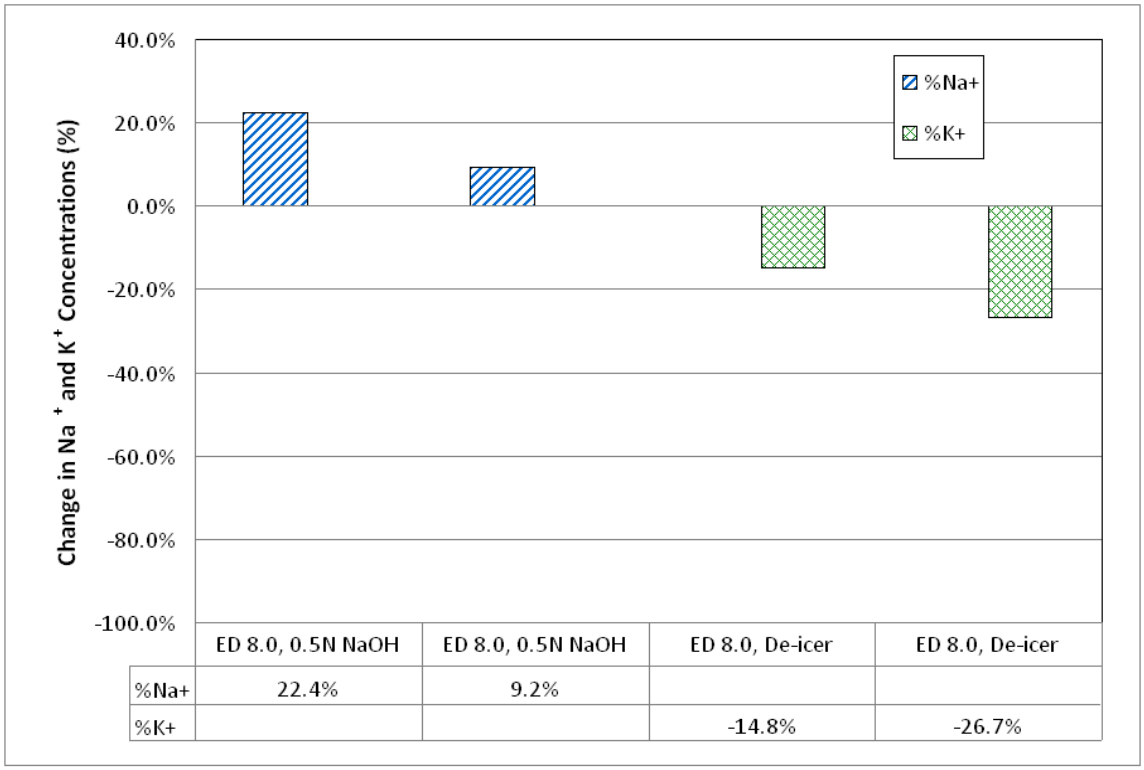

Figure 66 Percentage Change in Na^+ and K^+ Concentrations for High Binder Content Compacted HMA Made with ED RCA Tested in Deicer Solution and 0.5N NaOH+CH at 60°C

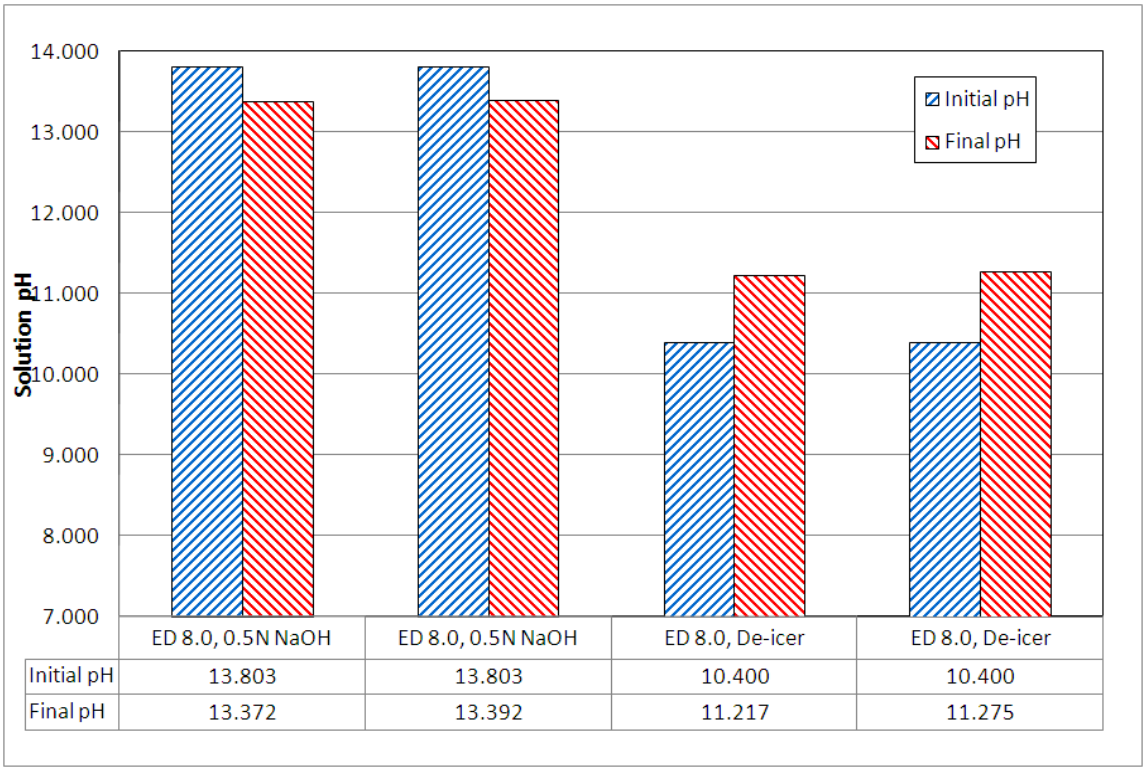

	ED 8.0, 0.5N NaOH	ED 8.0, 0.5N NaOH	ED 8.0, De-icer	ED 8.0, De-icer
Initial pH	13.803	13.803	10.400	10.400
Final pH	13.372	13.392	11.217	11.275

Figure 67 Comparison of Solution pH for High Binder Content Compacted HMA Made with ED RCA Tested in Deicer Solution and 0.5N NaOH+CH at 60°C

The solution analysis from the high binder content specimens appears to indicate that the volume change in 0.5N NaOH with CH is due to the binder-solution interaction, and that, in the deicer solution, it is due to a combination of the binder-solution interaction and some ASR.

4.2.4 Dilatometer Summary

The low reactivity of chert demonstrates that the primary test conditions, 0.5N NaOH + CH at 60°C, are relatively mild. The low reactivity is apparent in both the expansion data and the analysis of the test solution. Volume changes in compacted HMA specimens containing chert appear to be primarily due to an interaction between the asphalt binder and the alkaline solution. The expansion over time measured for both the RCAs in the dilatometer tests with RCA alone and solution analysis confirms that ASR occurred. The same binder-solution interaction is evident as a dominating

phenomenon in compacted HMA made with RCAs. However, some ASR may have occurred along with same binder-solution interaction when HMA containing ED RCA was tested with concentrated deicers.

4.3 Detailed Microstructure of Polished Chert

The samples were reacted with 0.5N NaOH solution saturated with CH at 60°C for varying time periods. Samples were removed at the following removal times: 2 days, 4 days, 7 days, and 28 days to confirm the occurrence of ASR in chert under the given test conditions. After the samples were removed, they were gently rinsed with acetone to remove any solution on the surface without removing or disturbing the reaction products.

4.3.1 Original Surface

An image of the typical appearance of the original surface of the chert particles before the reaction is presented in Figure 68 along with the average EDS analysis for the surface.

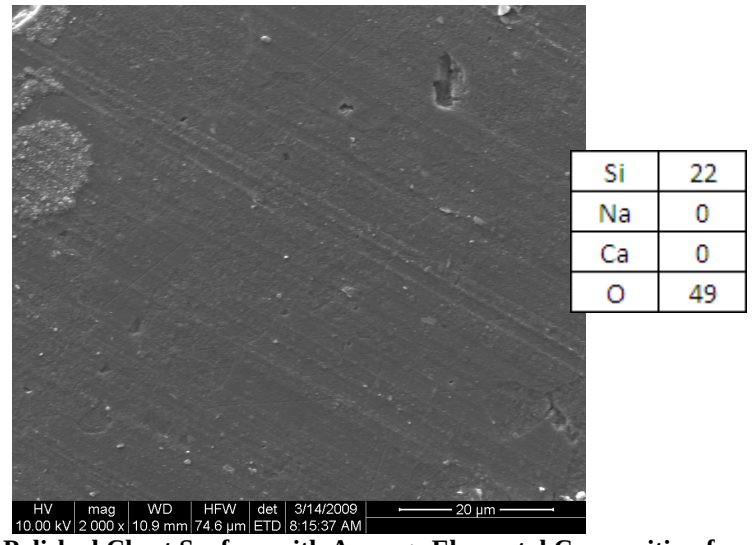

Figure 68 Original Polished Chert Surface with Average Elemental Composition from EDS Analysis

The surface is relatively smooth and neither sodium nor calcium was detected by the EDS analysis.

4.3.2 Two-Day Results

The surface of the chert specimen, reacted for two days, appeared relatively smooth with some etching due to dissolution as presented in Figure 69 along with the average EDS analysis for the surface.

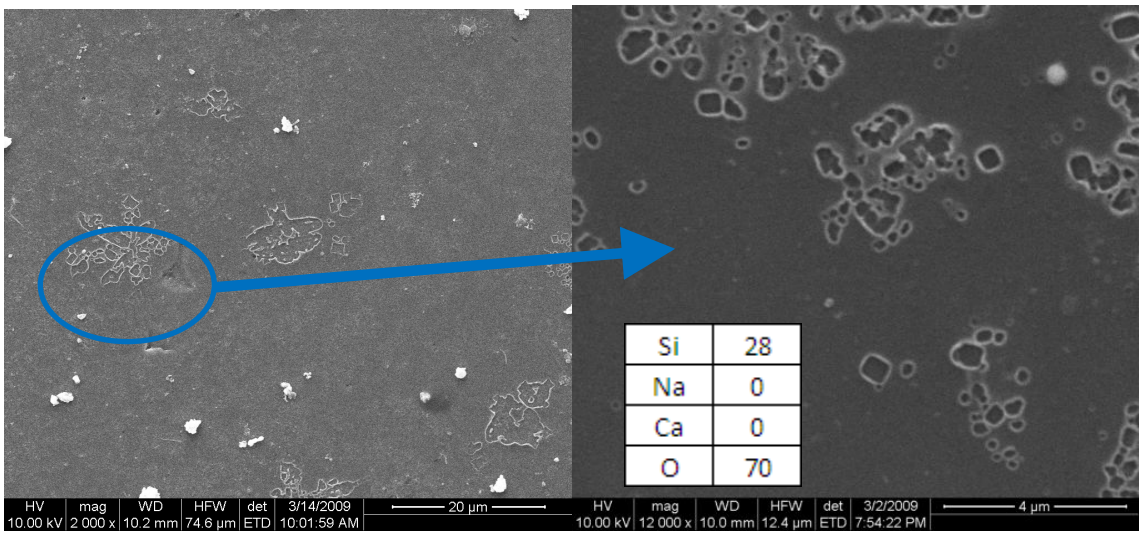

Figure 69 Surface of Specimen Reacted for Two Days with Average Elemental Composition from EDS Analysis

The EDS analysis indicates that this surface is essentially made of Si and O (i.e., silicon dioxide) without any presence of Na and Ca. Since the surface is still smooth, and no evidence of a product is provided by the EDS analysis, it can be concluded that no distinguishable reaction has taken place yet.

4.3.3 Four-Day Results

A few reaction sites were found along the edges of the specimen reacted for four days. An example of one of these sites is presented in Figure 70 along with the average EDS analysis for the product.

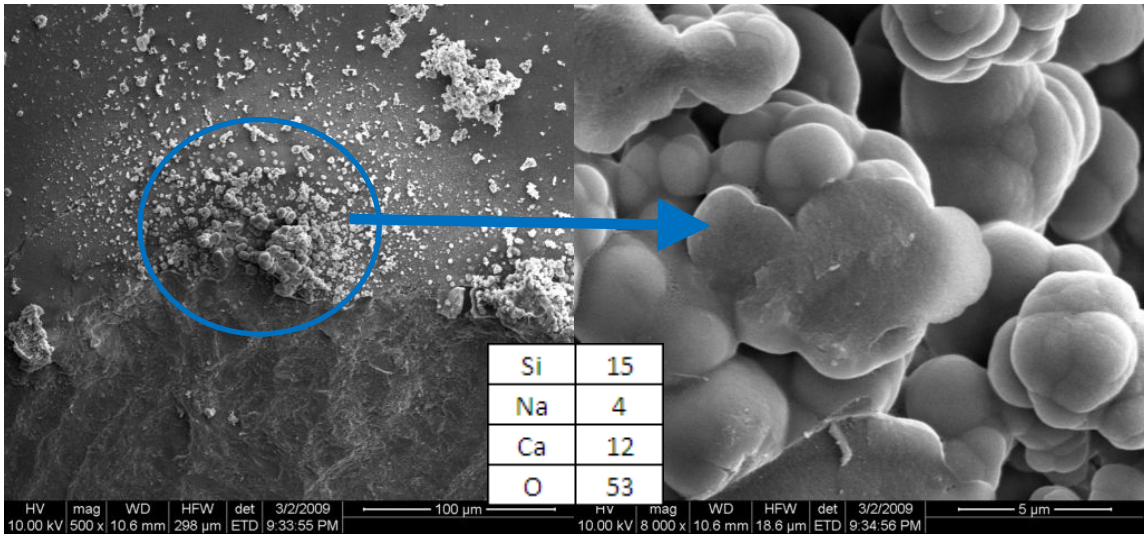

Figure 70 Deposit on Surface of Specimen Reacted for Four Days with Average Elemental Composition from EDS Analysis

The product appears to be ASR gel containing mainly Si with larger amounts of calcium than sodium.

4.3.4 Seven-Day Results

A small amount of reaction products were found on the surface of the specimen reacted for seven days. However, a site was observed along the edge of one of the chert particles where a significant product occurred. This site is presented in Figure 71 along with the average EDS analysis.

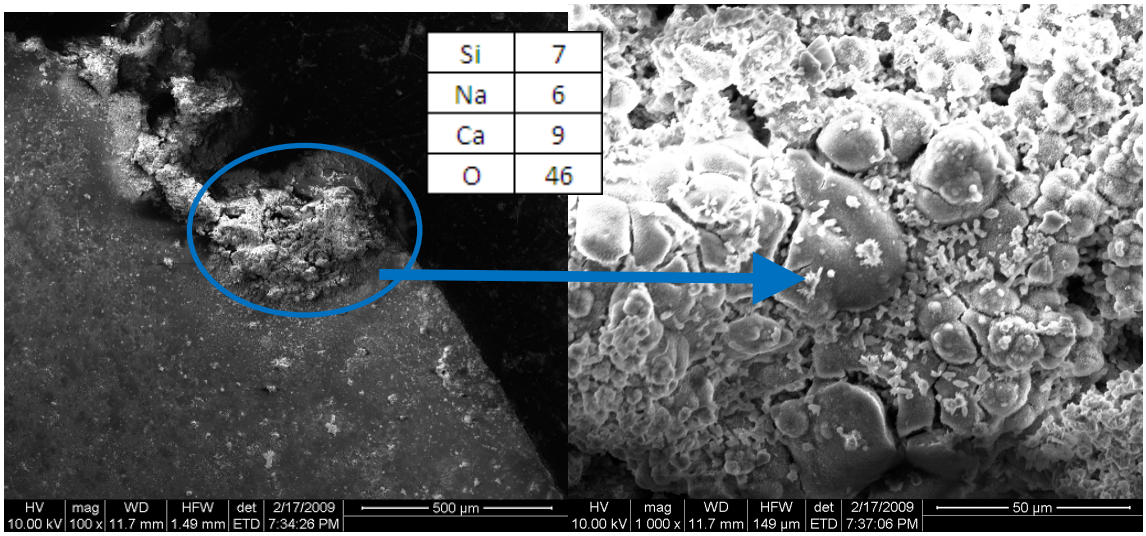

Figure 71 Gel Deposit on Edge of Chert Particle Reacted for Seven Days with Average Elemental Composition from Elemental Composition from EDS Analysis

The product from seven days reaction has a much larger ratio of sodium to calcium than the four-day reaction product.

4.3.5 Twenty-Eight Day Results

Numerous deposits were observed on the surface of the chert specimen that was reacted for twenty-eight days. An example of one of these deposits is presented in Figure 72 along with the average EDS analysis for the product.

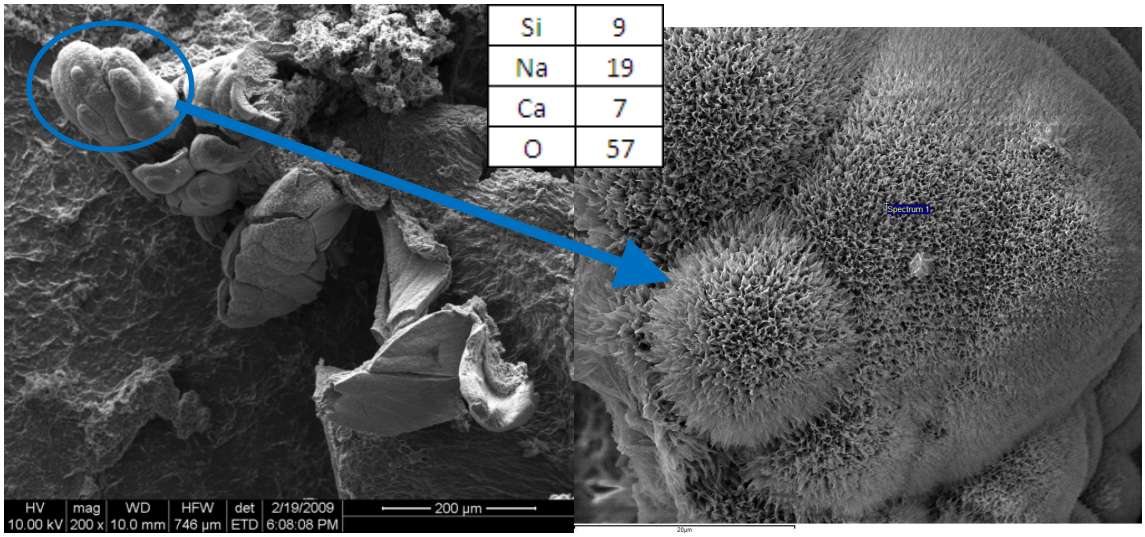

Figure 72 Gel Deposit on Surface of Chert Reacted for 28 Days with Average Elemental Composition from EDS Analysis

This product has much more sodium than the product observed at seven days reaction. The average ratios of sodium to calcium, sodium to silicon, calcium to silicon, and silicon to oxygen for the deposits on the surface at different ages are presented in Table 10.

Table 10 Average Elemental Ratios for Deposits at Different Reaction Ages

Age	Ave Na:Ca	Ave Si:O	Ave Na:Si	Ave Ca:Si
4	0.63	0.24	0.53	0.81
7	0.86	0.17	0.92	1.13
28	4.21	0.18	1.80	0.60

Elemental ratios corresponding to specimen of two days reaction are not available as no deposits were found on the surface of specimen after two days of reaction. The sodium to silicon ratio increases from four days to twenty-eight days. The calcium to silicon ratio increases from four to seven days, but then decreases from seven to twenty-eight days. The silicon to oxygen ratio decreases from four to seven days but then remains

relatively constant. The sodium to calcium ratio increases from four to twenty-eight days. At four and seven days, the ratio is less than unity, indicating that there is more calcium than sodium; but, at twenty-eight days, it indicates that there is almost twice as much sodium as calcium. This appears to indicate that calcium is initially the primary ion involved in the formation of the product but at later times sodium is the primary ion involved.

4.4 Beam Test

The results of the beam test are presented in Figure 73.

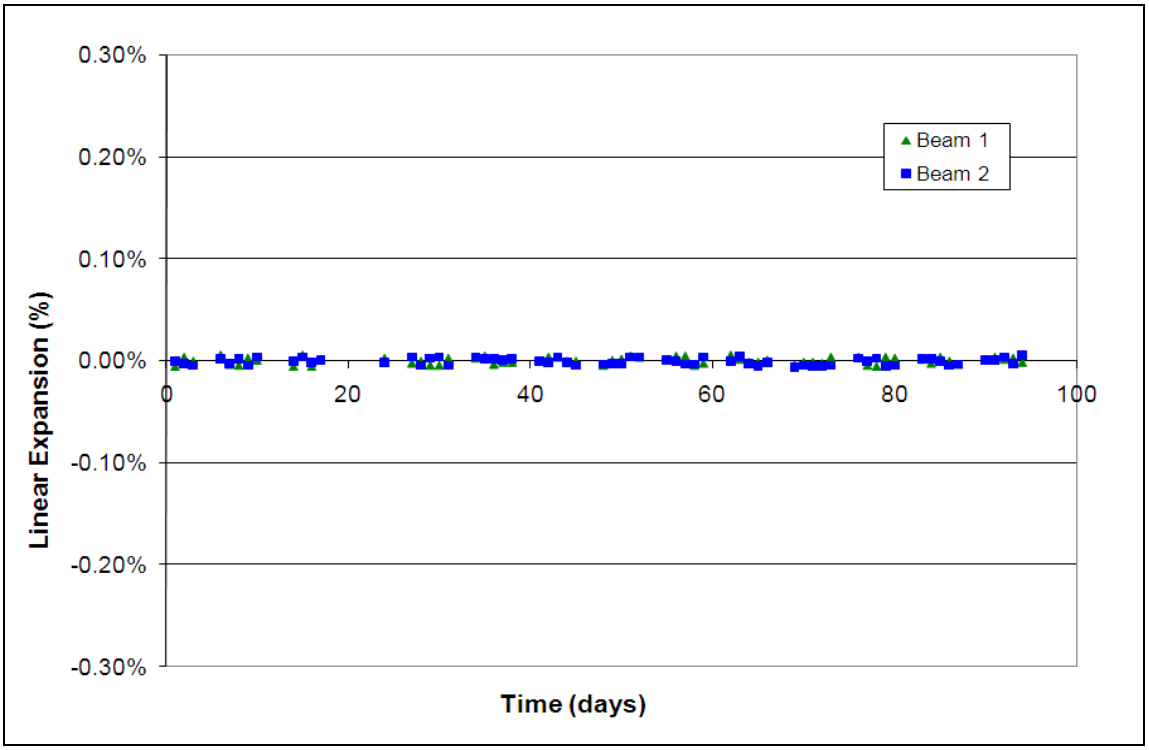

Figure 73 Expansion Results from Modified Beam Test

No increase in length of the beams was apparent from the beam tests. The noise in the data is likely due to the difficulty of mounting the measuring studs perfectly in the beam. The results of the beam tests partially support the results of the dilatometer tests.

Since the volume changes measured in the HMA dilatometer testing are believed to be a result of the interaction between the binder and the solution and not the ASR reaction, the lack of change in the beam lengths is consistent. The beam only measures effects caused by the aggregate and not due to changes in the solution or the mastic. Since the dilatometer measures volume changes in the whole system, it is expected to be more sensitive than the beam test. Since no expansion was recorded and proper placement of the measurement studs is very difficult, further testing of the beams was not conducted.

From the limited test results, it is expected that any volume change due to the binder-solution interaction will not be manifested as any measurable total solid volume change in the field. However, this may not be true in case of deicer reaction with HMA in the field. The experiments with accelerated conditions (direct immersion in concentrated K-acetate) showed that some ASR took place along with the binder-solution interaction. However, in the field, the degree of ASR depends on the degree of penetration of deicers through interconnected voids as well as cracks, which affects the number of reaction sites. More penetration and reaction sites can be responsible for a higher degree of ASR in some specific circumstances. It would be interesting to collect field performance data from HMA field sections made using reactive aggregate with extensive use of deicers. If no evidence of ASR is observed, it is possible to say that measurable ASR expansion due to deicers in HMA is probably a remote possibility.

4.5 Lottman Test

The results of the Lottman testing on compacted HMA specimens are presented in Table 11.

Table 11 Lottman Test Results

	Chert	ED RCA	HL RCA
TSR	80%	100%	96%
TSR_{ND}	82%	104%	101%
TSR_{NW}	103%	104%	106%
$TSR_{6.5}$	*	85%	95%
$TSR_{ND6.5}$	*	76%	91%
$TSR_{NW6.5}$	*	85%	95%

*Specimens were too soft to test

TSR is the standard tensile strength ratio of specimens conditioned in water at 60°C for 24 hours as compared to specimens left dry, as required by ASTM D 4867. The TSR_{ND} is the ratio of tensile strength of the specimens conditioned in 0.5N NaOH solution at 60°C for 24 hours to the tensile strength of those left dry. The TSR_{NW} is the ratio of tensile strength of the specimens conditioned in 0.5N NaOH solution at 60°C for 24 hours to the tensile strength of specimens conditioned in water at 60°C for 24 hours. The $TSR_{6.5}$ is the ratio of tensile strength of the specimens conditioned in water at 60°C for approximately 6.5 days to the tensile strength of those left dry. The $TSR_{ND6.5}$ is the ratio of tensile strength of the specimens conditioned in 0.5N NaOH solution at 60°C for approximately 6.5 days to the tensile strength of those left dry. The $TSR_{NW6.5}$ is the ratio of tensile strength of the specimens conditioned in 0.5N NaOH solution at 60°C for approximately 6.5 days to the tensile strength of specimens conditioned in water at 60°C for approximately 6.5 days.

None of the specimens showed a damage index below the 70% limit. The results for the chert specimens indicate that some moisture damage had occurred in specimens conditioned in both water and NaOH solution for 24 hours. Because of the variability of the Lottman results, the results for both RCAs indicate that little if any moisture damage occurred in 24 hours. These results are supported by observations made during the breaking of the specimens. After breaking, moisture was observed throughout the cross-section of the specimens made using chert. In addition, failure of the specimens occurred in the binder and at the binder aggregate interface, as presented in Figure 74.

Figure 74 Fracture Cross-Section of Chert Specimen Conditioned in Water for 24 Hours

In contrast, significant moisture was only observed in the outer 1/2 inch to 1 inch of the cross-section of the specimens made with RCA. Additionally, many of the aggregates were broken through the mortar fraction, as presented in Figure 75 .

Figure 75 Fracture Cross-Section of ED RCA Specimen Conditioned in Water for 24 Hours

Most of the broken mortar sections appeared dry, in contrast to the 6.5-day results presented below.

The results at approximately 6.5 days indicate that some moisture damage occurred in the specimens made with RCA. No results are available for the chert specimens because they became too soft to test successfully. For the ED RCA specimens, the NaOH solution is causing greater damage than the water alone. It appears that the same may be true for the HL RCA specimens but the difference may be due to the variability of the test results. The increased moisture damage is supported by visual observations made during the breaking of the specimens. Moisture was observed throughout the cross-sections of the specimens including in moisture in the mortar fractions of the broken aggregates, as presented in Figure 76.

Figure 76 Fracture Cross-Section of ED RCA Specimen Conditioned in Water for 6.5 Days

Less breakage of the mortar fractions was observed in comparison to the 24-hour specimens. In the specimens made using ED RCA, some failures at the aggregate-binder interface were observed for the granitic coarse aggregate from the RCA.

Since the binder grade selected for this study was chosen to reduce the stripping that was observed on loose HMA specimens made with chert during the initial

dilatometer at 70°C, the observed tensile strength losses may not be as significant as would be observed with other binders. However, the chert, which typically has high moisture susceptibility, shows much greater strength loss than the two RCAs, as expected. With a softer binder, the chert would likely fail to meet the 70% minimum TSR required by most agencies who use the Lottman test.

There appears to be a correlation between the coarse aggregate used in the original concrete and the moisture susceptibility of the HMA made from the RCA, which is also demonstrated by the micro calorimeter results, as presented below. This would indicate that ASR-RCA containing reactive coarse aggregate is more likely to be moisture sensitive, since HMA mixtures containing siliceous aggregates tend to have greater moisture susceptibility (*49-52*).

4.6 Micro Calorimeter

The heat-flows in the micro calorimeter for each test of unreacted chert (UC), chert reacted with 1N NaOH saturated with CH at 70°C for fourteen days (RC), Edwards RCA (ED), and Holloman RCA (HL)are presented in Figure 77.

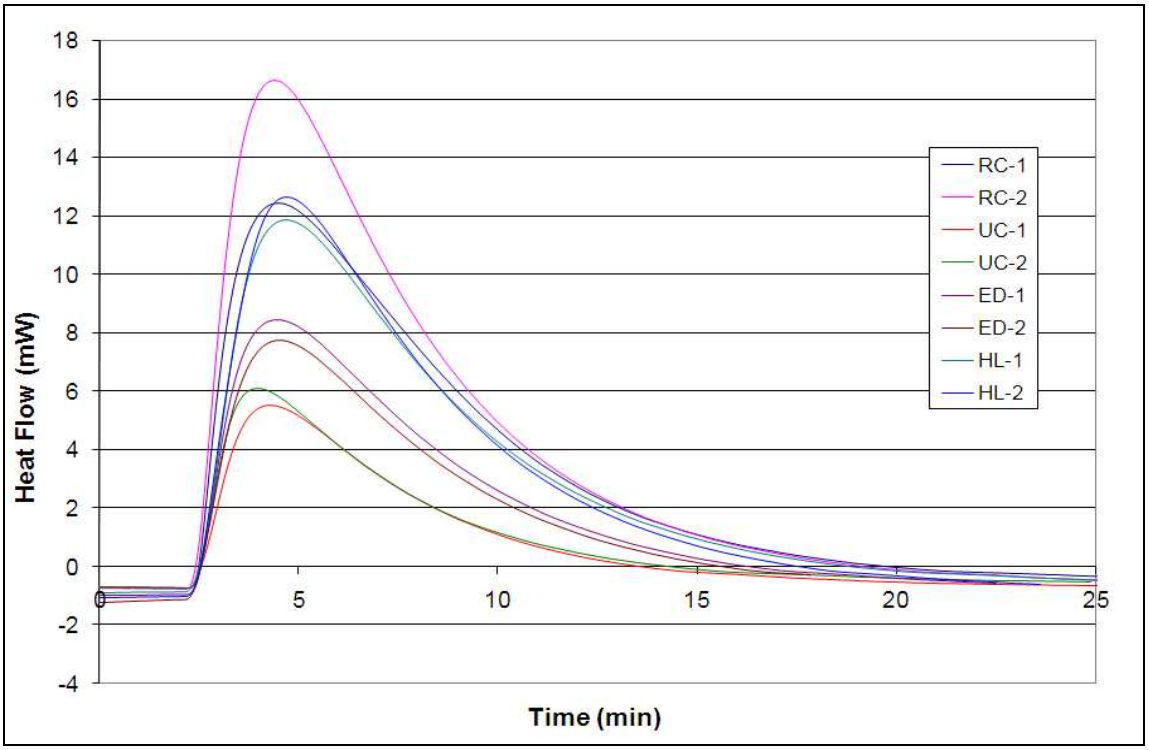

Figure 77 Heat Flow in Micro Calorimeter

The total energy of adhesion (TEA), as determined by integrating the area under the curve in Figure 77 for each test, is presented in Table 12. The TEA is proportional to the strength of the interfacial bond between the aggregate and the asphalt binder.

Table 12 Total Energy of Adhesion from Micro Calorimeter Test

Material	TEA (mJ/g)	CV
Unreacted Chert	295	16.8%
Reacted Chert	755	10.3%
Edwards RCA	425	11.6%
Holloman RCA	680	2.1%

The values presented in Table 12 are based on testing of two specimens. The unreacted chert has the lowest TEA, and the reacted chert has the highest TEA, with the two RCAs falling between the two. Neglecting the effects of surface area of the

specimens, the results agree with the Lewis Acid-Base theory used to estimate adhesion between two materials. Asphalt binders typically have a slightly acidic character and therefore are likely to bond better to basic materials. The unreacted chert is primarily composed of siliceous materials, which also tend to have an acidic character and therefore exhibit poor bonding with asphalt. The reacted chert has some basic character due to the ASR that has occurred at the aggregate surface. This would be similar to the effect of liquid anti-strip agents, which coat the aggregates and provide a more basic character prior to mixing with the binder. However, the products that may be increasing the adhesive energy may also have poor mechanical strength and therefore be of little value for increasing the strength of the bond. The coarse aggregates of the Edwards and Holloman RCAs are of a granitic and limestone, respectively. Since some of these aggregates would be broken down and end up in the finer fraction during crushing, it is anticipated that the nature of the coarse aggregate would influence the TEA. Mortar that has a basic nature is present in the samples as well, therefore, the combined effects of the coarse aggregate and mortar will determine the TEA. Since the granitic aggregate of the Edwards sample is less basic than the limestone of the Holloman sample, the lower TEA for Edwards seems reasonable.

The results of the micro calorimeter testing agree with the results of the Lottman testing. The micro calorimeter results predict that the unreacted chert should have the greatest moisture susceptibility, which was confirmed by the chert having the lowest TSR in the Lottman results. At 6.5 days, the ED RCA had lower strength ratios than the HL RCA, which agrees with the greater TEA for the HL RCA.

4.7 Differential Scanning Calorimeter / Thermogravimetric Analysis

The DSC was performed on samples of fresh artificial gel and gel that had been allowed to carbonate. The results from the fresh gel are presented in Figure 78.

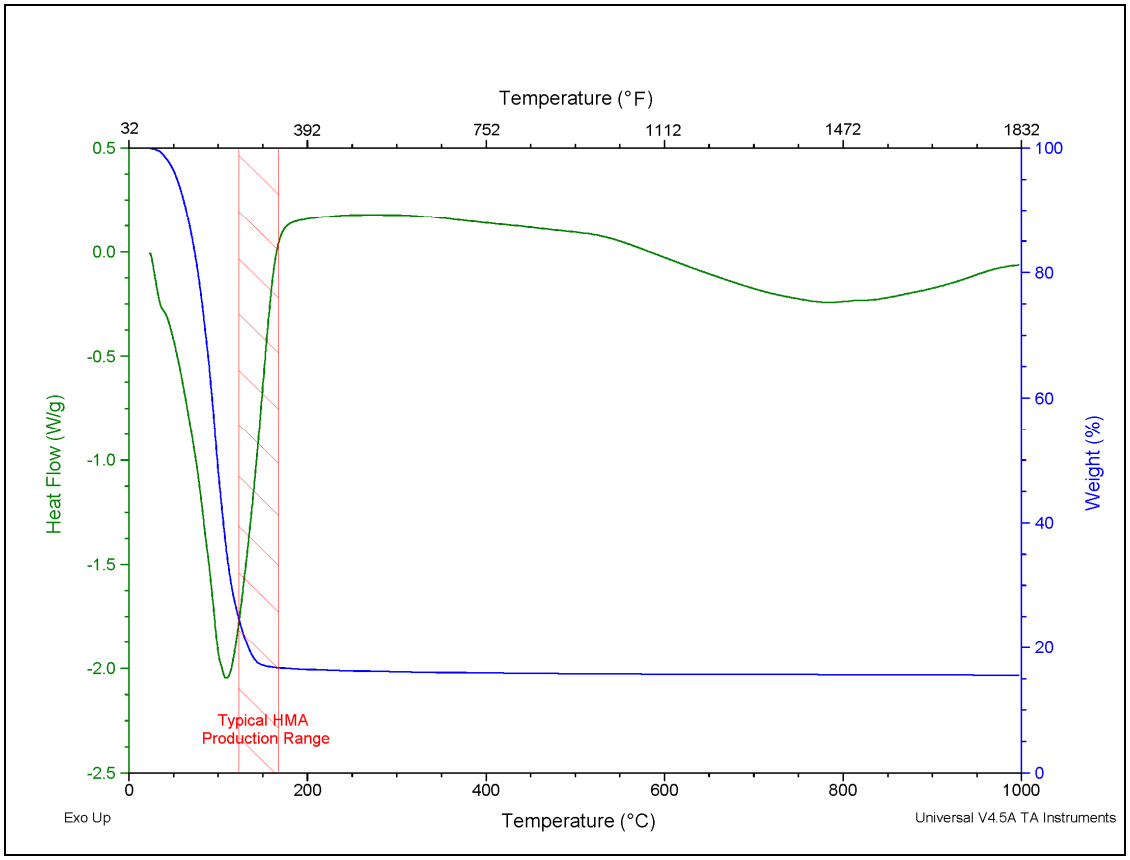

Figure 78 DSC and TGA Results from Non-Carbonated Gel

The initial endothermic peak (i.e., peak of negative heat flow) at 100°C is due to the removal of water from the gel. The artificial gel kept inside an environmental room at 23°C for two months in order to allow gel carbonation, which caused some portion of the gel to be converted to Ca-carbonate. The DSC/TG results of the carbonate gel are presented in Figure 79.

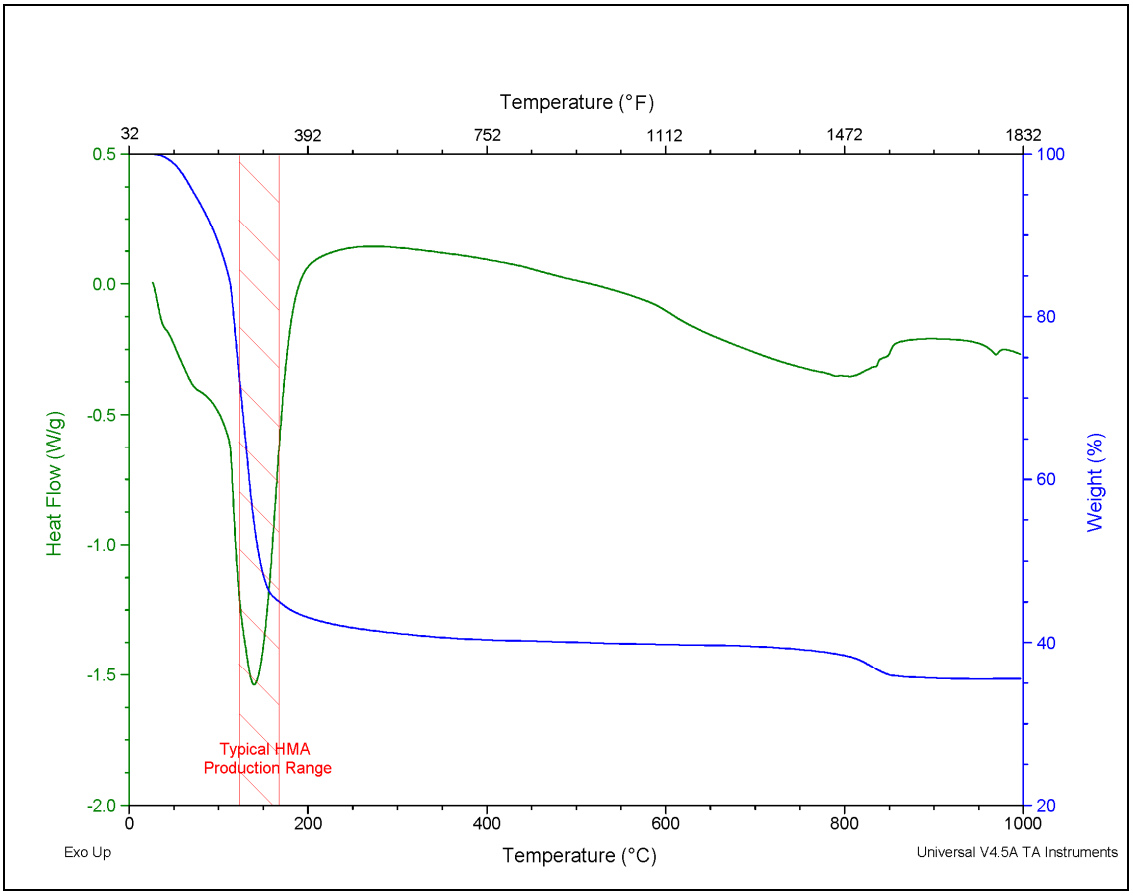

Figure 79 DSC and TGA Results from Carbonated Gel

The carbonated gel has similar results to the non-carbonated gel with an initial heat flow peak due to the loss of water but the peak is smaller since some of the gel has become carbonated. However, the peak at 800°C (1472°F) has become more defined, and a loss of weight due to the carbon dioxide is apparent. The second endothermic peak at 800°C represents decarbonation of Ca-carbonate formed during carbonation.

Carbonated gel will be less harmful within an HMA pavement as the carbonation will reduce the ability of the gel to reabsorb water and swell. Storing of ASR-RCA outdoors after it has been crushed will facilitate carbonation of the gel. In addition, since most of the water stored in the gel is lost between 100°C and 150°C (212°F and 302°F), extended drying in this temperature range would be preferred to ensure that the gel is fully dehydrated.

4.8 X-Ray Diffraction

The results of the XRD analysis of the filler fraction from ED RCA are presented in Figure 80.

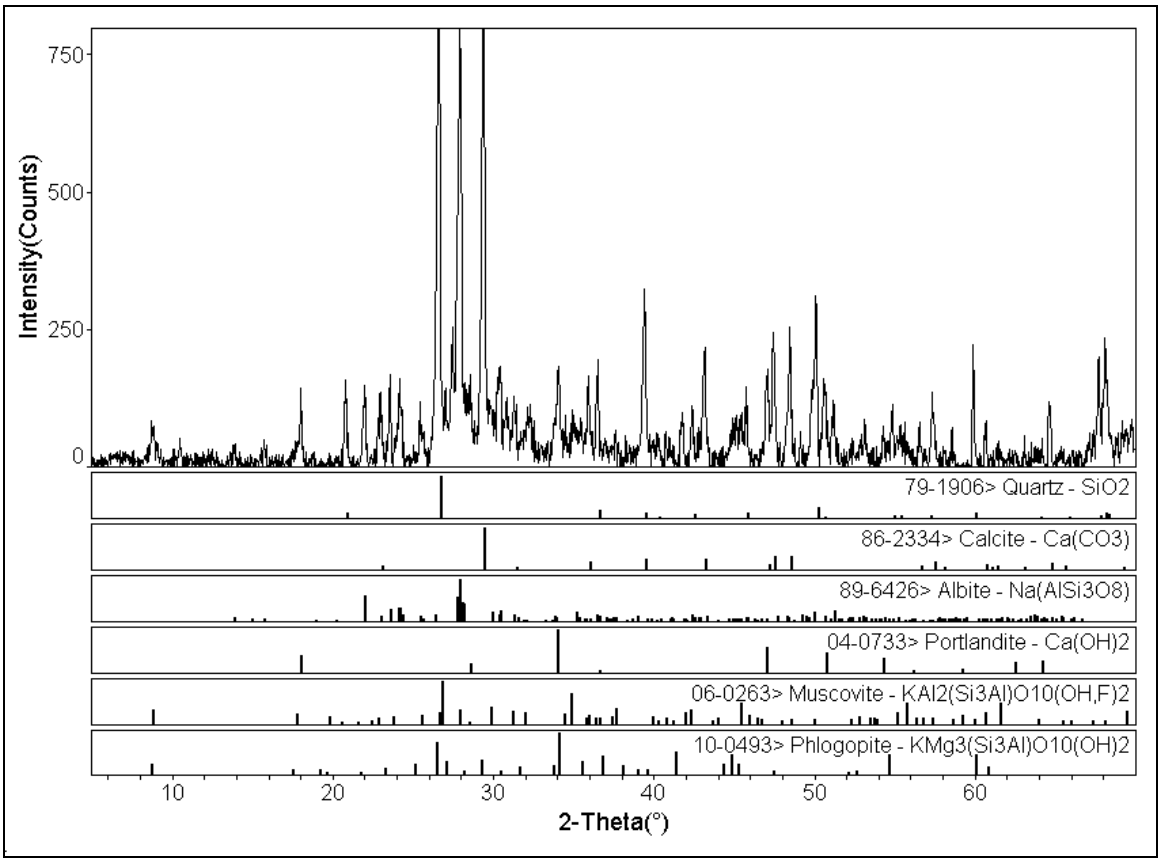

Figure 80 XRD Analysis of ED RCA Filler Fraction

The analysis indicates that the filler fraction is composed of quartz, calcite, portlandite, albite, muscovite, and phlogopite minerals. Quartz, albite, muscovite and phlogopite are from the granitic coarse aggregate as well as fine aggregate whereas Porlandite is from the mortar fraction of the ED RCA. The presence of calcite indicates that the cement paste and any gel that has concentrated to the filler fraction are carbonated. In addition, a slight hump in the analysis between approximately 25° and

35°, indicates the presence of amorphous material(s). The ASR gel as well as some C-S-H gel (from mortar) possibly constitutes the amorphous materials for the slight hump. This is an indication that gel is probably present in the filler fraction. However, since this hump is not very prominent and some C-S-H gel interferes with the results, the ASR gel concentration in the filler seems to be low and it does not represent solely the amorphous materials detected in XRD. Also, the analysis may underestimate the presence of gel since some of the gel has likely become carbonated to form calcite. The XRD analysis for the HL RCA filler fraction is similar as presented in Figure 81.

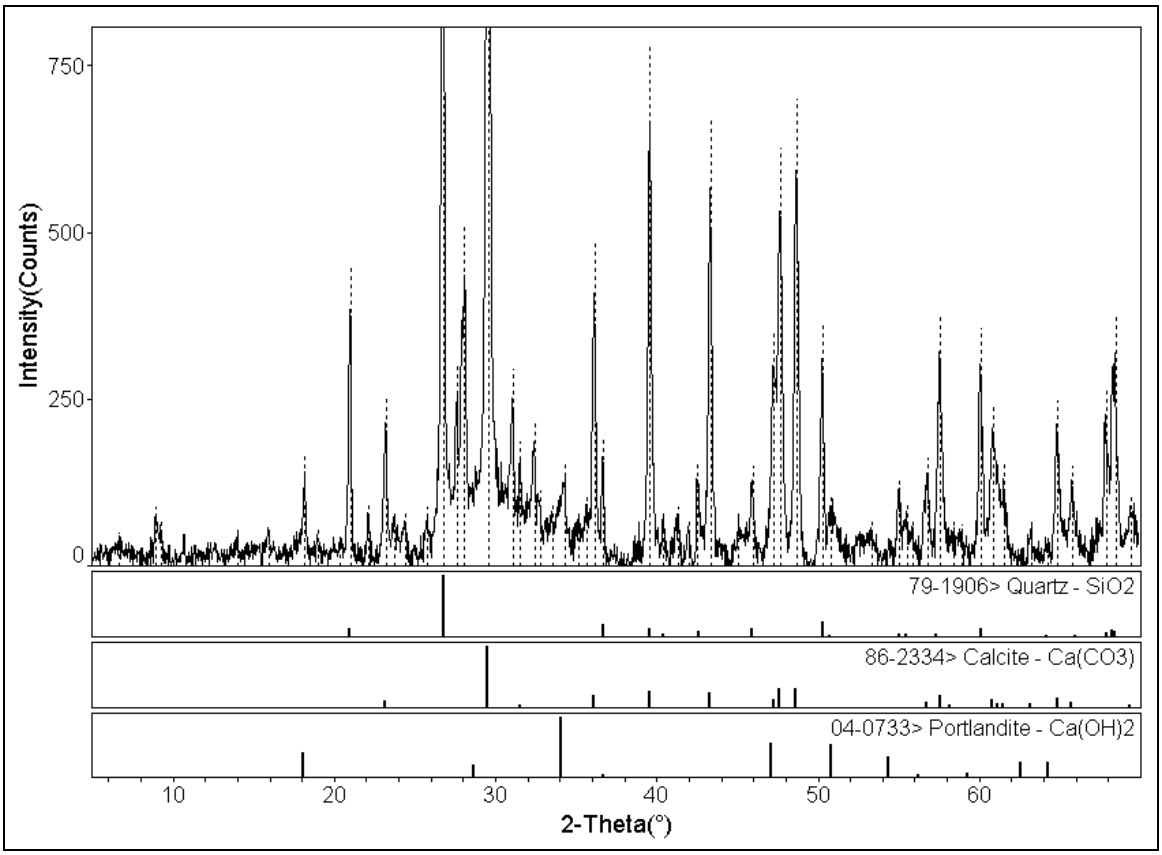

Figure 81 XRD Analysis of HL RCA Filler Fraction

As with the ED RCA filler, quartz, calcite, and portlandite are present in the filler fraction along with the hump indicating an amorphous material. For the HL RCA,

which contains a limestone coarse aggregate, there is more calcite than quartz. The presence of calcite in both the coarse aggregate of the original concrete and from carbonation of gel and the mortar fraction result in a larger peak for calcite than for quartz, which is only present in the fine aggregate. The magnitude of the hump is slightly higher in HL RCA than that in ED RCA, which possibly indicates the presence of more gel in HL RCA than ED RCA with the assumption that gel carbonation and C-S-H contribution in the hump is similar for both the RCAs. It is noteworthy that the fine aggregate is reactive in HL RCA which possibly facilitates concentration of gel in the finer fractions. Since both ASR-RCAs have the hump indicating the likely presence of gel, it appears to confirm the expectation that gel would concentrate to the finer fractions. Based on these limited results, it appears to be prudent to exclude the finer fractions from use in HMA to avoid the potential for expansion that they may cause due to re-hydration.

4.9 Micro-Deval

Results of the coarse and fine aggregate Micro-Deval tests are presented in Table 13 .

Table 13 Results from Micro-Deval Test

Material	Chert		HL RCA		ED RCA	
Size	Coarse	Fine	Coarse	Fine	Coarse	Fine
Average Mass Loss (%)	5%	13%	15%	13%	13%	16%
CV (%)	2.0%	5.6%	0.1%	0.2%	0.9%	9.2%

The results indicate that the RCAs have higher mass losses than chert in the Micro-Deval, as expected. This is likely due to the mortar contained in the RCAs, which is more likely to break down than the virgin aggregate. In addition, the results indicate that the fine fractions of the Chert and ED RCA have a higher mass loss than the coarse fraction, as expected. This is likely due to the increased surface area of the fine aggregates. For the ED RCA, the concentration of mortar to the finer fractions of the

RCA may also contribute to the increased mass loss. However, the fine fraction of the HL RCA showed a lower mass loss than the coarse fraction. Visual observation of the HL RCA particles before and after testing indicated that the limestone coarse aggregate was more susceptible to abrasion than the mortar that had accumulated in the fine fraction as discussed below.

The chert primarily consists of micro – and cryptocrystalline forms of silica (e.g., chalcedony as well as microcrystalline quartz). Some limestone particles always remain (by default) with the chert particles as fine chert aggregate was sieved from a chert-rich Texas gravel with limestone impurity. The chert particles were sharp, angular, and flat before testing in the Micro-Deval. After testing, the sharp edges and angular shape of the particles were maintained. The limestone particles in the chert fine aggregate had high texture and high angularity. However, after testing, the surfaces of the limestone particles were smoothed and the edges lost their sharpness. Due to the presence of these soft limestone particles, the mass loss of fine chert was recorded as relatively high. Otherwise, the mass loss for pure fine chert should be low, as expected. In that situation, the mass loss for both the RCAs will be higher than that for the virgin aggregate. A comparison of the chert particles before and after testing is presented in Figure 82.

a **b**

Figure 82 Stereomicroscope Images of Chert Particles (a) Before and (b) After Testing in the Micro-Deval

The coarse aggregate in the HL RCA is primarily limestone with minor amounts of rhyolitic rocks and quartzite. The limestone is relatively smooth and there are relatively high air voids in the concrete. The HL RCA coarse aggregate was very angular before the Micro-Deval test. After testing, the aggregates remained angular but their texture had been smoothed significantly. Therefore, the mass loss measured for the coarse aggregate was due to abrasion, which reduced the texture of the particles, and not due to particle breakdown. A comparison of the coarse HL RCA particles before and after testing is presented in Figure 83.

a **b**

Figure 83 Stereomicroscope Images of Coarse HL RCA Particles (a) Before and (b) After Micro-Deval Testing

The fine aggregate was primarily mortar and did not have as smooth of a texture as the coarse aggregate after testing. Some of the air voids in the fine fraction were filled with a white material that may be ASR gel. A comparison of the fine HL RCA particles before and after testing is presented in Figure 84.

a b

Figure 84 Stereomicroscope Images of Fine HL RCA Particles (a) Before and (b) After Micro-Deval Testing

Due to its brittle nature, the mortar fraction of the HL RCA was more likely to break up during the crushing process than the softer coarse limestone. Thus, more of the mortar concentrated to the finer fractions than the limestone. The soft limestone particles were more susceptible to abrasion in the micro-deval than the mortar fraction. Since there were greater quantities of limestone in the coarse fraction and greater quantities of mortar in the fine fraction, the coarse was more susceptible to abrasion in the micro-deval.

The coarse aggregate of the ED RCA is primarily granitic. The 13% loss for ED RCA coarse aggregate is higher than conventional granitic aggregate (3.5-7.5%), which is possibly due to ASR micro-cracking or the presence of mortar fractions. The ED fine aggregate was basically mortar with some pieces of coarse aggregate. A comparison of the fine ED RCA particles before and after testing is presented in Figure 85 . A slightly higher loss with fine aggregate is possible due to accumulation of more mortar fractions as well as gel. It seems that the nature of the samples for both coarse and fine fractions is similar which manifested as similar types of loss.

a b

Figure 85 Stereomicroscope Images of Fine ED RCA Particles (a) Before and (b) After Micro-Deval Testing

The differences between coarse and fine aggregate loss with ED RCA is not significant enough to verify that gel had accumulated in the finer fraction. The lower mass loss for the HL RCA fines and the fact that the ED RCA fines do not have a highly significant difference in mass loss from the coarse aggregate, indicate that the micro-deval test of the fine aggregate cannot be considered as a diagnostic tool to select or reject the ASR-RCA fines in HMA on the basis of the presence of ASR gel. A larger number of tests, satisfying statistical criteria, using several varieties of ASR-RCA are necessary in order to validate this conclusion. However, the micro-deval may still be used as a quality indicator for coarse and fine aggregate using the same guidelines as would be used for a typical RCA (*58-60*).

4.10 Freeze-Thaw

The results of the freeze-thaw testing are presented in Table 14.

Table 14 Freeze-Thaw Results

Material	Chert		ED RCA		HL RCA	
Size Fraction	Coarse	Fine	Coarse	Fine	Coarse	Fine
Average Loss (%)	0.7%	4.5%	1.1%	7.0%	2.8%	8.0%
CV	0.2%	5.5%	0.3%	3.3%	59.1%	4.4%

The RCAs have greater mass loss than the virgin chert aggregate from the freeze-thaw test, as expected. The possible presence of gel and micro-cracks in the mortar along with the greater porosity and lower strength of mortar compared to virgin aggregates are the likely causes of the higher mass loss for the RCAs. The high coefficient of variation (CV) for the coarse fraction of the HL RCA appeared to be due to the limestone coarse aggregate used in the concrete. In one of the samples, an aggregate particle had shattered as presented in Figure 86.

Figure 86 Stereomicroscope Image of Shattered Limestone Aggregate from HL RCA Coarse Aggregate Freeze-Thaw Test

All of the pieces of this particle passed through the sieve resulting in much higher loss than if only a small piece had broken off as appeared to have occurred with other particles. The tendency of the limestone particles to break down also explains why the HL RCA had greater mass loss than the ED RCA that contained granitic coarse aggregate.

The freeze-thaw test is performed on samples above 0.3 mm (No. 50 sieve). If the gel has preferentially concentrated to the minus 75µm (No. 200 sieve) fraction, then this test will not detect the effect of gel. Therefore, the freeze-thaw test does not appear to be able to detect the effect of gel in an ASR-RCA. However, it appears to be capable of detecting the effect of pre-existing micro-cracking due to ASR.

Although the micro-deval test is faster and simpler to perform than the freeze-thaw test, the freeze-thaw test seems more suitable for testing ASR-RCA. The damage caused to some limestone particles, as presented above, indicates that the freeze-thaw test can detect the presence of micro-cracks in the mortar and aggregate. In addition, there was a clear difference between the results of the coarse and fine fractions for the freeze-thaw test while the micro-deval did not seem to differentiate between the two size fractions. In addition, the micro-deval test appears to require some knowledge of the aggregates used in the concrete to make a good interpretation of the results from ASR-RCA. Therefore, it seems that the freeze-thaw test is more sensitive than micro-deval test to the effects of pre-existing ASR, especially micro-cracking.

4.11 Potential Distress Mechanisms

The potential distress mechanisms that might occur in HMA made with ASR-RCA are:

- Mechanical Degradation
- Existing ASR
- New ASR
- Binder Degradation

Mechanical degradation of the ASR-RCA may occur due to existing micro-cracks caused by ASR. These micro-cracks will be weak points within the aggregate particles and the pavement structure as presented Figure 87.

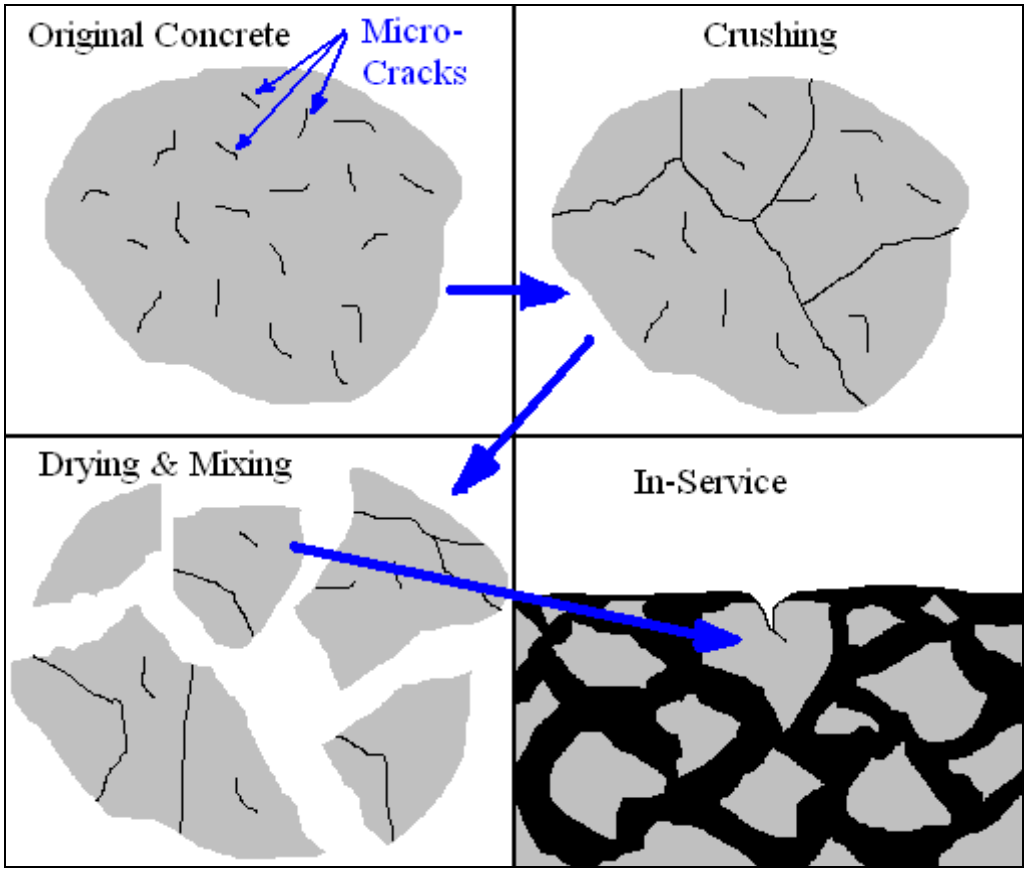

Figure 87 Effect of Micro-Cracks on ASR-RCA Breakdown

Micro-cracks may cause breakdown of the individual particles at several different stages of processing. The first of these is during crushing when micro-cracks will provide preferential planes for the breakdown of aggregates. However, the crushing process may not expose all micro-cracks. When the aggregates are dried and mixed with the asphalt binder, impacts between particles and with the mixing equipment may cause breaking along additional micro-cracks. Finally, while the HMA pavement is placed and in-service, traffic loadings may cause stress concentrations that will break down any micro-cracks that are still present. These cracks will be especially problematic if they allow moisture to enter the pavement structure and interact with the mortar fraction of the ASR-RCA.

Existing gel within the RCA particles may rehydrate and swell causing cracking within the pavement. However, if the gel is severely carbonated, the potential for rehydration of the gel will be greatly reduced. The longer the ASR-RCA is exposed to the atmosphere after crushing and prior to mixing with the asphalt binder, the greater the likelihood that the gel will be carbonated. Drying at high temperature (most effective in the case of a batch plant) will ensure additional carbonation (if the exposure outside in the first stage is not sufficient) as a second stage. Recall that the slow rate of carbonation was observed when the artificial gel kept outside for around two months time at room temperature. However, it is expected that long exposure of natural gel should ensure a considerable amount of carbonation before drying in an asphalt plant. It is noteworthy that the availability of calcium in the gel is another factor that controls the degree of carbonation.

Fresh faces of the reactive aggregate will be exposed during crushing. If moisture damage occurs or RCA particles at the surface of the pavement crack, then water may come into contact with the mortar fraction of the RCA. That water will then have a high alkalinity, which may initiate new ASR in the fresh faces of the reactive aggregates.

A reaction occurs between alkaline solution and asphalt binder. This reaction leads to swelling of the asphalt and weakening of the binder. In addition, moisture damage may occur without the alkaline solution especially for RCAs containing siliceous aggregates. Moisture damage may be more problematic if the pre-existing gel is not sufficiently dried and/or carbonated. This is an additional factor other than those applicable for any HMA-related moisture transport through interconnected voids and cracks, diffusion, etc.

5. FIELD IMPLICATIONS

The results presented in the previous section are from accelerated laboratory testing. As such, it is necessary to explore the differences in conditions between the laboratory testing and the field and what impact these differences will have on the field performance of HMA made with ASR-RCA.

5.1 Conditions

Although mild, the conditions used to accelerate the test process in the laboratory are still more severe than HMA made with ASR-RCA is likely to experience in the field. The dilatometer test is a constant immersion test while, in the field, the HMA will rarely be completely saturated. Also, the primary source of alkalis in the field are the mortar fractions attached with the RCA, provided enough moisture is available to release the mortar alkalis to form an alkaline pore solution. However, the application of deicers to an HMA pavement may provide additional alkalis.

It is anticipated that any volume change due to binder-solution interaction will not be manifested as any measurable total solid volume change in the field. However, this may not be true in the case of deicer reaction with HMA in the field. These experiments with accelerated conditions (direct immersion with K-acetate) showed that some ASR took place along with the main binder-solution interaction. However, in the field, the degree of ASR depends on the degree of penetration of deicers through interconnected voids as well as cracks and number of reaction sites. The more penetration and reaction sites can be responsible for a higher degree of ASR in some specific circumstances. It would be interesting to collect field performance data from HMA field sections made of reactive aggregate with extensive use of deicers. If no evidence of ASR or binder degradation is observed, it is possible to say that measurable expansion due to deicers in HMA is a probably a remote possibility.

The environmental conditions that the HMA will be subject to in the field will vary. Cycles of wetting and drying have been shown to exacerbate ASR in the field. In addition, temperature cycles, especially freeze-thaw cycles may accelerate deterioration

of the HMA and create a favorable situation for ASR. Along with the rate and type of deicer applications, these conditions are difficult to represent in the laboratory. Alkali redistribution, such as concentration of alkalis within certain areas of the pavement is also difficult to simulate in the laboratory.

5.1.1 Processing

An ASR-RCA is likely to go through several processing steps before being used in an HMA, many of which are likely to concentrate the reaction products in the finer fractions. These processing steps include crushing, sorting, handling, and mixing.

Since concrete is typically removed in large pieces, crushing is necessary to reduce these pieces to a size range suitable for use in HMA. ASR products tend to cause cracks and micro-cracks in the surrounding area due to their expansive pressure. Therefore, crushing will likely cause both the mortar fraction and the coarse aggregate to break at areas where ASR products have occurred due to the preexisting cracks in those areas. This will expose those products to mechanical action during the other steps. Alternatively, the ASR products may be separated from the larger particles during crushing. In this case, the ASR products will be found in the finer portions of the crushed material.

After the ASR-RCA is crushed, it is typically sorted into various size fractions by mechanical means, typically by shaking it over screens of particular sizes. This shaking action will cause some abrasion of the ASR-RCA as the particles collide. Since the ASR products have lower abrasion resistance than the mortar and aggregate portions of the concrete, the ASR products are likely to be removed and concentrated to the finer fractions more readily than the mortar and aggregate portions.

After sorting, the ASR-RCA would be placed into stockpiles until it is transferred to the HMA. Both the stockpiling and transfer operations may cause some additional abrasion due to the movement of the particles past one another. The ASR products are likely to concentrate to the finer fractions as described above.

During mixing, the ASR-RCA will be subject to additional abrasion, which will occur at higher temperatures. In a drum plant, this will occur as the ASR-RCA is lifted

and dropped by the flights of the drum. In a batch plant, this will occur in the aggregate dryer as the ASR-RCA is tumbled in a stream of hot air. Some additional abrasion may occur in the pugmill of the batch plant as the ASR-RCA is mixed with the hot asphalt binder. The effects of the different types of HMA production are discussed in the following section.

During each of the above steps, the ASR-RCA and any gel it contains have the potential for carbonation. This is especially true for the stockpiling step if the material is left in stockpiles exposed to the atmosphere for extended periods. A relatively lower pH of the RCA-water system (11.0-11.5) than normal non-carbonated concrete pore solution is possibly due to the combined effects of carbonation and dilution. The carbon dioxide and heat from the exhaust gases during aggregate drying for HMA production can also increase the carbonation of the ASR-RCA and any gel that it contains.

5.1.2 HMA Production

The type of HMA production will affect the degree to which the gel is dehydrated. There are two main types of HMA production, batch plants and drum plants. In addition, the emerging technology of warm mix asphalt (WMA) should be considered.

Batch plants are the type of plant most commonly used in Europe and are representative of the method used to produce the HMA specimens used in this study. A schematic of a typical batch plant is presented in Figure 88.

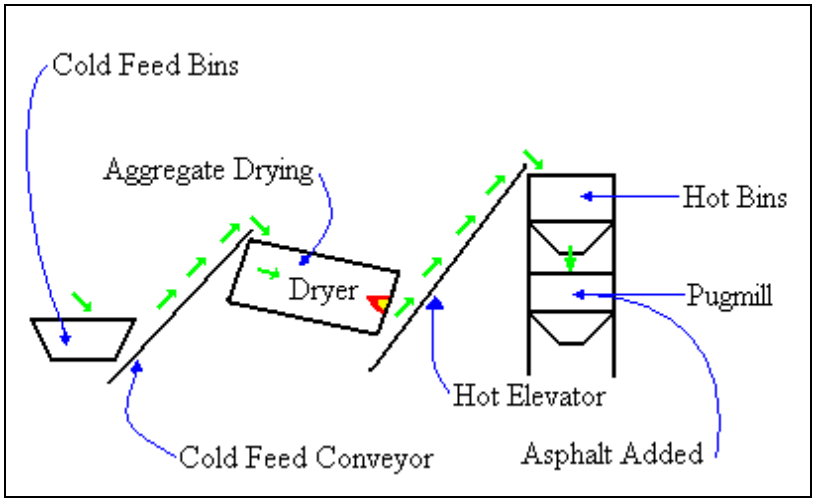

Figure 88 Schematic of Typical HMA Batch Plant

In a batch plant, the aggregates are thoroughly dried and then stored in hot bins. The desired amounts of each aggregate type are then transferred to the pugmill where it is mechanically mixed with the asphalt binder. Batch plants allow for greater control of the quantities of materials used in the HMA but have lower production rates than drum plants. The dehydration process, removal of water / moisture from ASR gel as well as mortar fractions, can most effectively achieved in the batch plant. It can also facilitate some additional carbonation.

Drum plants are the type of plant most commonly used in the United States. A schematic of a typical drum plant is presented in Figure 89.

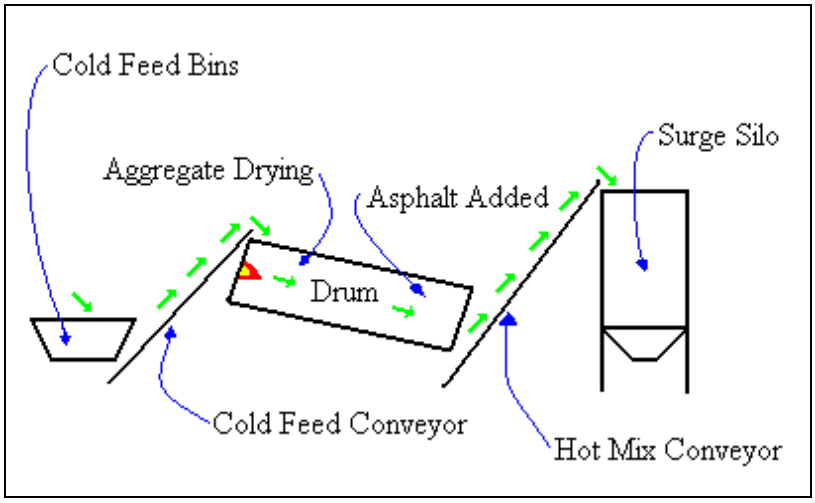

Figure 89 Schematic of Typical HMA Drum Plant

In the drum plant, the aggregates are introduced at the beginning of the drum and drying takes place as the aggregates move along the length of the drum. Continued loss of moisture from the aggregates when the asphalt binder is added is required to cause the asphalt to foam in order to better coat the aggregates. Since mixing is a continuous process in the drum plant, production rates are higher than for batch plants but control of material quantities is more limited. In addition, since there is a requirement for some moisture in the aggregates at the time of mixing, drum plants may not dehydrate the gel completely.

WMA is produced at temperatures of 28-55°C (50-100°F) lower than conventional HMA. The lower temperatures are achieved through the use of additives to the asphalt binder, which decrease its viscosity at high temperatures without significantly affecting the properties at the service temperatures. Because of the lower temperatures at which WMA is produced, the gel in RCA may not be fully dehydrated during the mixing process.

5.2 Potential Impacts

If water penetrates to the mortar of ASR-RCA, two potential reactions may occur according to the test results. One is ASR and the other is the reaction between an alkaline solution and the asphalt binder. A schematic of this is presented in Figure 59.

The test results indicate that the reaction between the alkaline solution and the asphalt binder occur more rapidly than ASR. Thus, softening of the binder will likely occur initially but may allow for greater moisture damage and then ASR at a later time. The asphalt binder provides some moisture protection to the ASR-RCA initially. However, moisture will eventually be available with varying degree to the mortar fractions through combination of diffusion, ASR micro-cracks in the RCA, and some kind of moisture damage. As a result, OH^- and alkali ions will be released and generate a mild alkaline solution (pH = 11.0-11.5), which can create some new ASR on the fresh aggregate surfaces in extreme cases. However, the pH of the solution may not be sufficiently high to develop any measurable new ASR. Deicer application can make the solution pH relatively high (~ 12.0) in certain circumstances, which can cause more ASR than without deicers. In PCC, gel imbibes additional water and swells, which creates expansive pressure. It is unusual that this additional water requirement will be satisfied in HMA pavement solely from external sources. Therefore, some new gels may form on fresh aggregate surfaces but they will not be expansive in general due to lack of moisture/water. Since the asphalt binder is a visco-elastic material, it will be able to absorb some of the expansion caused by ASR (if any), especially if the ASR occurs during periods of elevated temperature. As a result, solid volume increase due to binder-solution interaction (swelling) and expansion of new ASR gel (if any) or re-hydration (expansive) of existing gel will either not be manifested at all or would take longer than the service life of HMA pavement made using ASR-RCA. However, binder-solution interaction and any ASR may not be a primary cause of failure, but micro-crack formation due to ASR can create a favorable situation for another distress (especially moisture damage).

Although the dilatometer testing indicated that ASR might still occur in HMA made with ASR-RCA exposed to deicer solution at its original concentration, the dilatometer conditions can still be considered more severe than the field. In the dilatometer, the compacted HMA specimen was completely surrounded by a large quantity of solution that maintains a constant supply of deicer, but in the field the deicer

would only be applied at the surface. Therefore, only deicer that penetrated the HMA pavement through cracks or diffusion would be available for ASR. In addition, the deicer would be subject to washing away or dilution by rain or melted snow and ice.

ASR-RCA is likely to be weaker than virgin aggregates and other RCA's. As such, it will have a greater tendency to break down during HMA production and in service. Adjustments can be made to the input materials for HMA production to account for the change in the gradation of the ASR-RCA during processing. If the ASR-RCA breaks down at the surface of the pavement, it will allow for increased moisture ingress.

6. CONCLUSIONS AND RECOMMENDATIONS

The dilatometer test was used to successfully classify the expansion of the virgin aggregate and the two ASR-RCAs. For the virgin aggregate, increases in temperature or solution normality produced the expected increases in volumetric expansion. However, for the dilatometer tests of HMA, the interpretation of the results is not as clear due to the complexity of the system. The interactions occurring include:

- Saponification or neutralization of naphthenic acids in the asphalt binder by the alkaline solution and heat energy
- Emulsification of some of the asphalt binder
- Moisture damage or stripping of some asphalt from the aggregate surfaces exacerbated by high alkalinity and temperature
- Incomplete saturation of the compacted specimens or absorption by the dried aggregates following moisture damage

The tests using virgin aggregate indicate that asphalt binder provides some protection against ASR by blocking moisture access to the aggregates and by neutralizing some of the hydroxyl in the solution. There was evidence that ED HMA specimens tested in the potassium acetate deicer may have had some occurrence of ASR.

No expansion was measured in the modified beam test. This supports the observation that the reaction occurring in the compacted HMA dilatometer tests was primarily the saponification reaction between the naphthenic acids and the sodium hydroxide solution. The volume change due to saponification (swelling in the dilatometer test) was not manifested as measurable solid linear expansion in the beam test.

Virgin chert was found to have the highest moisture susceptibility of the aggregates tested. HMA specimens made with chert had the lowest TSR between wet and dry conditioned specimens in the Lottman test. In addition, the chert samples had the lowest total energy of adhesion in the micro calorimeter test, which also indicates the greatest moisture susceptibility. ED RCA had slightly higher moisture susceptibility

than HL as indicated by its lower values of TSR and TEA. This difference can primarily be attributed to the coarse aggregate used in the original PCC with the granitic aggregate from the ED RCA having greater moisture susceptibility than the limestone aggregate from the HL RCA.

Differential scanning calorimeter testing and thermogravimetric analysis of artificial gel indicates that the gel loses water at approximately 100°C (212°F), which is lower than the temperatures to which the aggregates are typically heated during HMA production. In addition, gel that was allowed to carbonate had a lower water content by weight and had additional weight loss due to the loss of carbon dioxide at approximately 800°C (1472°F). Carbonation of the gel will reduce the potential for the gel to re-expand if it comes into contact with water.

The micro-deval and freeze-thaw tests were unable to detect the presence of gel in the coarse or fine fractions of the RCA. However, these tests remain useful to check the quality of the aggregates, especially for the presence of excessive micro-cracks which could lead to aggregate breakdown during HMA production or in-service. It seems the freeze-thaw test is more sensitive than micro-deval test to detect the effect of pre-existing ASR, especially micro-cracking.

6.1 Use of ASR-RCA in HMA

6.1.1 Recommendations

The following guidelines are suggested for the use of ASR-RCA in HMA:

- Any restrictions placed on the use of conventional RCA should also be used for ASR-RCA.
- It is advisable to store the crushed ASR-RCA outdoors for as long as possible to increase the carbonation of the gel and the mortar fraction. Increased carbonation of the gel will reduce its potential for future expansion through re-hydration. Increased carbonation of the mortar fractions in RCA will reduce the pH of alkaline solution (11.0-11.5) that may be generated through moisture-cement mortar interactions. The generated alkaline solution will be consumed mostly through faster binder-solution interaction, and its availability for any new

ASR will greatly minimized. The expansion due to binder-solution reaction as well as some ASR (if any) will mostly be absorbed by the visco-elastic asphalt binder and may not be manifested as any measurable solid volume change in the fields. However, binder-solution interaction along with some ASR in isolated sites can enhance the possibility of other distresses, e.g. moisture damage. Therefore, the occurrence of any new widespread ASR in HMA made using ASR-RCAs is a remote possibility.

- An effective drying at high temperature in the plant is necessary to ensure effective dehydration of gel, which will minimize the availability of additional moisture inside HMA pavement. It would be preferable to produce the HMA in a Batch Plant (if available) as it facilitates effective drying.
- It is recommended not to use the fines and filler from ASR-RCAs as ASR gel may preferentially accumulate in the finer fractions during crushing and sieving as demonstrated by the XRD analysis earlier. A proper blending with good quality fine aggregates will reduce the necessary binder content of the mix thereby reducing its cost.
- Efforts need to be made in order to reduce interconnected voids in HMA mixtures and therefore the ability of moisture to infiltrate the HMA.
- Conservative moisture damage criteria based on moisture damage testing can be introduced in order to reduce the potential for the moisture related problems.
- Although a moisture-damage resistant design is desirable, engineers may choose to restrict the use of anti-stripping agents in HMA made with ASR-RCA as they may provide additional OH^- for reactions. The limited results of the Lottman and micro-calorimeter tests from this study indicate good bonding between the ASR-RCA and the asphalt binder, negating the need for anti-stripping agents.
- Attention should also be paid to the reaction products and micro-cracks from other distresses, such as delayed ettringite formation (DEF) and alkali-carbonate reaction (ACR) that may present along with ASR in the RCA. Ettringite decomposes at high temperatures (110-114°C) to form meta-ettringite ± AFm ±

hemihydrate ± gypsum. The ettringite can reform (an expansive reaction) depending on temperature and water vapor pressure conditions in HMA pavement with or without any external source of sulfate (e.g., sulfate from soil below).

- It is advisable not to use HMA made using ASR-RCA in the portions of airfield pavements prone to receive greater impact due to aircraft landing (e.g., runway) or high traffic frequency. However, placing a quality surface course made using virgin aggregate on top of HMA made using ASR-RCA will probably minimize this issue.
- It is recommended to determine the level of ASR distress and the reactivity of the aggregate before making the RCA from the ASR-affected PCC pavement. The FAA Advisory circular (AC No: 150/5380-8, 2004) can be used for this purpose. This will assist in determining the proper utilization of ASR-RCA in HMA pavements depending on climate, traffic, and deicer applications as well as selecting the remedial measures. This is described in the next sub-section.

6.1.2 Condition Assessment and Aggregate Reactivity of the ASR-Affected PCC Pavement

The procedure for condition assessment in terms of assessing ASR distress levels (e.g., low, medium, high) is briefly described below

- Visual observation of degree of map-cracking and other expansive features (e.g., joint seal damage, joint misalignment, heaving / blow up, trench drain damage)
- Petrographic examination of the core specimens to determine presence and extent of gel and micro-cracks
- Identification of any other distresses (e.g., Delayed ettringite formation, freeze-thaw, alkali carbonate reaction, sulfate attack etc.) based on both visual as well as petrographic observations
- Assessment of ASR distress (e.g., low, medium, high) based on a combined rating system (described in detail in AC No: 150/5380-8)

Aggregate (from PCC pavement) alkali silica reactivity can be determined by the following procedures:

- Prepare RCA and test the RCA by dilatometer (RCA-solution test) to determine the reactivity.
- Separate the aggregates followed by crushing to conduct ASTM C 1260 ASR mortar bar testing.
- Measure residual expansion of concrete specimens determine by dilatometer or procedure similar to ASTM C 1293. As dilatometer is not yet a standard ASR test procedure, it is recommended to use ASTM C 1260 or 1293 tests in parallel with dilatometer test.

Aggregate quality assessment can be performed by conducting freeze-thaw and/or micro-deval tests as these tests were found suitable to detect the effect of pre-existing ASR micro-cracking.

In general, a high aggregate reactivity should coincide with a high ASR distress in the field. However, depending on climatic conditions and mix design controls, a highly reactive aggregate may not always show always high ASR distress or a low reactive aggregate may not always show a low distress in the field. Therefore, combinations such as high reactivity-low distress or low reactivity-medium distress may occur in some circumstances. Therefore, importance should be given to both (i) degree of micro-cracking and gel abundance, and (ii) reactivity of the aggregate, in order to find a better utilization of the ASR-RCA. The recommended guidelines for use of ASR-RCA based on reactivity, distress level, and HMA pavement conditions are presented in Table 15.

Highly reactive aggregates from a PCC pavement suffering from high level of ASR distress to be used in an HMA pavement subject to severe climate, high traffic loadings, and deicer application is the most severe case presented in Table 15. The highly reactive aggregates increase the possibility that new ASR may occur in the HMA if the aggregates are exposed to alkaline solution. Use of a harder binder and lower interconnected air voids is recommended in order to reduce the moisture susceptibility of

the mix thereby protecting the aggregates from moisture exposure. The severe climate and deicer application will increase the potential for moisture damage and exposure to alkaline solution. High levels of distress in PCC pavement indicate that there will be larger amounts of gel and micro-cracks in the RCA. Larger amounts of gel require longer drying times to ensure that all of the moisture is removed from the gel and also greater carbonation to reduce the potential for re-expansion of the dried gel. The larger amounts of gel are also likely to concentrate to the finer fractions of the RCA, and therefore the fines should not be used. The increased amount of micro-cracking in the RCA will increase its tendency to break down especially under high traffic or near the surface.

Low reactive aggregates from a PCC pavement suffering from medium level ASR distress to be used in an HMA pavement subject to mild climate, low traffic loadings, and no deicer application is one of the milder cases presented in Table 15. Since the aggregate reactivity is low, moisture susceptibility is not as significant an issue as anticipated for highly reactive aggregates. Also, the mild climate and lack of deicers even further reduces the potentiality of any new ASR to occur. Therefore moisture susceptibility requirements are not as stringent as for highly reactive aggregates because formation of alkaline solution will be much less likely to cause additional ASR. The medium level of distress indicates that there are still likely to be significant amounts of gel and/or micro-cracks in the RCA. As a result, greater carbonation, and extended drying will be needed as explained previously for the high distress situation. Similarly, the restriction on the use of the fines needs to be maintained, and the effect of micro-cracking under high traffic or near the surface is applicable.

Table 15 Guidelines for Use of ASR-RCA Based on Aggregate Reactivity, Pavement Distress Level, and HMA Pavement Conditions

PCC Condition		HMA Conditions			Remediation Measures
Reactivity	Distress*	Climate**	Traffic	Deicer	
High	High	Mild	Low	No	low air void connectivity♥, intense carbonation♦ and extended drying (batch plant recommended), do not use in surface course, do not use fines
High	High	Severe	High	Yes	harder binder, low air void connectivity♥, intense carbonation♦ and extended drying (batch plant recommended), do not use in surface course, do not use fines
High	Low	Mild	Low	No	low air void connectivity♥, normal carbonation♠ and drying (drum or batch plant), may use in surface course with caution, use fines with caution
High	Low	Severe	High	Yes	harder binder, low air void connectivity♥, normal carbonation♠ and drying (drum or batch plant), do not use as a surface course, do not use fines
Low	Medium	Mild	Low	No	intense carbonation♦ and extended drying (batch plant recommended), do not use in surface course, do not use fines
Low	Medium	Severe	High	Yes	intense carbonation♦ and extended drying (batch plant recommended), do not use in surface course, do not use fines
Low	Low	Mild	Low	No	normal drying (drum or batch plant), may use in surface course with caution, use fines with caution
Low	Low	Severe	High	Yes	normal drying (drum or batch plant), may use in surface course with caution, do not use fines

* High and medium distress levels are anticipated to result in greater mass loss in the freeze-thaw and micro-deval tests.

** Low temperature and low rainfall combination represents mild climate whereas high temperature and high rainfall combination represents severe climate

♥ If the results of moisture susceptibility testing (such as the Lottman test) indicate strong resistance to moisture damage, then the requirement of low air void connectivity may be waived in order to minimize the cost.

♦ May need to keep ASR-RCA outdoors for longer time period and/or spread stockpiles more thinly, an approximation of degree of carbonation may be determined by measuring the pH of ASR-RCA immediately after crushing then measuring the pH of ASR-RCA that has been allowed to carbonate in the stockpiles. The reduction in pH will provide an approximation of the degree of carbonation.

♠ Carbonation as a result of normal stockpiling practices.

6.2 Additional Research

The recommendations presented in Table 15 are based on the limited results of this study. Additional research is needed to confirm that all of the remediation measures listed for each reactivity, distress level, and HMA condition are suitable and effective.

The effect of ASR-RCA fines was not definitively established in this study. Additional research into the impact of these fines on HMA properties is needed. Also, guidelines on blending ASR-RCA fines with fines from quality virgin aggregates need to be developed.

Determine the carbonation rates of ASR-RCA during field storage through pH monitoring and petrographic studies to provide guidelines regarding effective storage time.

Determine the moisture content of ASR-RCA at the completion of drying in the two different types of production facilities to provide guidelines regarding effective drying.

Generate large volume of moisture susceptibility data using different asphalt binders when combined with varieties of ASR-RCAs. Both Micro calorimeter and Lottman test should be used for this purpose in order to establish a better way to quantify the moisture susceptibility.

In order to understand fully the long-term effects of using ASR-RCA in HMA, a field study of sections of HMA pavement made with ASR-RCA should be conducted. Factors such as (i) high rainfall, dry climate, (ii) high traffic, low traffic, (iii) with and without deicers, (iv) cold and hot climate can be effectively incorporated during test section selection and design process. This will allow construction of test sections with extreme situations, e.g., (i) one section under high rainfall and traffic conditions with deicers application – high severity case, (ii) another section under dry climate, without deicers, less traffic – less severity case

The following data would need to be monitored during a long-term study:

- Alkalinity of solution within the HMA – efforts need to be made to verify whether current practice of pore solution extraction for PCC materials can be applied to HMA materials. Otherwise, different methods need to be explored.
- Solution pH in the HMA
- Expansion monitoring of the HMA pavement (similar to PCC pavement)
- Petrographic investigation of cores samples periodically taken from the test section – information pertaining to (i) occurrence of any ASR products, micro-cracks, (ii) binder softening and presence of microcracks in binder, will be gathered.

Another area for potential research would be a forensic study of in-service HMA pavements containing ASR reactive aggregates blended with normal RCA to which de-icing chemicals have been applied. This would examine the potential for reaction between reactive aggregates and deicing chemicals. The study would include:

- Petrographic examination of the aggregates to determine if ASR had occurred and, if so, to what extent
- Cracking initiating in the pavement layer of interest
- Climatic conditions (e.g., rainfall, relative humidity, temperature)
- De-icing solution application times and rates
- Alkalinity of solution within the HMA
- Solution pH in the HMA

REFERENCES

1. Lea, F.M. *Lea's Chemistry of Cement and Concrete*. 4th ed, P.C. Hewlett, ed. Arnold, London, 1998, pp. 1-1053.

2. Lane, D.S. *Alkali-Silica Reactivity: An Overview of a Concrete Durability Problem*. USA ASCE, New York, 1992, PP. 4-32.

3. Wang, H. and J.E. Gillott, Mechanism of Alkali-Silica Reaction and the Significance of Calcium Hydroxide. *Cement and Concrete Research*, Vol. 21, No. 4, 1991, pp. 647-654.

4. Chatterji, S. Role of Ca(OH)//2 in the Breakdown of Portland Cement Concrete due to Alkali-Silica Reaction. *Cement and Concrete Research*, Vol. 9, No. 2, 1979, pp 185-188.

5. Chatterji, S., N. Thaulow, A.D. Jensen, and P. Christensen. Studies of Alkali-Silica Reaction. Part 3. Mechanisms by which NaCl And Ca(OH)//2 Affect The Reaction. *Cement and Concrete Research*, Vol. 16, No. 2, 1986, pp. 246-254.

6. Chatterji, S., N. Thaulow, A.D. Jensen, and P. Christensen. Mechanisms of Accelerating Effects of NaCl and Ca(OH)2 on Alkali-Silica Reaction. *Proceedings of the 7th International Conference on Alkali-Aggregate Reaction in Concrete*. Ottawa, Canada, 1986. pp. 115-124.

7. Chatterji, S., N. Thaulow, and A.D. Jensen. Studies of Alkali-Silica Reaction: Part 4. Effect of Different Alkali Salt Solutions on Expansion. *Cement and Concrete Research*, Vol. 7, No. 5, 1987, pp. 777-783.

8. Chatterji, S., N. Thaulow, and A.D. Jensen. Studies of Alkali-Silica Reaction, Part 6. Practical Implications of a Proposed Reaction Mechanism. *Cement and Concrete Research*, Vol. 18, No. 3, 1988, pp. 363-366.

9. Chatterji, S., N. Thaulow, and A.D. Jensen. Studies of Alkali-Silica Reaction. Part 5. Verification of a nNewly Proposed Reaction Mechanism. *Cement and Concrete Research*, Vol. 19, No. 2, 1989, pp. 177-183.

10. Chatterji, S. Mechanisms of Alkali-Silica Reaction and Expansion. *Proceedings of the 8th International Conference on Alkali-Aggregate Reactio*n, Kyoto, Japan, 1989, pp. 101-106.

11. Chatterji, S. and M. Kawamura. Electrical Double Layer, Ion Transport and Reactions in Hardened Cement Paste. *Cement and Concrete Research*. Vol. 22, 2002. pp. 774-782.

12. Chatterji, S. Chemistry of Alkali-Silica Reaction and Testing of Aggregates. *Cement and Concrete Composites*, Vol. 27, No. 7-8, 2005, pp. 788-795.

13. Ponce, J.M. and O.R. Batic. Different Manifestations of the Alkali-Silica Reaction in Concrete According to the Reaction Kinetics of the Reactive Aggregate. *Cement and Concrete Research*, Vol. 36, No. 6, 2006, pp. 1148-1156.

14. Rivard, P., J.-P. Ollivier, and G. Ballivy. Characterization of the ASR Rim: Application to the Potsdam Sandstone. *Cement and Concrete Research*, Vol. 32, No. 8, 2002, pp. 1259-1267.

15. Hansen, W.C. Studies Relating to Mechanism by Which Alkali-Aggregate Reaction Produces Expansion in Concrete. *American Concrete Institute Journal*, Vol. 15, No. 3, Jan 1944, pp. 213-227.

16. McGowan, J.K., Vivian, H.E. Studies in Cement-Aggregate Reaction: Correlation Between Crack Development and Expansion of Mortars, *Australian Journal of Applied Science*, Vol. 3, 1952, pp. 228–232.

17. Power, T.C. and Steinour, H.H. An Investigation of Some Published Researches on Alkali-Aggregate Reaction. I. The Chemical Reactions and Mechanism of Expansion. *Journal of the American Concrete Institute*, Vol. 26, No. 6, 1955, pp. 497-512.

18. Prezzi, M., P.J.M. Monteiro, and G. Sposito. Alkali-Silica Reaction, Part I: Use of the Double-Layer Theory to Explain the Behavior of Reaction-Product Gels. *ACI Materials Journal*, Vol. 94, No. 1, 1997, pp. 10-17.

19. Prezzi, M., P.J.M. Monteiro, and G. Sposito. Alkali-Silica Reaction - Part 2: The Effect of Chemical Admixtures. *ACI Materials Journal*, Vol. 95, No. 1, 1998, pp. 3-10.

20. Rodrigues, F.A., P.J.M. Monteiro, and G. Sposito. The Alkali-Silica Reaction: The Effect of Monovalent and Bivalent Cations on the Surface Charge of Opal. *Cement and Concrete Research*, Vol. 31, No 11, 2001, pp. 1549-1552.

21. Diamond, S. and L.J. Struble. Swelling Properties of Synthetic Alkali-Silica Gels. *Journal of the American Ceramic Society*, Vol. 64, No. 11, 1981, pp. 652-655.

22. Figg, J. ASR-Inside Phenomena and Outside Effects (Crack Origin and Pattern). *Proceedings of the 7th International Conference on Alkali-Aggregate Reaction in Concrete*. Ottawa, Canada, 1986, pp. 152-156.

23. Kuo, S-S., H.S. Mahgoub, and A. Nazef. Investigation of Recycled Concrete Made with Limestone Aggregate for a Base Course in Flexible Pavement. In *Transportation Research Record: Journal of the Transportation Research Board, No. 1787*, TRB, National Research Council, Washington, D.C., 2002. pp. 99-108.

24. Saeed, A., M. Hammons, D. Feldman, and T. Poole. *Evaluation, Design and Construction Techniques for Airfield Concrete Pavement Used as Recycled Material for Base*. IPRF Report. IPRF-01-G-002-03-5. July 2006.

25. Azari, H., R. Lutz, P. Spellerberg. *Precision Estimates of Selected Volumetric Properties of HMA Using Absorptive Aggregate*. NCHRP Web-Only Document 109. December 2006.

26. Chini, A.R., S-S. Kuo, J. M. Armaghani, and J.P. Duxbury. Test of Recycled Concrete Aggregate in Accelerated Test Track. *Journal of Transportation Engineering*, Vol. 127, No. 6, 2001, pp. 486-492.

27. Cuttell, G.D., M.B. Snyder, J. M. Vandenbossche, and M.J. Wade. Performance of Rigid Pavements Containing Recycled Concrete Aggregates. In *Transportation Research Record: Journal of the Transportation Research Board, No. 1574*. TRB, National Research Council, Washington, D.C., 1997, pp. 89-98.

28. Cawley, B., C. Luedders, B. Smith, C. Hill, J. Harrington, et. al. *Transportation Applications Of Recycled Concrete Aggregate*. FHWA State of the Practice National Review. September 2004.

29. Kikuchi, M., A. Yasunaga, and K. Ehara. Total Evaluation of Recycled Aggregate and Recycled Concrete. *Proceedings of the 3rd International RILEM Symposium on Demolition and Reuse of Concrete and Masonry*, Odense, Denmark, 1994, pp. 367-377.

30. Merlet, J.D. and P. Pimienta. Mechanical and Physico-Chemical Properties of Concrete Produced with Coarse and Fine Recycled Concrete Aggregates. *Proceedings of the 3rd International RILEM Symposium on Demolition and Reuse of Concrete and Masonry*, Odense, Denmark, 1994, pp. 343-354.

31. Obla, K., H. Kim, and C. Lobo. *Crushed Returned Concrete as Aggregates for New Concrete*. Final Report to the RMC Research & Education Foundation. September 2007.

32. Sommer, H. Recycling of Concrete for the Reconstruction of the Concrete Pavement on the Vienna-Salzburg Motorway. *Proceedings of the 3rd International RILEM Symposium on Demolition and Reuse of Concrete and Masonry*, Odense, Denmark, 1994, p. 433-444.

33. Topcu, I.B. Physical and Mechanical Properties of Concretes Produced with Waste Concrete. *Cement and Concrete Research*, Vol. 27, No. 12, 1997, pp. 1817-1823.

34. Topcu, I.B., and S. Sengel. Properties of Concretes Produced with Waste Concrete Aggregate. *Cement and Concrete Research*, Vol. 34, No. 8, 2004, pp. 1307-1312.

35. Wainwright, P.J., A. Trevorrow, Y. Yu, and Y. Wang. Modifying the Performance of Concrete Made with Coarse and Fine Recycled Concrete Aggregates. *Proceedings of the 3rd International RILEM Symposium on Demolition and Reuse of Concrete and Masonry*, Odense, Denmark, 1994, pp. 319-330.

36. Yagishita, F., M. Sano, and M. Yamada. Behaviour of Reinforced Concrete Beams Containing Recycled Aggregate. *Proceedings of the 3rd International RILEM Symposium on Demolition and Reuse of Concrete and Masonry*, Odense, Denmark, 1994, pp. 331-342.

37. Anon. Concrete Runway Recycled as Asphalt Runway. *Highway and Heavy Construction*, Vol. 127, No. 9, 1984, pp. 44-46.

38. Heins, D. *Evaluation of Asphalt Mixes Made from Reclaimed Concrete Aggregates.* Iowa Department of Transportation: Office of Materials. 1986.

39. Paranavithana, S. and A. Mohajerani. Effects of Recycled Concrete Aggregates on Properties of Asphalt Concrete. *Resources, Conservation and Recycling*, Vol. 48, No. 1, 2006, pp. 1-12.

40. Wong, Y.D., D.D. Sun, and D. Lai, Value-Added Utilisation of Recycled Concrete in Hot-Mix Asphalt. *Waste Management*, Vol. 27, No. 2, 2007, pp. 294-301.

41. Cross, S.A., M.N. Abou-Zeid, J.B. Wojakowski, and G. A. Fager, Long-Term Performance of Recycled Portland Cement Concrete Pavement. In *Transportation Research Record: Journal of the Transportation Research Board, No. 1525*. TRB, National Research Council, Washington, D.C., 1996, pp. 115-123.

42. Bruinsma J.B., Peterson K.R., and Snyder M.B., Chemical Approach to Formation of Calcite Precipitate from Recycled Concrete Aggregate Base Layers. In *Transportation Research Record: Journal of the Transportation Research Board, No. 1577*. TRB, National Research Council, Washington D.C., 1997, pp. 10-17.

43. Gottfredsen, F.R. and F. Thogersen. Recycling of Concrete in Aggressive Environment. *Proceedings of the 3rd International RILEM Symposium on Demolition and Reuse of Concrete and Masonry*, Odense, Denmark, 1994, pp. 309-320.

44. Li, X. and D.L. Gress. Mitigating Alkali–Silica Reaction in Concrete Containing Recycled Concrete Aggregate. In *Transportation Research Record: Journal of the*

Transportation Research Board, No. 1979. TRB, National Research Council, Washington D.C., 2006, pp. 30–35.

45. Kiggundu, B.M., and Roberts, F.L., *Stripping in HMA Mixtures: State-of-the-Art and Critical Review of Test Methods*. Report 88-02, National Center for Asphalt Technology, Auburn University, Alabama, 1988.

46. Masad, E., E.Arambula, A.R. Abbas, R.A. Ketcham, and A. Epps-Martin, Non-Destructive Measurement of Moisture Transport in Asphalt Mixtures. *Journal of the Association of Asphalt Paving Technologists*, Vol. 76, 2007.

47. Caro, S., E.Masad, A.D. Bhasin, and D.N. Little, Moisture Damage Susceptibility, Part I: Mechanisms. *International Journal of Pavements Engineering*, Vol. 9, No. 2, April 2008, pp. 81-98.

48. Arambula, E., E. Masad, and A. Epps-Martin. Moisture Susceptibility of Asphalt Mixtures with Known Field Performance Evaluated with Dynamic Analysis and Crack Growth Model. In *Transportation Research Record: Journal of the Transportation Research Board, No. 2001*. TRB, National Research Council, Washington D.C., 2007, pp. 20-28.

49. Bhasin, A., J. Howson, E. Masad, D.N. Little, and R.L. Lytton. Effect of Modification Processes on Bond Energy of Asphalt Binders. In *Transportation Research Record: Journal of the Transportation Research Board, No. 1998*. TRB, National Research Council, Washington D.C., 2007, pp. 29-37.

50. Bhasin, A., D.N. Little, K.L. Vasconcelos, and E. Masad. Surface Free Energy to Identify Moisture Sensitivity of Materials for Asphalt Mixes. In *Transportation Research Record: Journal of the Transportation Research Board, No. 2001*. TRB, National Research Council, Washington D.C., 2007, pp. 37-45.

51. Caro, S., E. Masad, G. Airey, A. Bhasin, and D. Little. Probabilistic Analysis of Fracture in Asphalt Mixtures Caused by Moisture Damage. In *Transportation Research Record: Journal of the Transportation Research Board, No. 2057*. TRB, National Research Council, Washington D.C., 2008, pp. 28-36.

52. Birgisson, B., R. Roque, G.C. Page, and J. Wang. Development of New Moisture-Conditioning Procedure for Hot-Mix Asphalt. In *Transportation Research Record: Journal of the Transportation Research Board, No. 2001*. TRB, National Research Council, Washington D.C., 2007, pp. 46-55.

53. Mukhopadhyay A.K., S. Chang-Seon, and D.G. Zollinger. Activation Energy of Alkali-Silica Reaction and Dilatometer Method, In *Transportation Research Record, Journal of the Transportation Research Board, No. 1979*, TRB, National Research Council, Washington D.C., 2006, pp. 1-11.

54. Sarkar, S.L., D.G. Zollinger, A.K. Mukhopadhyay. *Handbook for Identification of Alkali-Silica Reactivity in Airfield Pavement*, Advisory Circular No. 150/5380-8. FAA, U.S. Department of Transportation, 2004.

55. Chang-Seon, S., A.K. Mukhopadhyay, and D. Zollinger. Evaluation of Alkali - Silica Reactivity Potential of Aggregate and Concrete by Using the Dilatometer Method: Performance Based Approach, In *Transportation Research Record, Journal of the Transportation Research Board, No. 2020*, TRB, National Research Council, Washington D.C., 2007, pp. 10-19.

56. Robertson, R.E., J.F. Branthaver, P.M. Harnsberger, J.C. Petersen, S.M. Dorrence, J.F. McKay, T.F. Turner, A.T. Pauli, S-C. Huang, J.-D. Huh, J.E. Tauer, K.P. Thomas, D.A. Netzel, F.P. Miknis, T. Williams, J.J. Duvall, F.A., Barbour, and C. Wright. *Fundamental Properties of Asphalts and Modified Asphalts, Volume I*. Interpretive Report, FHWA-RD-99-212. U.S. Department of Transportation, Federal Highway Administration, McLean, V.A. 2001.

57. Vasconcelos, K.L., A. Bhasin, and D.N. Little. Calorimetric Measurement of Adhesion between Bitumen and Aggregate used in Asphalt Mixtures. *International Symposium on Asphalt Pavements and Environment*. 2008.

58. Meininger, R. Micro-Deval vs. L. A. Abrasion. *Rock Products*, Vol. 107, No. 4, April 2004, pp. 33-35.

59. Rogers, C. A., M. L. Bailey, and B. Price. *Micro-Deval Test for Evaluating the Quality of Fine Aggregates for Concrete and Asphalt*. Report EM-96, Ontario Ministry of Transportation, June 1991.

60. Rogers, C. A., M. L. Bailey, and B. Price. Micro-Deval Tests for Evaluating the Quality of Fine Aggregates for Concrete and Asphalt. In *Transportation Research Record, Journal of the Transportation Research Board, No. 1301*, TRB, National Research Council, Washington D.C., 1991, pp. 68-76.

61. Arla, D., A. Sinquin, T. Palermo, C. Hurtevent, A. Graciaa, and C. Dicharry. Influence of pH and Water Content on the Type and Stability of Acidic Crude Oil Emulsions. *Energy and Fuels*, Vol. 21, No. 3, May/June 2007, pp. 1337-1342.

62. Brandal, Ø., J. Sjoblom, and G. Øye. Interfacial Behavior of Naphthenic Acids and Multivalent Cations in Systems with Oil and Water. I. A Pendant Drop Study of Interactions Between n-Dodecyl Benzoic Acid and Divalent Cations. *Journal of Dispersion Science and Technology*, Vol. 25, No. 3, May 2004, pp. 367-374.

63. Brandal, Ø., A-M.D. Hanneseth, and J. Sjoblom. Interactions Between Synthetic and Indigenous Naphthenic Acids and Divalent Cations Across Oil-Water Interfaces:

Effects of Addition of Oil-Soluble Non-Ionic Surfactants. *Colloid and Polymer Science*, Vol. 284, No. 2, November 2005, pp. 124-133.

64. Ese, M-H., and P.K. Kilpatrick. Stabilization of Water-in-Oil Emulsions by Naphthenic Acids and Their Salts: Model Compounds, Role of pH, and Soap: Acid Ratio. *Journal of Dispersion Science and Technology*, Vol. 25, No. 3, May 2004, pp. 253-261.

65. Kiran, S.K., E.J. Acosta, and K. Moran. Evaluating the Hydrophilic-Lipophilic Nature of Asphaltenic Oils and Naphthenic Amphiphiles Using Microemulsion Models. *Journal of Colloid and Interface Science*, Vol. 336, No. 1, August 2009, pp. 304-313.

66. Magnusson, H., A-M.D. Hanneseth, and J. Sjöblom. Characterization of C80 Naphthenic Acid and Its Calcium Naphthenate. *Journal of Dispersion Science and Technology*, Vol. 29, No. 3, 2008, pp. 464-473

67. Mendez, Z., R.E.Anton, and J-L. Salager. Surfactant-Oil-Water Systems Near the Affinity Inversion. Part XI. pH Sensitive Emulsions Containing Carboxylic Acids. *Journal of Dispersion Science and Technology*, Vol. 20, No. 3, 1999, pp. 883-892.

68. Rikka, P. *Spectometric Identification of Naphthenic Acids Isolated from Crude Oil*, Thesis, Texas State University-San Marcos. December 2007.

69. Zhang, A., Q. Ma, W.A. Goddard, and Y. Tang. *Improved Processes to Remove Naphthenic Acids*. Annual Technical Progress Report, California Institute of Technology, 28 April 2004.

70. Pospisil, K., A. Frybort, A Kratochvil, and J. Machackova. Scanning Electron Microscopy Method as a Tool for the Evaluation of Selected Materials Microstructure. *Transactions on Transport Sciences*. Ministry of Transport of the Czech Republic. 1 November 2008, pp. 13-20.

APPENDIX A

STANDARD QUESTIONNAIRE SENT TO AFBS

Material availability:

1. Is ASR-damaged recycled concrete aggregate (RCA) material currently available in your facilities? If available in which form?
2. Is RCA in a form of stockpile available? If yes then how old is the stockpile? We need relatively fresh materials.
3. Do you make finished RCA with recommended gradation?
4. What is the possibility that you can remove a confirmed ASR affected slab (partially) and crush using your onsite crusher and then donate us the crushed material for our research. We are willing to pay the shipping charge.
5. Whether ASR concentrates only in top 2-3 inches and rest of the concrete looks good?
6. Whether you are doing only patch work (removal of top ASR affected layer) or full depth repair (in case the whole slab is ASR affected)
7. Whether ASR-RCA in your facility is an accumulation of crushing slabs or foundation / base or combination of both?
8. If the material is not available at this time, are you planning to remove any alkali-silica reacted (ASR) slabs and make RCA within the next 4-8 weeks?
9. Do you have HMA mixtures in service that contain RCA as aggregates - specifically RCA that was crushed from PCC that was affected by ASR?

Historical information

10. What type and dosage of **deicer** that was applied, if any?
11. Do you think that the use of deicer triggered the ASR,?
12. Can RCA from areas with and without deicer application be selected?
13. What is the type of reactive aggregate(s) in ASR-affected concrete? Whether both coarse and fine aggregates are reactive or only one is reactive?
14. Availability of info pertaining to mix design (with and without SCMs, w/cm, etc.)?
15. Any information pertaining to climatic parameters such as temperature cycles, wet-dry cycles, moisture, rainfall, external source of alkalis and sulfates (if any)
16. How old is the pavement?
17. Is there any other visible or suspected distress (e.g., freeze/thaw, DEF, sulfate attack, corrosion problem etc.) other than ASR?

Level of ASR distress:

18. What is the **level of ASR-distress** (e.g., low, medium, and high)? If information is available then following criteria can be applied to categorize the distress level as low, medium and high
    a) Upheaved shoulders, buckled pavements, closing expansion joints, damaged utility trenches, significant map-cracking, presence of white gel products

along the map cracks – symptoms of significant concrete expansion - **High ASR distress**

b) presence of poor ASR related map-cracking and other ASR symptoms - **Low distress**

Can you send us some pictures or reports to get an idea about the level of ASR distress visually?

19. Confirmation of ASR by petrography - Can you send us some **petrographic report** (if available)? Otherwise, do you have any cores that you may have taken earlier to verify ASR inside the pavement or any other purpose? Can you donate us those cores for assessment?

APPENDIX B

AVAILABLE INFORMATION FROM THE INITIALLY IDENTIFIED AIR FORCE BASES

Source	POC	Material Availability	Petrographic Report	Nature of Damage	Deicer Application	Pavement Age	Type of Reactive Aggregate	Top Part or Whole Depth
Dover AFB	Earl Waller	Unable to provide ASR-RCA samples	No petrography Only UFAM	Map-cracks observed at places, Concrete with granite aggregate looks ok; Little ASR with concrete with river run aggregates	E-36, full strength, deicer possibly triggered ASR	Various ages from 10-60 years, Asphalt overlay, sample will be contaminated by AC	**Old river run** – possibly reactive; Later on **Granite** aggregate possibly not reactive	It seems ASR is not a big issue here
Holloman AFB, NM	John Hamann,	Materials received from top 2-3 inches	No such good petrography report	all levels of ASR, Trench drain damage, Cracking without significant expansion; Pictures shows map-cracks; No other distresses (?);	No deicer, mild dry climate	Stockpiles ~ 8 months old, early 1990s, 13-17 years	**Natural sand?**? No such other distress although SO_3 in soil high, cement content was high	Top 2-3 inches, patch work is going on
Seymour Johnson AFB, North Carolina	Darlene Varani	ASR-RCA received	No petrography, ASR confirmed based on personal experience and visual distresses	Medium ASR distress, 1.5// exp. Joint closed by 2 years and 4// joint reduced to 1// by 5-10 yrs, asphalt shoulder heaving; pictures show map-cracks but not prominent, Other distresses - unknown	No deicer; Hot and humid climate and periodic hurricane and tropical storm	1959	Not sure	Probably full depth??
Grand Junction, CO, AFB	Ed stores / Jason Virzy, phone	March-April (stockpiles) or 30 inch dia cores any time			No use of deicer			Whole depth
Ft. Campbell AFB, Kentucky	David Kiefer / Roy Tyler, phone	Not available, they have no plan to remove any ASR affected slabs in near future		Exp. Joint closed in a matter of months, expansion with negligible cracking	Li application			
Edwards AFB	Ken Crawford		Presence of ASR was	Map cracking observed but	Dry climate (desert), ASR	1950s, 40+ years no such	Little rock wash –	Looks like ASR

			confirmed in Lab in 1995, In 2004 report the presence of ASR gel was confirmed on aggregate surface, around aggregates and in cracks	not significant (1995 report); map-cracking more severe at the runways and taxiways intersections; ASR not been identified as a problem or concern, no spalling, shallow superficial cracks; ASR is growing	solely not responsible for more crack development in recent years; carbonation, drying shrinkage, ASR due to wet/dry cycles with high T inside, traffic loads	problem	alluvial deposits of granitic and volcanic (rhyolite, andesite and basalt), chert etc.; slowly reactive aggregates; 0.4 w/c, 3 inch max. size aggregate, 2.5-5.5 air, no SCMs, 6 sacks cement	in deeper portion but no such solid proof; Full depth along the joints
Omaha, NE Airport	David Roth, e-mail	Do not have ASR effected concrete stock piles, don't know whether they are going to do any repair work in near future						
Navy	Greg Cline, e-mail	NO response yet						
Atlanta AFB	Quintin Watkins	ASR-RCA not available, rubbles from slated pavements available but they need further crushing						
NM DOT	Bryce Simons	No RCA, they don't deal with RCA, However they can remove slabs crushed by the private industry. Available, locations need to be selected	No petrography available for the present locations, Pictures and reports – not easily and quickly available	Severe ASR damage, All level of distresses, North Mexico – severe freeze/thaw cycles; sulfate present in soils; other distresses are not confused with ASR	both with and without deicer application, sand with salt	2000's and older	From Rio Grande drainage basin – gravel (?)	

APPENDIX C

TEST PROTOCOL FOR DETERMINATION OF ALKALI-SILICA REACTIVITY OF AGGREGATE, MORTAR, AND CONCRETE USING DILATOMETER

Scope

This test method covers the determination of free volume expansion of aggregates (both coarse and fine aggregate) alone due to alkali-silica reaction (ASR) as a function of time. Dilatometer test is also used to determine the ASR expansion of mortar and concrete specimens.

Referenced Documents

1 Mukhopadhyay A.K., Shon Chang-Seon, and Zollinger D.G. “Activation Energy of Alkali-Silica Reaction and Dilatometer Method”, Transportation Research Record, Journal of the Transportation Research Board, No. 1979, concrete materials 2006.

2 Shon Chang-Seon, Mukhopadhyay A.K, Zollinger D.G (2007), “Evaluation of Alkali - Silica Reactivity Potential of Aggregate and Concrete by Using the Dilatometer Method: Performance Based Approach”, Journal of Transportation Research Record, Concrete Materials 2007, No. 2020, pp. 10-19 - **was nominated for the best practice-ready paper award** by the Design and Construction Group of the Transportation Research Board of the National Academics, Washington D.C in the area of design and construction.

3 S.L. Sarkar, Dan G. Zollinger, Anal K Mukhopadhyay, “Handbook for Identification of Alkali-Silica Reactivity in Airfield Pavement”, Advisory circular, AC No: 150/5380-8, 2004, U.S. Department of Transportation Federal Aviation Administration. – *The dilatometer test method is discussed as a new rapid test method that could be routinely applied during construction.*

4. Chang-Seon Shon, Shondeep L. Sarkar, and Dan. G. Zollinger, A New Rapid Test Method to Predict LiNO3 dosage for Controlling ASR Expansion, *Proceeding of 7th*

CANMET/ACI International Conference on Superplasticizers and Other Chemical Admixtures in Concrete, Berlin, SP-217, pp.423-436, October 2003.

5 Shon Chang-Seon, Mukhopadhyay A.K, Zollinger D.G., "Evaluation of Alkali-silica Reaction Potential of Aggregate Using Dilatometer Method", Proceedings of Transportation & Development Institute (T&DI) of the American Society of Civil Engineer's Airfield and Highway Pavement Specialty Conference, April 30 – May 3, 2006, Atlanta, USA.

6 Verbeck, George J., "Dilatometer Method for Determination of Thermal Efficient of Expansion of Fine and Coarse Aggregate," Highway Research Board, Proceedings of the Thirtieth Annual Meeting, Jan. 9-12, 1951.

Apparatus

The device proposed to measure the free volume expansion of aggregate (both coarse and fine aggregates), mortar and concrete is called "the dilatometer". The detailed drawings of the dilatometer are shown in the figure below. In short, it consists of a stainless steel cylinder, a Teflon-coated brass lid, a stainless steel hollow tower and a steel float. At the top of the tower, a casing is installed to ensure proper alignment of the LVDT and the float. To ensure that air bubbles can be easily removed, the inner surface of the lid is designed at a specific angle upwards. As the stainless steel rod moves inside the LVDT, electrical signals are generated. Therefore the physical phenomenon (i.e. movement of the rod) is converted into a measurable signal. This provides a sufficiently high accuracy in the measurement of a certain volume change in the small area of the NaOH solution surface in the tower. A thermocouple is immersed in the NaOH solution to monitor the temperature inside the container. The LVDT signal and temperature are recorded simultaneously by a data acquisition – computer system.

Preparation of Alkalinity Solution

The 1 N, 0.5N and 0.25N NaOH solutions are prepared by diluting 40, 20 and 10g of sodium hydroxide crystals into 0.9 Liter of distilled water. Then water is added to raise

the total volume of solution to 1 liter. $Ca(OH)_2$ is separately added to the prepared NaOH solutions till the solutions become saturated with respect to $Ca(OH)_2$.

Aggregate Preparation

Use the 80% of aggregate out of 100% total volume of cylindrical container.

1. The weight of the oven dried aggregate is measured and then placed in the dilatometer
2. The aggregates are soaked for 15-16 hours (overnight) in an alkaline solution at room temperature.
3. The dilatometer is subjected to 3 hrs vacuuming the following day to remove entrapped air.
4. The dilatometer is then placed in a water bath to raise the temperature to the target temperature.
5. A second round of vacuuming at target temperature is then applied for 1 hr.
6. The stainless steel float is inserted into the tower and the casing is securely placed at the top of the tower. An airtight situation is ensured through the use of O-rings in all the three junctions (lid-tower, tower-casing, casing-LVDT housing etc.) in the dilatometer system
7. The dilatometer is then placed in the oven. It takes around 4-5 hrs for the alkaline solution to be equilibrated with the temperature of the oven.
8. LVD movement after the stabilizing period represent movement due to ASR
9. LVDT movement and temperature are continuously recorded through data acquisition system till 75-100 hours with 1 hour data interval

A summary of the above steps is presented in the table below. Furthermore, concrete / mortar specimens of specific dimensions are also tested using dilatometer at different levels of soak solution alkalinities by following the above steps. In general, it takes around 7-8 days for mortar testing and 15-20 days for concrete testing.

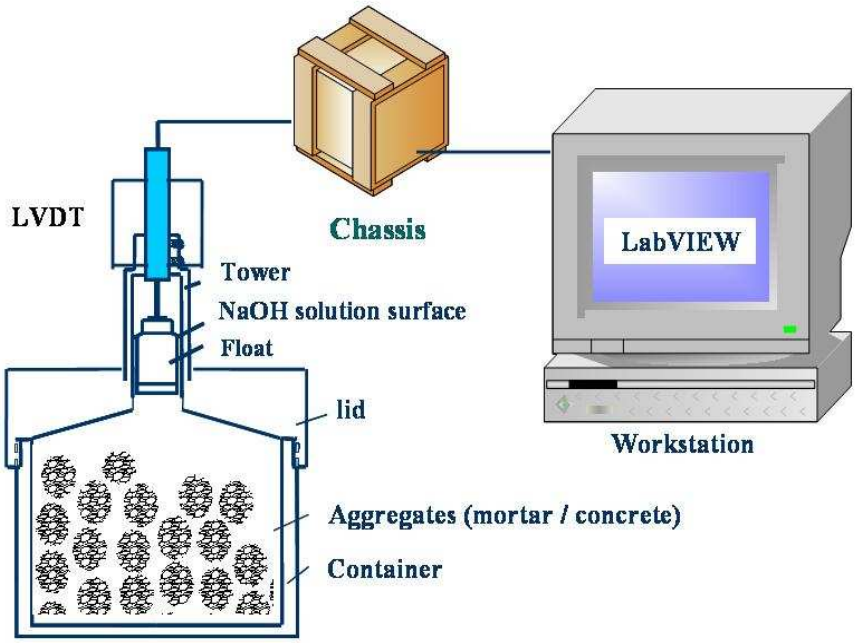

Dilatometer Setup

Proposed Sample Preparation of Aggregate

Step	Time	Temp.	Purpose/ Process
Aggregate Saturation	12 hrs.	Room	Saturation
Vacuuming (Agg. + sol.)	2 hrs.	Room	Remove entrapped air
Preheating dilatometer	2 hrs.	Room to Target	
Vacuuming (Agg. + sol.)	45 min.	Target	
Dilatometer stabilization	5 hrs.	Target	Set LVDT
ASR Measurement	150-170 hrs.	Target	Measure ASR exp.

Calibration Procedure

A calibration procedure is developed in order to determine the net LVDT displacement due to ASR. The steps of the calibration procedure are described below

- Three dilatometer tests, i.e., two with aggregate-solution and one with aggregate-water are conducted at the same temperature and time for an aggregate. Permissible COV% based on two replicas of aggregate-solution tests will serve as a verification of repeatability within the laboratory. It is to be noted that the COV% can be more in case of highly heterogeneous aggregates because of variability in two different dilatometer samples.
- The data are recorded and monitored for at least 4 days
- Once the test is stopped, the LVDT movement (inch) and temperature are plotted as a function of time (hours) for both aggregate-solution and aggregate-water tests.
- A reference time on the LVDT movement (y-axis) - time (x-axis) plot is then chosen based on the time when the dilatometer temperature reaches the target temperature (temperature-time plot) and become stabilized (approximately after 4-5 hours from the beginning of the test at oven).
- All LVDT readings after the reference time (item 5.4) are subtracted from the LVDT reading at reference time to obtain the LVDT displacement due to aggregate-solution and aggregate-water interaction.
- A downward LVDT movement for aggregate-water tests is obvious because of permanent pressure build up situation created by complete air-right situation inside dilatometer and incomplete aggregate saturation (if any).
- The rate of downward movement of aggregate-solution tests should be lower than that at aggregate-water test as it is a net effect of downward movement due to pressure build up and incomplete saturation and upward movement due to ASR
- The difference in the magnitude between the LVDT movements of aggregate-solution and aggregate-water test represents the LVDT displacement due to ASR
- The percent LVDT displacement due to ASR is then calculated based on the following procedure.

Calculation Procedure for Percent Displacement

The percent LVDT displacement is calculated based on the following mathematical relation:

$$E_n(\%) = \frac{\Delta V_{ASR}}{V_{aggregate}} \times 100$$

$E_n(\%)$ = Percent Expansion at n hours

Where: $V_{aggregate}$ = Initial Volume of Aggregate

ΔV_{ASR} = Volume change of Aggregate at n hours

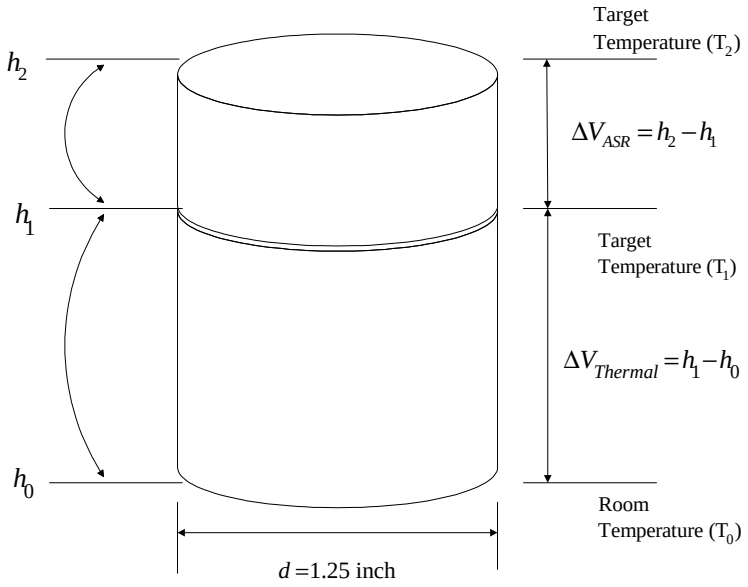

A schematic volume change due to ASR expansion

The above analysis is conducted for all the tested aggregates. An upward net ASR movement is observed for all the tests. Therefore, it can be postulated that dilatometer measures free volume expansion due to ASR.

Determination of the Characteristic Parameters of ASR

The measured expansion – time relationship is then modeled using the following mathematical relationship in order to calculate the ultimate ASR expansion (ε_0) of aggregates, the theoretical initial time of ASR expansion (t_0), and the rate constant (β).

$$\varepsilon = \varepsilon_0 . e^{-(\frac{\rho}{t-t_0})^{\beta}}$$

where:

ε_0 = ASR Ultimate Expansion

β = Slope of the logarithmic rate of expansion with respect to time

t_0 = Initial time of ASR Expansion (hr)

ρ = Time corresponding to an expansion (ε_0 / e)

Actually, the model is used to predict expansion as a function of time. The above parameters are determined using a new procedure called System identification Method (SID) at the best match between predicted and measured expansion. The calculation to determine the four parameters is based on iteration process and a computer program in MATLAB is developed for this purpose. The expansion (in %) and time (in hrs) are the necessary input for the MATLAB software and the ultimate expansion, the rate constant, and the ASR theoretical time are the relevant outputs.

The COV% based on 2 rate constants from two aggregate-solution tests needs to be within 15% in order to satisfy the repeatability requirements.

VITA

Brian James Geiger
geiger.brian.j@gmail.com
103 South General Bruce Drive
Temple, TX 76504

EDUCATION:

M.S. in Civil Engineering August 2010
Texas A&M University, College Station, TX

B.S. in Civil Engineering December 2007
Michigan Technological University, Houghton, MI

Drafting Certificate
Tuscola Technology Center, Caro, MI

WORK EXPERIENCE:

Technician/Receptionist: October 2009 – Present
Winkler Service and Parts, Inc., Temple, TX

Research Assistant: June 2008 – September 2009
Texas A&M Department of Civil Engineering, College Station, TX

Teaching Assistant: January 2008 – May 2008
Texas A&M Department of Civil Engineering, College Station, TX

Civil Engineering Intern: May 2007 - August 2007, May 2006 - September 2006, May 2005 - August 2005
Civil Engineering Co-op: May 2004 - November 2004
Soil and Materials Engineers, Inc., Bay City, MI

Drafting Co-op/Intern: December 2002-August 2003
Cass River Land Surveys, Caro, MI

EXTRA-CURRICULAR ACTIVITIES:

Treasurer: Michigan Tech ASCE student chapter, Spring 2007 - Fall 2007
Freshman Representative: Michigan Tech Undergraduate Student Government, Fall 2003 - Spring 2004
Junior Representative: Michigan Tech Undergraduate Student Government, Fall 2005 - Spring 2006
Senior Representative: Michigan Tech Undergraduate Student Government, Spring 2007
Elections Committee Chair: Michigan Tech Undergraduate Student Government, Spring 2007
Board Member: Friends of the Van Pelt Library, Fall 2005 - Fall 2007